

NORTHWESTERN UNIVERSITY

Luteinizing Hormone Receptor Signaling Regulates MAP2D Phosphorylation in Preovulatory
Granulosa Cells

A DISSERTATION

SUBMITTED TO THE GRADUATE SCHOOL
IN PARTIAL FULFILLMENT OF THE REQUIREMENTS

for the degree

DOCTOR OF PHILOSOPHY

Field of Cell and Molecular Biology

Integrated Graduate Program in Life Sciences

By

Maxfield Patrick Flynn

CHICAGO, ILLINOIS

December 2008

© Copyright by Maxfield P. Flynn 2007
All Rights Reserved

ABSTRACT

Luteinizing Hormone Receptor Signaling Regulates MAP2D

Phosphorylation in Preovulatory Granulosa Cells

Maxfield P. Flynn

The actions of luteinizing hormone (LH) to induce ovulation and luteinization of preovulatory follicles are mediated principally by activation of cAMP-dependent protein kinase (PKA) in granulosa cells. PKA activity is targeted to specific cellular locations by A-kinase anchoring proteins (AKAPs). I previously showed that follicle-stimulating hormone (FSH) induces expression of the AKAP microtubule-associated protein (MAP) 2D and that MAP2D co-immunoprecipitates with PKA regulatory subunits in rat granulosa cells. Here I describe a rapid and targeted dephosphorylation of MAP2D at Thr256/Thr259 after treatment with LH receptor agonist hCG. This event is mimicked by treatment with forskolin or a cAMP analog and blocked by the PKA inhibitor myristoylated-PKI, indicating a role for PKA signaling in phosphoregulation of granulosa cell MAP2D. I show that Thr256/Thr259 dephosphorylation is blocked by the protein phosphatase (PP) 2A inhibitor okadaic acid and demonstrate interactions between MAP2D and PP2A by co-immunoprecipitation and microcystin-agarose pulldown. I also show that MAP2D interacts with glycogen synthase kinase (GSK) 3 β and is phosphorylated at Thr256/Thr259 by this kinase in the basal state. Increased phosphorylation of GSK3 β at Ser9 and PP2A B56 δ subunit at Ser566 is observed after treatment with hCG, corresponding to LH receptor-mediated inhibition of GSK3 β and activation of PP2A, respectively. MAP2D dephosphorylated at Thr256/Thr259 appears to redistribute into a vimentin-enriched cell fraction

coincident with hCG-stimulated phosphorylation of vimentin on two PKA sites (Ser38 and Ser72). I show that MAP2D is localized to vimentin filaments and microtubules in granulosa cells and that LH receptor activation induces remodeling of the vimentin cytoskeleton. MAP2D binds directly to immobilized vimentin protein in overlay assays and this binding is diminished by GSK3 β phosphorylation of MAP2D *in vitro*. These results are consistent with the hypothesis that LH-stimulated dephosphorylation of MAP2D may facilitate the progesterone biosynthesis that is obligatory for fertility by altering intermediate filament dynamics.

ACKNOWLEDGEMENTS

I would like to express my profound gratitude to a number of people who supported me during this work. First, I thank my mentor, Dr. Mary Hunzicker-Dunn, who has provided me invaluable support, guidance, scientific insight, and enthusiasm through all of my time in her lab. I am equally grateful to Dr. Evelyn T. Maizels, who has become a mentor for me in life as well as science, providing encouragement and advice in even the most difficult circumstances. I thank the members of our lab, past and present, Dr. Youngkyu Park, Dr. Carl Peters, Zach Feiger, and, in particular, Dr. Hena Alam, who taught me much by example with her wisdom and perseverance, and Amelia Karlsson, who has been a knowledgeable colleague and a dear friend. I would also like to thank my committee members, Dr. Lester Binder, Dr. Adriana Ferreira, and Dr. Kelly Mayo, for their mentorship, guidance, and advice. Additionally, I thank Dr. Daniel Carr and Sarah Fiedler, who performed the recombinant MAP2D solid phase overlay assays and provided advice on AKAP signaling, Dr. Robert Goldman and Dr. Ying-hao Chou, who provided advice and reagents for vimentin research, Dr. Angus Nairn, Dr. Jung-Hyuck Ahn, and Dr. Thomas McAvoy, who contributed PP2A B56 δ antibodies and provided advice on PP2A signaling, and Dr. Teng-Leong Chew at the Northwestern Cell Imaging Facility for microscopy training and assistance. I would like to acknowledge the Endocrinology Training Grant and the Medical Scientist Training Program at Northwestern University for financial support. Last, I would like to acknowledge that this work relies heavily on the sacrifice of many research animals and hope that each one of us will continue to respect and advocate for the humane treatment of the animals that make much of our work possible.

LIST OF ABBREVIATIONS

AKAP, A-kinase anchoring protein

C, PKA catalytic subunit

CaMK, Ca²⁺/calmodulin-dependent protein kinase

CDK, cyclin-dependent kinase

DMSO, dimethylsulfoxide

EGF, epidermal growth factor

Epac, Exchange protein activated by cAMP

ERK, extracellular signal-regulated kinase

FSH, follicle-stimulating hormone

GSK, glycogen synthase kinase

hCG, human chorionic gonadotropin

IDPN, β,β' -iminodipropionitrile

LH, luteinizing hormone

LHRH, luteinizing hormone releasing hormone

MAP, microtubule-associated protein

MAPK, mitogen-activated protein kinase

MEK, MAPK kinase

MTBD, microtubule-binding domain

MLC, myosin light chain

Myr-PKI, myristoylated PKA inhibitor

P-450 SCC, cytochrome P-450 side chain cleavage enzyme

PI, phosphatidylinositol

PKA, cAMP-dependent protein kinase

PMSF, phenylmethylsulfonyl fluoride

PMSG, pregnant mare serum gonadotropin

PO, preovulatory

PP, protein-phosphatase

R, PKA regulatory subunit

RIA, radioimmunoassay

STI, soybean trypsin inhibitor

StAR, steroidogenic acute regulator protein

8-CPT-cAMP, 8-(4-chlorophenylthio) cAMP

8-pCPT-2'-O-Me-cAMP, 8-(4-chlorophenylthio)-2'-O-methyl cAMP

DEDICATION

For Kira

And for my parents

TABLE OF CONTENTS

<u>CHAPTER I: INTRODUCTION</u>	13
HYPOTHALAMIC-PITUITARY-OVARIAN AXIS	13
GONADOTROPINS AND FOLLICLE MATURATION	16
LH RECEPTOR SIGNALING.....	18
<i>cAMP/PKA Signaling</i>	18
<i>Other Signaling Pathways</i>	21
GRANULOSA CELL CYTOSKELETON.....	23
<i>Microtubules</i>	23
<i>Actin Microfilaments</i>	24
<i>Intermediate Filaments</i>	24
MAP2 FAMILY PROTEINS.....	25
<i>MAP2 and Cytoskeletal Interactions</i>	27
<i>MAP2 as a Signaling Scaffold</i>	28
MAP2 PHOSPHORYLATION	29
<u>CHAPTER II: LUTEINIZING HORMONE RECEPTOR ACTIVATION IN OVARIAN GRANULOSA</u>	
<u>CELLS PROMOTES PROTEIN KINASE A-DEPENDENT DEPHOSPHORYLATION OF MAP2D</u>	31
SUMMARY.....	31
INTRODUCTION.....	32
RESULTS	34
DISCUSSION	58
<u>CHAPTER III: MAP2D PHOSPHORYLATION REGULATES BINDING TO VIMENTIN</u>	
<u>INTERMEDIATE FILAMENTS</u>	65
SUMMARY.....	65

	10
INTRODUCTION	66
RESULTS	68
DISCUSSION	93
<u>CHAPTER IV: MATERIALS AND METHODS</u>	102
<u>CHAPTER V : CONCLUSIONS AND FUTURE DIRECTIONS</u>	110
CONCLUSIONS	110
FUTURE DIRECTIONS.....	111
<u>REFERENCES</u>	114
<u>CURRICULUM VITAE</u>	128

LIST OF FIGURES

<i>Figure 1 Regulation of ovarian follicle maturation by pituitary gonadotropins</i>	15
<i>Figure 2 Luteinizing hormone receptor signaling in preovulatory granulosa cells</i>	19
<i>Figure 3 MAP2 family proteins</i>	26
<i>Figure 4 Ovarian granulosa cell MAP2D exists in a phosphorylated state and is susceptible to an endogenous phosphatase activity</i>	35
<i>Figure 5 Phosphorylation of MAP2D at Thr256/Thr259 is rapidly decreased upon LH-receptor stimulation</i>	39
<i>Figure 6 cAMP/PKA-dependent signaling participates in the LH receptor-mediated decrease in phosphorylation of MAP2D Thr256/Thr259</i>	42
<i>Figure 7 PP2A-preferential treatment with the Ser/Thr phosphatase inhibitor okadaic acid blocks the hCG-induced decrease in MAP2D phosphorylation at Thr256/Thr259</i>	46
<i>Figure 8 Co-immunoprecipitation and affinity-pull-down analyses reveal interactions between MAP2D and PP2A, but not PPI catalytic subunits</i>	48
<i>Figure 9 GSK3 inhibitors block basal state phosphorylation of MAP2D at Thr256/Thr259</i>	51
<i>Figure 10 Modulation of MAP2D at Thr256/Thr259 through LH-mediated regulation of both GSK3β and PP2A .</i>	55
<i>Figure 11 Ovarian granulosa cell MAP2D co-isolates with vimentin intermediate filaments</i>	70
<i>Figure 12 MAP2D colocalizes with the vimentin intermediate filament and microtubule cytoskeletons in granulosa cells</i>	74
<i>Figure 13 MAP2D and vimentin intermediate filament localization is dependent on microtubule stability in granulosa cells</i>	76
<i>Figure 14 Granulosa cell MAP2D binds to vimentin in a phosphorylation-dependent manner</i>	79
<i>Figure 15 In vitro GSK3β phosphorylation regulates direct binding between MAP2D and vimentin</i>	82
<i>Figure 16 LH receptor activation results in vimentin phosphorylation at PKA sites</i>	86
<i>Figure 17 LH receptor signaling stimulates reorganization of the vimentin cytoskeleton</i>	88
<i>Figure 18 Vimentin disruption stimulates increased progesterone secretion by granulosa cells</i>	91

Figure 19 MAP2D functions as a scaffold for LH receptor signaling in preovulatory granulosa cells which may regulate vimentin cytoskeletal dynamics..... 94

CHAPTER I: INTRODUCTION

The mid-cycle surge in luteinizing hormone (LH) from the pituitary triggers acute changes in the function of the ovarian preovulatory (PO) follicle. In particular, LH binding to the LH receptors of PO granulosa cells promotes dramatic alterations in gene expression and signal transduction, particularly via the cAMP/PKA pathway. These changes stimulate a variety of events essential for fertility, including oocyte maturation, ovulation, steroidogenesis, and luteinization, and it is likely that these critical events require substantial changes in the granulosa cell cytoskeleton. I explore how LH receptor activation of the cAMP/PKA pathway in PO granulosa cells influences the A-kinase anchoring protein (AKAP) MAP2D and the granulosa cell cytoskeleton and propose a role for MAP2D in the process of LH-dependent follicle maturation.

Hypothalamic-Pituitary-Ovarian Axis

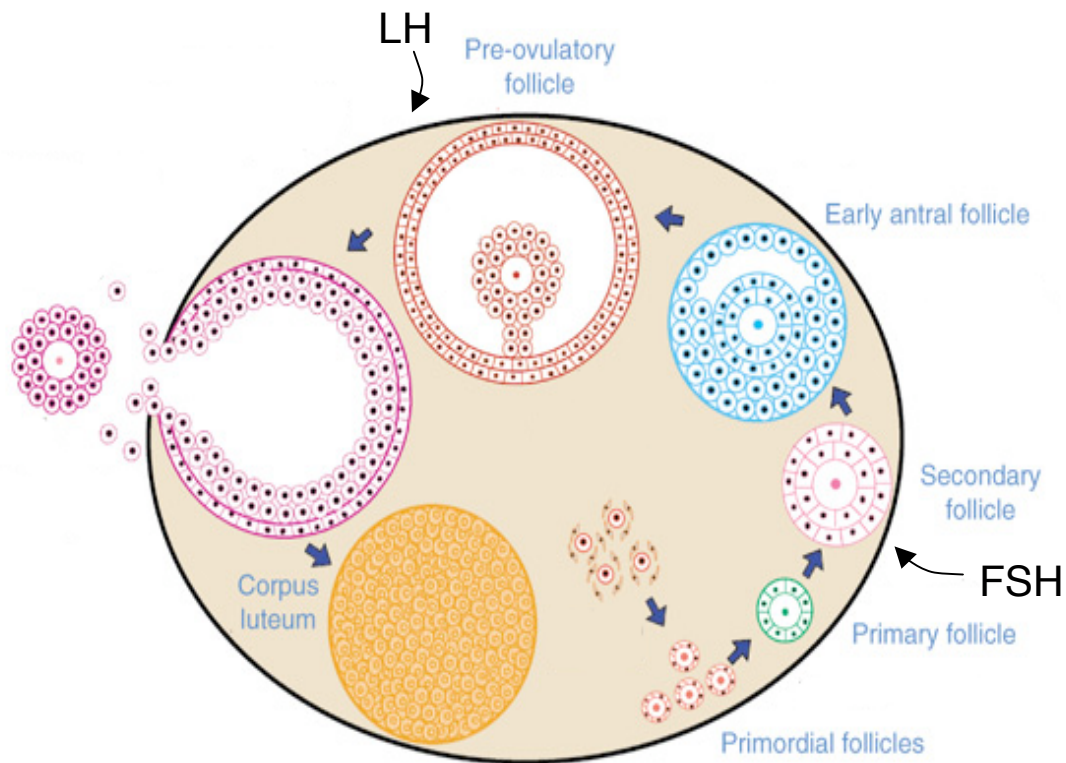
At the time of puberty, as development of the hypothalamus reaches maturity, specialized neurons projecting from the arcuate nucleus of the medial basal hypothalamus to the median eminence release pulsatile secretions of the luteinizing hormone releasing hormone (LHRH or GnRH) into the portal vessels (1). These pulses of LHRH act on gonadotrophs of the anterior pituitary expressing cell surface LHRH receptors, resulting in the pulsatile release of the pituitary gonadotropins, follicle stimulating hormone (FSH), and luteinizing hormone (LH). FSH and LH are released in various amounts, depending largely on feedback signals from the ovary in the form of steroids and other ovarian factors, such as the inhibins and activins (2).

The ovarian follicle, located in the outer cortex of the ovary, is the basic unit of ovarian function, and the pituitary-derived gonadotropins primarily act on ovarian follicles to promote their maturation (1) (Fig. 1). The less mature primary and secondary follicles, also referred to as preantral follicles, consist of a central oocyte surrounded by a thin layer of granulosa cells. In the case of secondary follicles, this layer is more than one cell-layer thick and is also surrounded by a layer of thecal cells (1). Low levels of LH secreted by the pituitary bind to receptors on thecal cells of preantral follicles to stimulate secretion of androgens, precursors for the production of estradiol by the granulosa cells (2). FSH binds to FSH receptors of granulosa cells of these preantral follicles to induce the expression of P-450 aromatase in these cells, enhancing their ability to convert thecal androgens into estradiol (3, 4). FSH also stimulates proliferation and differentiation of granulosa cells in the preantral follicle, and induces the expression of LH receptors in these cells (5) to prepare the enlarging follicles for the approaching LH surge (2).

As follicles mature to tertiary follicles, granulosa cell layers continue to proliferate and a fluid-filled space, called the antrum, forms between the mural granulosa cells, on the wall of the follicle, and cumulus granulosa cells, in the cumulus oophorus surrounding the oocyte (1). Mural granulosa cells express high levels of steroidogenic enzymes and LH receptors, whereas cumulus granulosa cells have fewer LH receptors and have lower steroidogenic activity (6-9), but develop specialized junctional communications with the oocyte in what is called the cumulus-oocyte complex (1, 10). A cohort of follicles, called antral or preovulatory (PO) follicles, rapidly increase in size and produce even greater levels of estradiol. Rising levels of estradiol, along with other factors, provide negative feedback on pituitary secretion of FSH and positive feedback on pituitary secretion of LH. This positive feedback on LH secretion reaches a peak at mid-cycle,

Figure 1 Regulation of ovarian follicle maturation by pituitary gonadotropins

FSH binds FSH receptors on granulosa cells of the preantral ovarian follicles resulting in granulosa cell proliferation and differentiation, and expression of genes encoding a variety of proteins, including LH receptors and MAP2D. A mid-cycle surge of LH activates LH receptors on granulosa cells of the PO (antral) follicle triggering events leading to ovulation and steroidogenesis. The ovulated follicle luteinizes to become the corpus luteum (adapted from (11)).



resulting in a surge of LH which activates LH receptors on granulosa cells and triggers events leading to enhanced progesterone steroidogenesis, ovulation, and luteinization of the theca and granulosa cell layers (1). These luteinizing cells will differentiate to become the corpus luteum, a “transient endocrine gland” (12). Levels of steroidogenic enzymes are increased as the corpus luteum becomes the main site of progesterone biosynthesis to support pregnancy and provide feedback to the pituitary to keep gonadotropin levels low (12). During pregnancy, the corpus luteum is controlled and maintained by hormones from the pituitary, decidua, and placenta, in particular prolactin, from the pituitary and later the trophoblast, and estradiol, from the ovary and later the trophoblast. Autocrine regulation by androgens and progesterone from the corpus luteum also plays a role in the rodent ovary (12). Without oocyte fertilization and implantation, or at the end of pregnancy, progesterone production is markedly decreased. Luteal cells undergo programmed cell death and the corpus luteum becomes drastically remodeled into a connective tissue rich corpus albicans (12). Falling progesterone levels allow the cycle to begin again with the release of gonadotropins from the pituitary.

Gonadotropins and Follicle Maturation

The gonadotropins, LH and FSH, are glycoprotein hormones composed of two peptide subunits, α and β , which bind noncovalently. The α subunit is common to LH and FSH, as well as thyroid stimulating hormone (TSH) and hCG. The β subunit of each hormone is distinct and confers a unique activity to each hormone (1). It should be noted, however, that both LH and hCG may bind and activate the LH receptor and hCG is often used in studies requiring LH receptor activation in PO granulosa cells (1).

FSH receptors, expressed on granulosa cells, are seven membrane-spanning G-protein coupled receptors which bind only FSH through interaction with a large extracellular N-terminal domain. Activation of FSH receptors in preantral granulosa cells results in signal transduction through the cAMP/PKA, Ca^{2+} , and phosphatidylinositol(PI) 3-kinase pathways (13). Their activation leads to increased expression of a number of factors important for follicular maturation, including the α subunit of the hormone inhibin, which feeds back to repress pituitary FSH production; P-450 aromatase, an important enzyme in estrogen production; cytochrome P-450 cholesterol side chain cleavage enzyme (P-450 SCC) and 3β -hydroxysteroid dehydrogenase, which are important for production of progesterone; and increased expression of membrane receptors for LH and EGF, both of which are necessary for ovulation (10, 13). FSH receptor activation also induces expression of a number of signaling proteins in granulosa cells, including the AKAP MAP2D (14).

LH receptors, expressed by theca-interstitial cells and by granulosa cells in large PO follicles, are seven membrane-spanning G-protein coupled receptors which may bind both LH and hCG through interaction with a large extracellular N-terminal domain. Activation of PO granulosa cell LH receptors during the LH surge is essential for ovulation. LH receptor null mice and humans with disrupting mutations of LH receptors are infertile with follicle development arrested at the early antral stage but no PO follicles, ovulation, or corpora lutea present (15, 16). Activation of LH receptors in PO granulosa cells results in signal transduction predominantly through the cAMP/PKA pathway, though PKA-independent signaling may also occur (13). LH receptor activation by the LH surge promotes expression of genes required for a number of events including suppression of granulosa cell division, cumulus expansion, final maturation of

the oocyte, remodeling and rupture of the follicle wall, and differentiation of granulosa and theca cells to form the corpus luteum (13, 17). In addition, steroid hormone biosynthesis is increased by persistent elevation of levels of P-450 SCC (18), a key enzyme in progesterone synthesis, and of the steroidogenic acute regulator protein (StAR) (19), which is involved in the transfer of cholesterol across the mitochondrial membrane.

LH Receptor Signaling

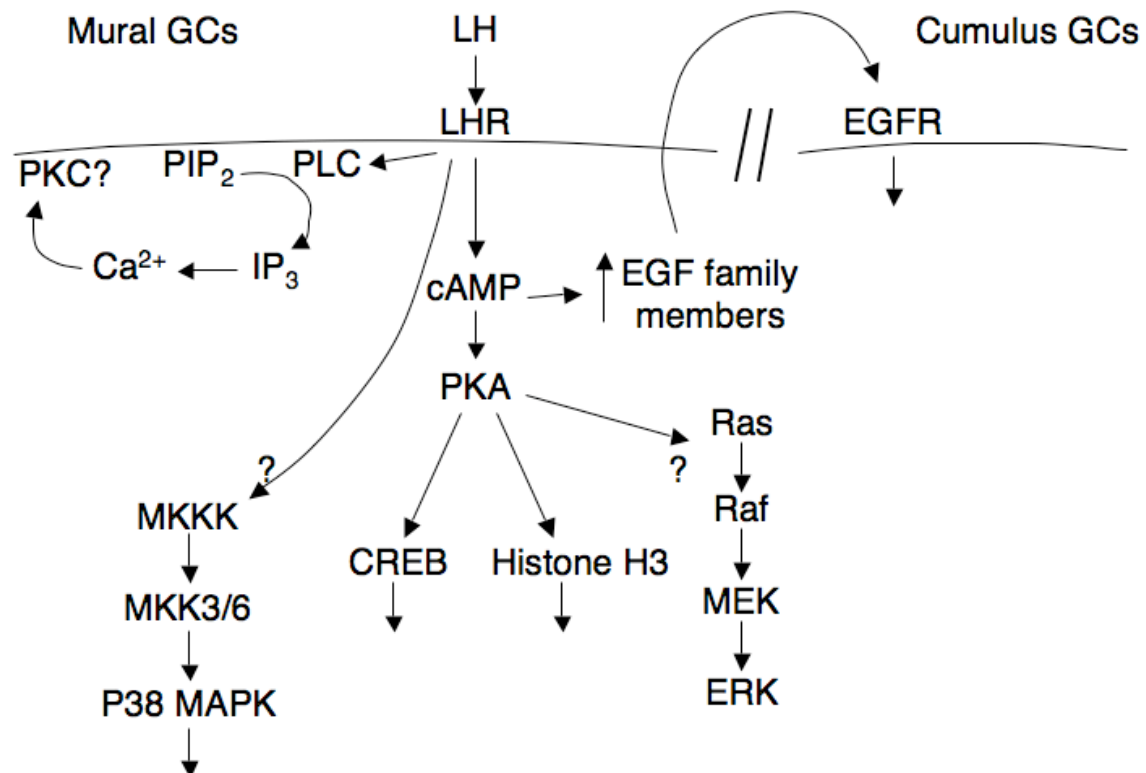
cAMP/PKA Signaling

The LH receptor couples to and activates Gs (20, 21) and adenylyl cyclase, resulting in increased synthesis of cAMP (22-24), and accounting for, it is believed, the majority of LH responses (Fig. 2). This is supported by the ability of the adenylyl cyclase activator forskolin and cell-permeable cAMP analogs to mimic LH-induced expression of a number of target genes (25-27).

In granulosa cells, increased cAMP as a result of LH receptor signaling predominantly activates cAMP-dependent protein kinase (PKA) (28). While it is also possible for LH-receptor mediated increases in cAMP to activate the cAMP-activated guanine nucleotide exchange factor Epac or a cyclic nucleotide-gated channel (29-32), signaling to these alternate cAMP pathways in PO granulosa cells has not been reported. PKA is a tetrameric holoenzyme consisting of a dimeric regulatory (R) subunit and two catalytic (C) subunits. Binding of cAMP to the R subunits causes the release of the active C subunits and allows phosphorylation of PKA substrates. PKA may be inhibited with the small molecule inhibitor H89, a competitive ATP antagonist, or the selective, cell-permeable C subunit inhibitor peptide myristoylated-PKI (Myr-PKI). PKI, the active portion of the ubiquitous PKA inhibitor protein, functions as a pseudo-

Figure 2 Luteinizing hormone receptor signaling in preovulatory granulosa cells

LH activates the LH receptor (LHR) to stimulate signaling via PKA to targets including the MEK/ERK pathway, histone H3, and CREB. LH receptors also signal via the p38 MAPK and IP_3/Ca^{2+} pathways. cAMP signaling by LH receptors also induces release of EGF-family members from mural granulosa cells, which bind and activate EGF receptors on cumulus granulosa cells. (Adapted from (13).)



substrate, attaching to the substrate binding site of the C subunits and blocking interactions with other PKA substrates. Inhibition of PKA in granulosa cells blocks the induction of a number of LH responses, including progesterone biosynthesis (33).

PKA activation in granulosa cells by LH receptor-mediated increases in cAMP results in phosphorylation of the classical PKA substrate CREB on Ser133 (34, 35). This phosphorylation is blocked by PKA inhibition (34). Phosphorylation-dependent binding of CREB to cAMP response elements in the promoter regions of a number of LH-responsive target genes, including the gene encoding StAR, has been demonstrated (36), revealing the fundamental importance of CREB phosphorylation by PKA for progesterone biosynthesis.

LH receptor phosphorylation and activation of ERK is also PKA-dependent, based on studies with H89 and Myr-PKI (34). Interestingly, in PO granulosa cells PKA regulates ERK by influencing signaling at a step upstream of MEK, as increased MEK phosphorylation by LH receptor signaling is H89-sensitive (34). The upstream site of this regulation has not been determined in granulosa cells but may involve activation of Ras, as reported for LH receptor signaling in primary Leydig cells (37). Thus, the mechanism of ERK activation by LH receptor signaling contrasts sharply with that of FSH receptor signaling, which involves disinhibition of ERK signaling by PKA-dependent phosphorylation and disassociation of an ERK-associated phosphotyrosine phosphatase (38). The role of ERK activation in PO granulosa cells is not clear, though involvement in expression of LH-responsive genes, including induction of StAR, has been postulated based on data showing that the MEK inhibitor PD98059 blocks downstream transcription activation of these genes (25, 39). Furthermore, a number of LH target genes,

including StAR (36, 39, 40) and P-450 SCC (41, 42), require binding of SF-1 for expression and SF-1 phosphorylation by ERK stabilizes this transcription factor in the active conformation (43).

Lastly, LH receptor signaling leads to phosphorylation of histone H3 on Ser10, which likely contributes to reorganization of gene promoters. This phosphorylation is also PKA-dependent, based on studies with H89 (34), but whether this occurs by direct-phosphorylation by PKA or via another phospho-regulatory mechanism downstream of PKA has not been evaluated.

Other Signaling Pathways

Based on studies in heterologous cells expressing LH receptors, it has been postulated that LH signaling increases inositol trisphosphate (IP₃) and intracellular Ca²⁺ levels through activation of PLC (44), and this signaling appears to be independent of cAMP (45, 46). Indeed, LH receptor signaling increases IP₃ in rat granulosa cells (47). However, while LHR activation of G_s and adenylyl cyclase has been well characterized, the identity of other G proteins that may activate the IP₃/Ca²⁺ pathway in granulosa cells remains unclear, though the involvement of β/γ subunits released by Gi₂ activation has been proposed (20, 21, 48, 49).

The downstream effects of LH-mediated increases in intracellular Ca²⁺ have not been definitively determined in granulosa cells. Ca²⁺ increases may activate one of the Ca²⁺/calmodulin-dependent protein kinases (CaMKs), which appear to be important for progesterone production, based on experiments using the CaMK inhibitor Kn93 (33). LH-mediate rises in Ca²⁺ may also activate one or more PKC isoforms, a hypothesis supported by the ability of PMA (phorbol myristate acetate, an activator of many PKC isoforms) added to subovulatory concentrations of LH to mimic a number of effects of ovulatory LH concentrations,

including progesterone production and luteinization of granulosa cells (50). Contrary to these studies, however, LH receptor activation does not promote the activation of the conventional (α and β ; Ca^{2+} -dependent) or novel (δ and ϵ) classes of PKC isoforms in granulosa cells by a variety of criteria (34). However, LH receptor activation is reported to stimulate membrane translocation of the atypical PKC isoform PKC ζ in PO granulosa cells (51), which may induce P-450 aromatase expression (52).

LH receptor signaling also phosphorylates p38 MAPK in PO granulosa cells (34). The upstream kinases MKK3 and MKK6 are also phosphorylated (53). Signaling into this pathway appears to be independent of PKA, based on the inability of H89 to block its phosphorylation (34), and the signaling targets of the p38 MAPK pathway are unknown (13).

As reviewed above, LH receptors in cumulus cells are expressed at far lower levels than in mural cells (54). In spite of this apparent insensitivity, LH receptor signaling still influences events in cumulus granulosa cells, such as cumulus expansion and the cumulus cell-mediated modulation of oocyte maturation (10). A mechanism for this seeming paradox may have been revealed recently by studies showing the expression of the epidermal growth factor (EGF) family members amphiregulin, epiregulin, and beta-cellulin on the surface of mural granulosa cells in response to LH-stimulated cAMP signaling (55). Addition of these factors to cultured cumulus-oocyte complexes (consisting of oocytes surrounded only by the cumulus layer of granulosa cells) mimicked LH-stimulated oocyte maturation, but this effect required the presence of cumulus granulosa cells (55). A model for mural to cumulus granulosa cell communication was proposed in which EGF family members are released from the surface of mural granulosa cells in response to cAMP-dependent LH receptor signaling and these factors then bind to and activate

EGF receptors on the surface of cumulus granulosa cells resulting in activation of signaling necessary for support of oocyte maturation and ovulation (10). Data supporting this model include an observed increase in EGFR activating phosphorylation occurring at a time slightly after the more immediate LH receptor signaling events in mural granulosa cells (55, 56), and a block in oocyte maturation after treatment with EGF receptor kinase inhibitors (55).

Granulosa Cell Cytoskeleton

Similar to the majority of animal cells, the granulosa cell cytoskeleton is composed of a complex network of three distinct components: microtubules, microfilaments, and intermediate filaments. Numerous studies have examined the role of the granulosa cell cytoskeleton in such functions as membrane receptor dynamics and topography (57), intracellular lysosome and endosome movement (58, 59), and steroidogenesis (60-62) at a variety of stages of differentiation. However, a clear understanding of cytoskeletal changes induced by LH receptor signaling in PO granulosa cells remains elusive.

Microtubules

PO granulosa cell microtubules, in a pattern common to many cell types, are organized in a fibrous network emanating from a centrosomal organizing center into the cell periphery (63). In mature granulosa cells obtained from human patients receiving hCG treatment for ovulation prior to IVF treatment, induction of increased cAMP levels by a variety of methods produced little or no change in the microtubule pattern (64). Treatment of similarly obtained cells with hCG produced no measurable change in synthesis of α - or β - tubulin (65). As observed in other cell models, taxol treatment of rat PO granulosa cells leads to increased bundling of

microtubules around the centrosomal organizing center (66), and treatment with microtubule disruptors such as nocodazole or colchicine resulted in complete disintegration of microtubule networks (58, 61, 67).

Actin Microfilaments

Actin microfilaments in PO granulosa cell are organized into abundant stress fibers which stretch the length of the cell and into the periphery (66). In mature human granulosa cells from IVF patients, increased cAMP levels promoted disassembly of actin stress fibers leaving centrally-localized staining (64), and treatment of similar cells with hCG resulted in decreased synthesis of actin and a number of other actin-associated proteins (65, 68).

Intermediate Filaments

The most abundant intermediate filament protein in PO granulosa cells is vimentin, a class III intermediate filament protein (67, 69, 70). While some types of keratin may also be prevalent in less mature human granulosa cells, these are decreased during granulosa cell maturation to the PO phenotype and are not detected at all in rat, porcine, and bovine granulosa cells (69, 70), emphasizing the importance of vimentin as these cells mature.

Vimentin is organized into filamentous structures in granulosa cells, and these filaments are well spread around the nucleus and into the peripheral cytoplasm of PO granulosa cells (66). Vimentin is considered one of the most phosphorylated polypeptides in granulosa cells by some estimates (67), and phosphorylation of vimentin by a variety of kinases, including PKA (71-74), is often correlated with reorganization or destabilization of vimentin filaments. In agreement with this, increased cAMP levels in mature human granulosa cells from IVF patients have been

shown to promote destabilization of vimentin filaments in the cytosolic periphery of the cell and thickening of vimentin filaments surrounding the nucleus (64). Vimentin destabilization in other steroidogenic cell types, including adrenal cells and LH-responsive testicular Leydig cells, is thought to result in increased transport of cholesterol ester droplets to the mitochondrial membrane for steroid production (75-77).

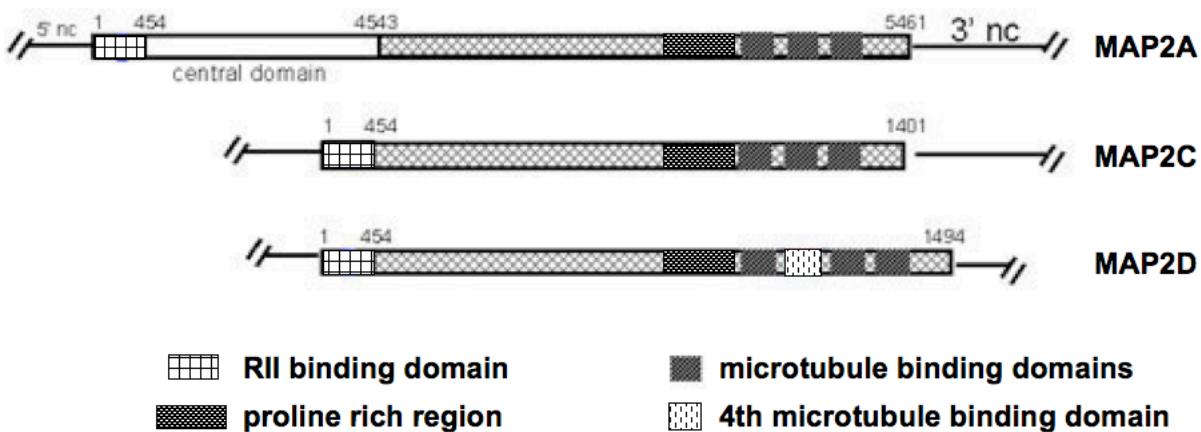
A similar collapse of the peripheral vimentin cytoskeleton into a thickened peri-nuclear region is observed following microtubule destabilization by nocodazole or colchicine (67, 78-84). It is thought that this phenomenon is due to the dependence of the vimentin on microtubule-dependent transport of vimentin particles for the formation of filaments (reviewed in (85)). Interestingly, destabilization of microtubules, which results in this vimentin remodeling, has been reported to result in increased progesterone production (61) similar to the effects of vimentin remodeling in other steroidogenic cells (75).

MAP2 Family Proteins

The MAP2 proteins (reviewed in (86)) are a family of heat-stable proteins abundant in the mammalian central nervous system where they are important in modulation of cytoskeletal dynamics, neuronal plasticity and neurite outgrowth (87). The human MAP2 proteins consist of two groups of four isoforms generated by alternative splicing: high molecular weight isoforms, MAP2A and MAP2B, and low molecular weight isoforms, MAP2C and MAP2D. MAP2C and MAP2D contain the same N- and C-terminal regions as the high molecular weight isoforms, but lack a central domain found in MAP2A and MAP2B (Fig. 3). All isoforms have at least three microtubule binding domains (MTBD), containing conserved KXGS motifs, in their C-termini as well as a highly conserved proline-rich domain just N-terminal to the MTBD (88, 89). MAP2D

Figure 3 MAP2 family proteins

The human MAP2 proteins consists of four isoforms generated by alternative splicing: high molecular weight isoforms, MAP2A and MAP2B, and low molecular weight isoforms, MAP2C and MAP2D. All isoforms have at least three C-terminal microtubule binding domains (MTBD), a highly conserved proline-rich domain, and an N-terminal RII binding domain. MAP2D and some MAP2B splice variants contain a 4th tubulin binding domain.



and some MAP2B splice variants contain an additional 93-bp insertion encoding a 4th tubulin-binding domain (90-92). The N-terminal region of MAP2 proteins contain a unique 31 residue domain which allows binding to the RII subunits of the PKA holoenzyme (93, 94), the functional definition of an AKAP. We recently described expression of the low molecular weight MAP2D isoform in PO granulosa cells where it binds to R subunits of the PKA holoenzyme (14) and may be important for LH receptor signaling.

MAP2 and Cytoskeletal Interactions

MAP2 family members were first isolated from brain tissue and their ability to bind to a number of cytoskeletal elements in neurons has been extensively studied (reviewed in (86, 95)). Perhaps best recognized is the capacity of MAP2 to bind to microtubules, via the MTBD (96), which results in increased microtubule assembly (97), stability and rigidity (98-100), and microtubule bundling in heterologous systems (101, 102). In addition to the MTBD, the presence of the nearby proline-rich domain also is important for binding to microtubules (103, 104). MAP2 similarly may bind to and bundle actin microfilaments (105, 106), also via the MTBD, resulting in increase stability of microfilaments. Observations of binding to both microtubules and microfilaments in neuronal cells have lead to the hypothesis that MAP2 may coordinate simultaneous reorganization of microfilaments and microtubules during neurite outgrowth (87, 107). Lastly, MAP2 has been reported to bind to at least two classes of intermediate filaments, vimentin and neurofilaments (83, 108-112), apparently using a binding site different than that used for microtubules (113), and it has been shown that MAP2 may form cross-bridges between microtubules and intermediate filaments (114). Phosphorylation of MAP2 appears to regulate

binding to each of these cellular components (101, 105, 106, 108), indicating the importance of MAP2 phospho-regulation in cytoskeletal dynamics.

MAP2 as a Signaling Scaffold

MAP2 was the first A-kinase anchoring protein (AKAP) to be identified and was initially recognized based on its ability to bind the RII subunits of the PKA holoenzyme (115). AKAPs, as a functional class of proteins, generally consist of a RII-binding domain and a specific subcellular targeting domain. The targeting domain allows localization of the AKAP and associated PKA holoenzyme to specific cellular locations and, in this way, may focus cAMP/PKA signaling on particular cellular locations and substrates (reviewed in (116, 117)). Recently it has been recognized that AKAPs not only bind PKA, but can also function as scaffolds to coordinate signaling cascades by binding phosphodiesterases, phosphatases, additional kinases, and other signaling proteins (118). Confinement of PKA and other associated signaling cascades to the AKAP scaffold in a discrete cellular location is thought to increase the efficiency of signaling and eliminate inappropriate cross-talk among pathways (118).

The hypothesis that MAP2 family proteins may serve as signaling scaffold for molecules in addition to PKA is supported by a variety of evidence. MAP2 isoforms may be heavily phosphorylated by a large number of kinases (86), as discussed below, and it is reasonable to hypothesize that one or more of these kinases may bind MAP2. Also, protein phosphatase (PP) 2A and PP1 have activity against MAP2 and so the AKAP may interact with these signaling proteins (119). Finally, it has been observed that MAP2C may directly interact with the Src homology 3 (SH3) domains of the Src-family non-receptor tyrosine kinase Fyn and Grb2 (120-122).

MAP2 Phosphorylation

MAP2 proteins may be heavily phosphorylated, reaching up to 46 moles of phosphate per mole of protein in high molecular weight isoforms (86). At least 15 predicted sites of phosphorylation are conserved in the lower molecular weight MAP2D isoform, particularly the Ser and Thr residues in the C-terminal proline-rich and microtubule-binding domains (86). MAP2 may be phosphorylated *in vitro* at numerous sites by a wide variety of kinases, including PKA (123), CaMK II (124), PKC (125, 126), microtubule affinity regulating kinases (127), Src-family kinases (120), and proline directed kinases, including GSK3, CDKs, and MAPK superfamily kinases (119, 128, 129). In addition, MAP2 may be dephosphorylated at various sites *in vitro* by PP1, PP2A, and PP2B (119, 130, 131). Phosphorylation at a number of sites can alter the association between MAP2 and various cytoskeletal components (101, 105, 106, 108), which may modulate the stability and dynamics of these cytoskeletal networks (86).

MAP2D in granulosa cells appears to be highly phosphorylated (14). I have focused on the phosphorylation state of two residues, Thr256/Thr259 (equivalent to Thr1620/Thr1623 in the higher molecular weight isoforms), located in the proline-rich domain adjacent to the first MTBD. Phosphorylation of MAP2D on Thr256/Thr259 in granulosa cells is coincident with FSH-induced increases in MAP2D expression (14) and the majority of the MAP2A/2B present in growth cones of hippocampal neurons is also phosphorylated at these residues (132). These residues are 100% conserved in mouse, rat and human species and are also highly conserved in the corresponding domain of the related MAP, tau (133). Thr256/Thr259 residues are *in vitro* targets for the proline-directed kinases GSK3, CDKs, and MAPK superfamily kinases (119) as are the corresponding residues in tau (Ser199/Ser202) (134). Moreover, phosphorylation of

Thr256/Thr259 in COS-1 cells overexpressing both MAP2C (a low molecular-weight isoform similar to MAP2D) and GSK3 β inhibits microtubule bundling consistent with reduced binding of MAP2C to microtubules (101).

Upon LH receptor activation in the PO granulosa cell, the substantial majority of LH receptor signaling is carried out by the cAMP/PKA pathway, initiating events such as steroidogenesis, ovulation, and luteinization which likely necessitate fundamental changes in the granulosa cell cytoskeleton. Coincident with these new demands, MAP2D, a protein with unique abilities to direct PKA signaling and to modulate cytoskeletal dynamics, is expressed. In the following studies, I characterize the phospho-regulation of MAP2D by LH receptor signaling and begin to elucidate its role in coordinating PKA signaling and cytoskeletal changes in the PO granulosa cell.

CHAPTER II: LUTEINIZING HORMONE RECEPTOR ACTIVATION IN
OVARIAN GRANULOSA CELLS PROMOTES PROTEIN KINASE A-DEPENDENT
DEPHOSPHORYLATION OF MAP2D

Summary

The actions of LH to induce ovulation and luteinization of PO follicles are mediated principally by activation of PKA in granulosa cells. PKA activity is targeted to specific locations in many cells by A-kinase anchoring proteins (AKAPs). We previously showed that FSH induces expression of MAP2D, an 80 kD AKAP, in rat primary granulosa cells, and that MAP2D co-immunoprecipitates with PKA regulatory subunits in these cells. Here I report a rapid and targeted dephosphorylation of MAP2D at Thr256/Thr259 after treatment with hCG, an LH receptor agonist. This event is mimicked by treatment with forskolin or a cAMP analog and is blocked by the PKA inhibitor myristoylated-PKI, indicating a role for cAMP and PKA signaling in phospho-regulation of granulosa cell MAP2D. Furthermore, I show that Thr256/Thr259 dephosphorylation is blocked by the PP2A inhibitor okadaic acid and demonstrate interactions between MAP2D and PP2A by co-immunoprecipitation and microcystin-agarose pulldown. I also show that MAP2D interacts with GSK3 β and is phosphorylated at Thr256/Thr259 by this kinase in the basal state. Increased phosphorylation of GSK3 β at Ser9 and the PP2A B56 δ subunit at Ser566 is observed after treatment with hCG and appears to result in LH receptor-mediated inhibition of GSK3 β and activation of PP2A, respectively. Taken together, these results show that the phosphorylation status of the AKAP MAP2D is acutely regulated by LH receptor-mediated modulation of kinase and phosphatase activity via PKA.

Introduction

Granulosa cells of mature PO ovarian follicles respond to a mid-cycle surge of pituitary LH by altering gene expression to promote luteinization and ovulation. These responses are initiated through binding of LH to surface LH receptors. The LH receptor is a seven transmembrane protein that couples to the stimulatory guanine nucleotide-binding protein G_s and signals to adenylyl cyclase (135). Activation of adenylyl cyclase rapidly increases the local concentration of the second-messenger cAMP resulting in activation of PKA (28). cAMP and PKA are largely responsible for early events of LH signaling which drive granulosa cell differentiation and steroid synthesis and culminate in ovulation of the oocyte (27, 34, 35, 136, 137).

PKA is a tetrameric holoenzyme consisting of a dimeric R subunit and C subunits. Binding of cAMP to the R subunits causes the release of the active C subunits and allows phosphorylation of PKA substrates. PKA is often targeted to specific cellular locations by AKAPs, a family of proteins functionally identified by their binding affinity for PKA R subunits (reviewed in (138, 139)). Cellular localization of AKAPs and associated PKA holoenzyme is achieved by interaction between an AKAP targeting domain and a cellular organelle or structure, such as a component of the cytoskeleton. Targeting of PKA activity by AKAPs increases the specificity of PKA action by controlling its access to various substrates. However, AKAPs also bind to a variety of signaling molecules, including other kinases, phosphatases, phosphodiesterases, and PKA substrates. Thus, the scaffolding function of AKAPs may allow for spatial regulation of numerous cellular signaling events.

We previously showed that FSH induces the expression of an 80-kDa AKAP in granulosa cells as they mature to a PO phenotype (140). We identified this AKAP as MAP2D, a low molecular weight splice variant of the MAP2 family of proteins (14). MAP2 family members are well characterized as neuronal microtubule-associated proteins and AKAPs and are expressed as splice-variants from a single gene (141-143). They contain an N-terminal R-subunit binding domain that allows for binding to PKA (115, 123). MAP2 isoforms also bind to numerous cytoskeletal elements including microtubules, via three or four C-terminal MTBDs; microfilaments, also via MTBDs; and, perhaps, intermediate filaments (reviewed in (86)) (83, 105, 106, 110, 112, 113).

The high-molecular weight MAP2A and MAP2B isoforms appear to be highly phosphorylated at serine/threonine residues *in vivo*, and at least 15 phosphorylatable residues are conserved in the low-molecular weight MAP2D isoform (reviewed in (86)). Two residues, Thr256/Thr259 (equivalent to Thr1620/Thr1623 in MAP2A/B), are present in a proline-rich domain that lies immediately N-terminal to the first MTBD. These residues are phospho-regulated *in vitro* by a variety of proline directed kinases (119) and by protein-phosphatase 1 (PP1) and/or PP2A (119). Similar regulation has been observed in cultured neurons (132) and rat brain tissue (131). Furthermore, phosphorylation of these residues was observed in COS-1 cells overexpressing both GSK3 and the highly homologous MAP2C isoform and resulted in regulation of microtubule binding affinity and microtubule polymerization dynamics (101).

Recently we showed that MAP2D in granulosa cells is phosphorylated at Thr256/Thr259 coincident with its FSH-induced expression (14). Based on the physiological expression of this predominately neuronal protein in the ovary at a time when the organ is exposed to the mid-cycle

surge of LH, I sought to investigate the *in vivo* phosphorylation state of MAP2D in PO ovarian granulosa cells, to identify the kinase(s) that promote phosphorylation at Thr256/Thr259, and to determine the effects of LH on the phosphorylation state at these sites. My results show that cAMP/PKA-dependent LH receptor signaling promotes a rapid decrease in phosphorylation at Thr256/Thr259. This change appears to be mediated by a simultaneous activation of PP2A activity, which I identify as a MAP2D binding partner, and inhibition of GSK3, another MAP2D binding partner and the predominant Thr256/Th259 kinase in granulosa cells.

Results

Ovarian granulosa cell MAP2D exists in a phosphorylated state and is susceptible to an endogenous phosphatase activity.

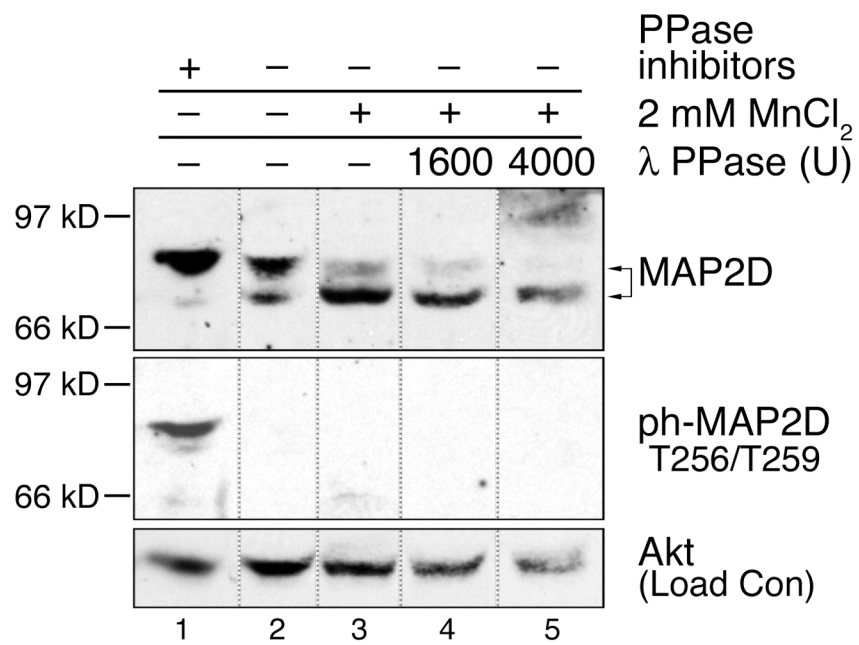
Based on previous reports that phosphorylation of MAP2 family proteins at multiple sites may result in changes in electrophoretic mobility (141, 144-146), the electrophoretic mobility of MAP2D in rat PO granulosa cell lysates was analyzed by Western blot. MAP2D protein migrated through polyacrylamide gel in at least two distinct bands (Fig. 4). When cell extracts were incubated (30 min at 30°C) in buffer containing standard phosphatase inhibitors, the majority (89%) of MAP2D protein was detected in a slower migrating band at approximately 80 kDa (Fig. 4, lane 1). The remaining MAP2D protein (11%) was detected in a faster migrating band at approximately 70 kDa.

To verify that the presence of two MAP2D bands resulted from distinct phosphorylation states of MAP2D, lysates were incubated (30 min at 30°C) in buffers with variable permissiveness toward phosphatase activity or in the presence of exogenous phosphatase activity. When phosphatase inhibitors were removed from the incubating buffer, 37% of MAP2D

Figure 4 Ovarian granulosa cell MAP2D exists in a phosphorylated state and is susceptible to an endogenous phosphatase activity

Rat PO granulosa cells were collected and lysed by sonication in buffer with the phosphatase inhibitors EDTA, sodium orthovanadate, sodium fluoride, and sodium pyrophosphate (lane 1; Complete Buffer A), buffer without phosphatase inhibitors (lane 2; Minimal Buffer A), or buffer with $MnCl_2$ (lanes 3-5; $MnCl_2$ Phosphatase Reaction Buffer). For further details, see *Materials and Methods*. Clarified lysates were incubated at 30°C for 30 min following addition of no phosphatase (lanes 1-3) or 1600 U (lane 4) or 4000 U (lane 5) of Lambda protein phosphatase (PPase). Arrows indicate faster (~70 kDa) and slower (~80 kDa) migrating MAP2D bands. Positions of Mr standards are indicated. Western blots of lysates were probed with the indicated antibodies. Total Akt levels were analyzed by Western blotting and used as a loading control (Load Con). Lines between lanes indicate cropped images. Results are representative of three separate experiments.

Figure 4



was now detected in the faster migrating band (Fig. 4, lane 2). The addition of 2 mM MnCl₂, which can activate phosphatases including PP2A under certain conditions (147, 148), further increased the proportion of MAP2D protein in the faster band (to 70%; lane 3). Finally, the addition of Lambda phosphatase increased the proportion of MAP2D protein in the faster band to up to 78% (lanes 4 and 5). These results confirm that the majority of MAP2D in ovarian granulosa cells exists in a phosphorylated state and suggest that this phosphorylation may be susceptible to endogenous phosphatase activity. I also evaluated the migration position of MAP2D phosphorylated on Thr256/Thr259 in the proline-rich domain using a phospho-specific antibody developed against a synthetic peptide containing these sites (Cell Signaling Technology; Danvers, MA). MAP2D phosphorylated at Thr256/Thr259 was detected at the size comparable to the slower migrating MAP2D band, but only in the presence of phosphatase inhibitors (~80 kDa; lane 1). These results also show that additional sites are phosphorylated on MAP2D, based on the abundance of MAP2D at 80 kDa under conditions in which Thr256/Thr259 signal is not detected (lane 2).

Phosphorylation of MAP2D at Thr256/Thr259 is rapidly decreased upon LH-receptor stimulation.

Based on the ability of LH receptor signaling to modulate many critical functions in PO granulosa cells (27, 34, 35, 136, 137), I analyzed the phospho-regulation of MAP2D Thr256/Thr259 in PO granulosa cells isolated from PMSG-primed rats upon activation of the LH receptor by the LH receptor agonist hCG. Cultured cells were treated with or without hCG for various times and Western blots of total cell lysates were probed with phospho-specific antibody.

MAP2D phosphorylation at Thr256/Thr259 was readily detected in untreated cells (Fig. 5A, lanes 1, 6, and 8). Treatment with hCG (lanes 2-5 and 7) caused a rapid decrease in Thr256/Thr259 phosphorylation, with a significant decrease to $18 \pm 3\%$ ($n=28$, $p<0.01$) of untreated control by 10 min. The timing of this decrease in phosphorylation occurred as early as 2 min and lasted as long as 1 h, corresponding with activation of PKA as demonstrated by increased phosphorylation of CREB at Ser133, a direct PKA target in granulosa cells (34, 35). Changes in phosphorylation of MAP2D at a different site, Ser136, were not observed after hCG treatment (Fig. 5A). These results indicate that MAP2D undergoes a rapid and specific decrease in Thr256/Thr259 phosphorylation upon activation of LH receptor signaling.

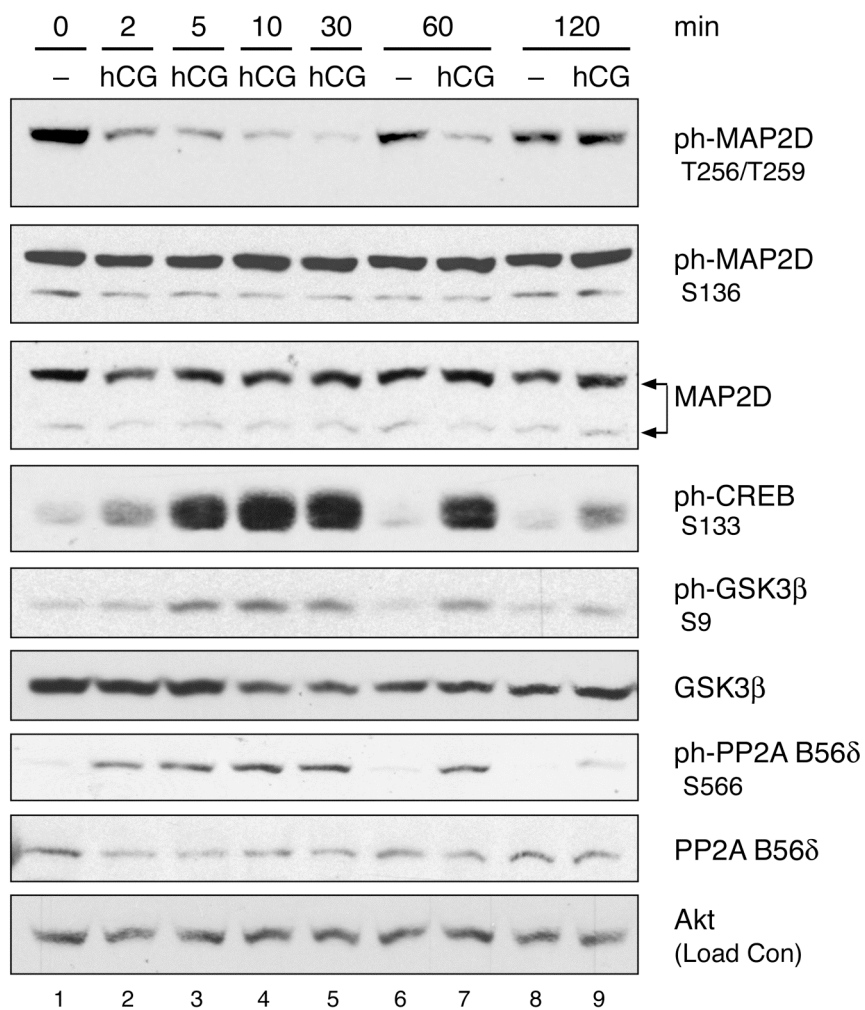
To verify that the decrease in MAP2D Thr256/Thr259 phosphorylation is a physiological response to hormone *in vivo*, PMSG-primed rats were treated with 50 IU hCG by intraperitoneal injection for various times before preparation of whole ovarian extracts. Results show that phosphorylation of MAP2D at Thr256/Thr259 is readily detected in ovarian extracts from saline-injected rats (Fig. 5B, lane 1) and decreased to approximately 20% of vehicle control by 2 h post-hCG injection (compare lanes 1 and 3). The *in vivo* timing of MAP2D dephosphorylation corresponded with activation of PKA as demonstrated by increased phosphorylation of CREB at Ser133. These results confirm that a decrease in MAP2D phosphorylation at Thr256/Thr259 occurs *in vivo* as well as in cultured cells in response to activation of LH receptor signaling.

Figure 5 Phosphorylation of MAP2D at Thr256/Thr259 is rapidly decreased upon LH-receptor stimulation

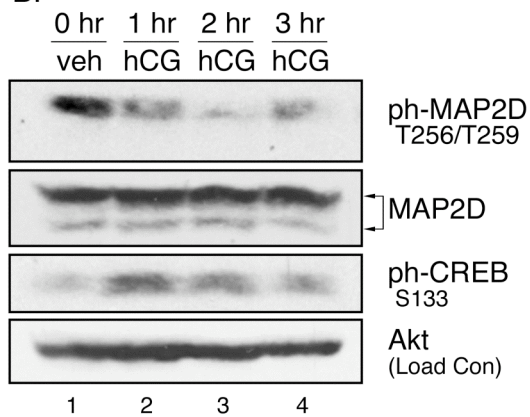
In *Panel A*, PO granulosa cells from PMSG-primed rats were isolated and plated overnight on fibronectin. Cells were then left untreated (–) or treated with 1 IU/ml hCG for the indicated times. Western blot results are representative of three separate experiments. In *Panel B*, PMSG-primed rats were injected with 50 IU hCG or saline (veh) for the indicated times before ovaries were harvested and whole ovary extracts prepared in homogenization buffer, as described in *Materials and Methods*. Clarified homogenates were used for Western blot. Results are representative of two separate experiments.

Figure 5

A.



B.



LH-dependent decrease in MAP2D phosphorylation at Thr256/Thr259 occurs via cAMP and PKA signaling.

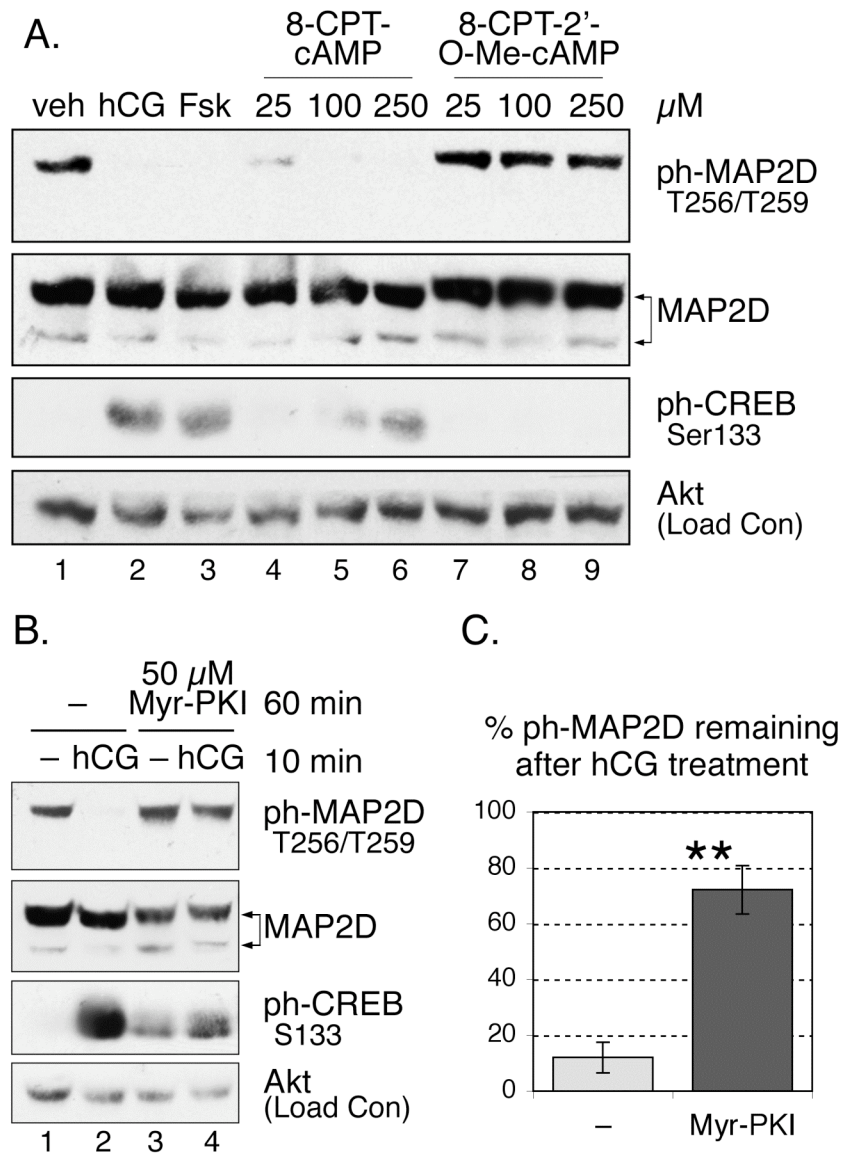
As cAMP is recognized as the predominant second messenger downstream of LH receptor signaling in granulosa cells, I determined the role of cAMP in the LH-dependent decrease in MAP2D phosphorylation at Thr256/Thr259 using the direct pharmacological adenylyl cyclase activator forskolin and the cell permeable cAMP analogue, 8-CPT-cAMP. Treatment of granulosa cells for 10 min with forskolin or 8-CPT-cAMP activated PKA signaling, as evidenced by increased phosphorylation of CREB at Ser133 (Fig. 6A, compare lane 1 versus lanes 3 and 6, respectively). Similarly forskolin (Fig. 6A, lane 3) or 8-CPT-cAMP (lanes 4-6) mimicked the effect of hCG and induced decreases in phosphorylation of MAP2D at Thr256/Thr259 to undetectable levels, compared to untreated cells (lane 1). These results indicate that increased cAMP signaling is sufficient to cause a decrease in MAP2D phosphorylation at Thr256/Thr259.

Increased production of cAMP leads to activation of a number of cAMP-dependent signaling pathways. Most commonly, cAMP activates PKA. In some cells, cAMP has also been shown to activate signaling independently of PKA by binding to the Rap1 guanine nucleotide exchange factor, Epac (Exchange protein activated by cAMP) (31, 149). To investigate whether the LH-dependent decrease in MAP2D phosphorylation at Thr256/Thr259 is PKA dependent, granulosa cells were treated for 10 min with 8-pCPT-2'-O-Me-cAMP, a cell permeable cAMP analogue capable of activating Epac but not PKA (150). As shown in Fig. 6A, no decrease in phosphorylation of MAP2D at Thr256/Thr259 was observed in 8-pCPT-2'-O-Me-cAMP-treated

Figure 6 cAMP/PKA-dependent signaling participates in the LH receptor-mediated decrease in phosphorylation of MAP2D Thr256/Thr259

In *Panel A*, PO granulosa cells were left untreated (–) or treated with 1 IU/ml hCG, 10 μ M forskolin (Fsk), or the indicated concentrations of 8-CPT-cAMP or 8-pCPT-2'-O-Me-cAMP for 10 min, as indicated. In *Panel B*, PO granulosa cells were left untreated (–) or pretreated with 50 μ M myristoylated-PKI (Myr-PKI) for 60 min and then left untreated (–) or treated with 1 IU/ml hCG for 10 min, as indicated. Western blot results are representative of 4 separate experiments. In *Panel C*, Thr256/Thr259 phosphorylated MAP2D levels were quantified by densitometric analysis of Western blot results, as stated under *Materials and Methods*, and normalized to total MAP2D protein levels. Values for hCG-treated samples are expressed as the percentage of the corresponding untreated (–) controls (100%), with no inhibitor pretreatment (–) or 60 min Myr-PKI pretreatment, as indicated. Values are the mean \pm SE from four separate experiments. **, $p < 0.05$.

Figure 6



cells compared with untreated cells (lanes 7-9 versus lane 1). These results suggest that cAMP activation of PKA, not Epac, is necessary for this effect.

To confirm this role for PKA, granulosa cells were pretreated for 1 h with the heat-stable, cell-permeable PKA inhibitor Myr-PKI prior to treatment for 10 min with or without hCG. Myr-PKI pretreatment inhibited PKA activation under hCG treatment, as evidenced by decreased phosphorylation of CREB at Ser133 (Fig. 6B, compare lanes 1 and 2 versus lanes 3 and 4). PKA inhibition by Myr-PKI significantly prevented the LH-dependent decrease in MAP2D phosphorylation at Thr256/Thr259 (Fig. 6C; $12 \pm 5.5\%$ of ph-MAP2D remains after hCG-treatment with no inhibitor present versus $72 \pm 8.6\%$ of ph-MAP2D in the presence of Myr-PKI; $n=4$, $p<0.05$). These results indicate that PKA activation is necessary for the observed decrease in MAP2D Thr256/Thr259 phosphorylation.

LH-dependent decrease in MAP2D phosphorylation at Thr256/Thr259 is blocked by pre-treatment with a PP2A-selective concentration of the Ser/Thr-phosphatase inhibitor okadaic acid.

Both PP2A and PP1 are capable of dephosphorylating synthetic MAP2A/B peptides at Thr1620/Thr1623 (equivalent to Thr256/Thr259 in MAP2D) in *in vitro* reactions (119) and a Ser/Thr phosphatase appears to be involved in phospho-regulation of this site in cultured neurons (132) and rat brain tissue (131). In the following experiments, the involvement of PP2A and/or PP1 in the LH-receptor mediated phospho-regulation of MAP2D at Thr256/Thr259 was evaluated. At appropriate doses, okadaic acid and tautomycin have been reported to be preferential inhibitors of PP2A and PP1, respectively (151-153). Granulosa cells were pretreated

with a PP2A-preferential dose (0.2 μ M) of okadaic acid prior to treatment with or without hCG. Western blot analysis of cell lysates showed that okadaic acid pretreatment reduced the LH-dependent decrease in MAP2D phosphorylation at Thr256/Thr259 (Fig. 7A, compare lanes 1 and 2 versus lanes 3 and 4). This reduction was found to be significant (Fig. 7B; $8.7 \pm 2.8\%$ of ph-MAP2D remains after hCG treatment with no inhibitor present versus $72 \pm 12\%$ of ph-MAP2D in the presence of okadaic acid; $n=4$, $p<0.01$).

Pretreatment of granulosa cells with a PP1-preferential dose (1 μ M) of tautomycin did not block the LH-dependent decrease in MAP2D phosphorylation at Thr256/Thr259 (Fig. 7C). Tautomycin, however, blocked the hCG-stimulated dephosphorylation of MLC2 at Ser19, a known target of PP1 (154). These results suggest that the decrease in phosphorylation of MAP2D Thr256/Thr259 after LH receptor activation is mediated, at least in part, by PP2A activity but not by PP1 activity.

Co-immunoprecipitation and affinity-pull-down analyses from PO granulosa cells reveal interactions between MAP2D and PP2A catalytic subunits.

Based on my indirect evidence for the involvement of PP2A in MAP2D phosphoregulation, I determined if there is an interaction between MAP2D and PP2A in ovarian granulosa cells. Affinity-pull-down analysis was performed from clarified granulosa cell lysates using microcystin-agarose, an affinity reagent that binds both PP2A and PP1. As expected, microcystin-agarose precipitated both PP2A and PP1 (Fig. 8, lane 8). The microcystin-agarose pulldown assay also isolated MAP2D from granulosa cell lysates, suggesting that MAP2D forms interactions with one or both of these Ser/Thr phosphatases. Immunoprecipitation analyses were

Figure 7 PP2A-preferential treatment with the Ser/Thr phosphatase inhibitor okadaic acid blocks the hCG-induced decrease in MAP2D phosphorylation at Thr256/Thr259

In *Panel A*, PO granulosa cells were left untreated (–) or pretreated with 0.2 μ M okadaic acid (OA) for 60 min and then left untreated (–) or treated with 1 IU/ml hCG for 10 min, as indicated. Western blot results are representative of four separate experiments. In *Panel B*, Thr256/Thr259 phosphorylated MAP2D levels were quantified by densitometric analysis of Western blot results, as stated under *Materials and Methods*, and normalized to total MAP2D protein levels. Values are for hCG-treated samples expressed as the percentage of the corresponding untreated (–) controls (100%), with no inhibitor pretreatment (–) or 60 min okadaic acid pretreatment, as indicated. Values are the mean \pm SE from four separate experiments. ***, $p < 0.01$. In *Panel C*, PO granulosa cells were left untreated (–) or pretreated with 1 μ M tautomycin (TAU) for 5.5 h and then left untreated (–) or treated with 1 IU/ml hCG for 10 min, as indicated.

Figure 8 Co-immunoprecipitation and affinity-pull-down analyses reveal interactions between MAP2D and PP2A, but not PP1 catalytic subunits

Detergent soluble PO granulosa cell extracts were subjected to co-immunoprecipitation (IP) and affinity-pull-down analyses as described in *Materials and Methods*. IPs were performed with MAP2 (HM-2) monoclonal antibody (Sigma), PP2A-c (1D6) monoclonal antibody (Upstate Biotechnology/Millipore), or control (Con) antibody against an irrelevant epitope (HA-Tag monoclonal antibody, Cell Signaling Technology). Pulldown analysis was performed with microcystin-agarose (MC, Upstate Biotechnology/Millipore), a PP2A/PP1 affinity-pull-down reagent. Input, unbound, and bound immunoprecipitated proteins were probed by Western blot with the indicated rabbit polyclonal antibodies. Input reflects 5% of total lysate, unbound reflects 13.3% of total unbound fraction, and bound reflects 100% of immunoprecipitated/pulled-down protein. Immunoprecipitation results are representative of three separate experiments.

also performed using monoclonal antibodies specifically recognizing PP2A catalytic subunit, MAP2 protein, or an irrelevant epitope (anti-HA-Tag mAb). Immunoprecipitation of PP2A catalytic subunit co-immunoprecipitated MAP2D (Fig. 8, lane 7). Conversely, MAP2D immunoprecipitation co-immunoprecipitated PP2A catalytic subunit but did not co-immunoprecipitate PP1 catalytic subunit (lane 6). Taken together, these results suggest that MAP2D forms a complex in granulosa cells with PP2A but not with PP1.

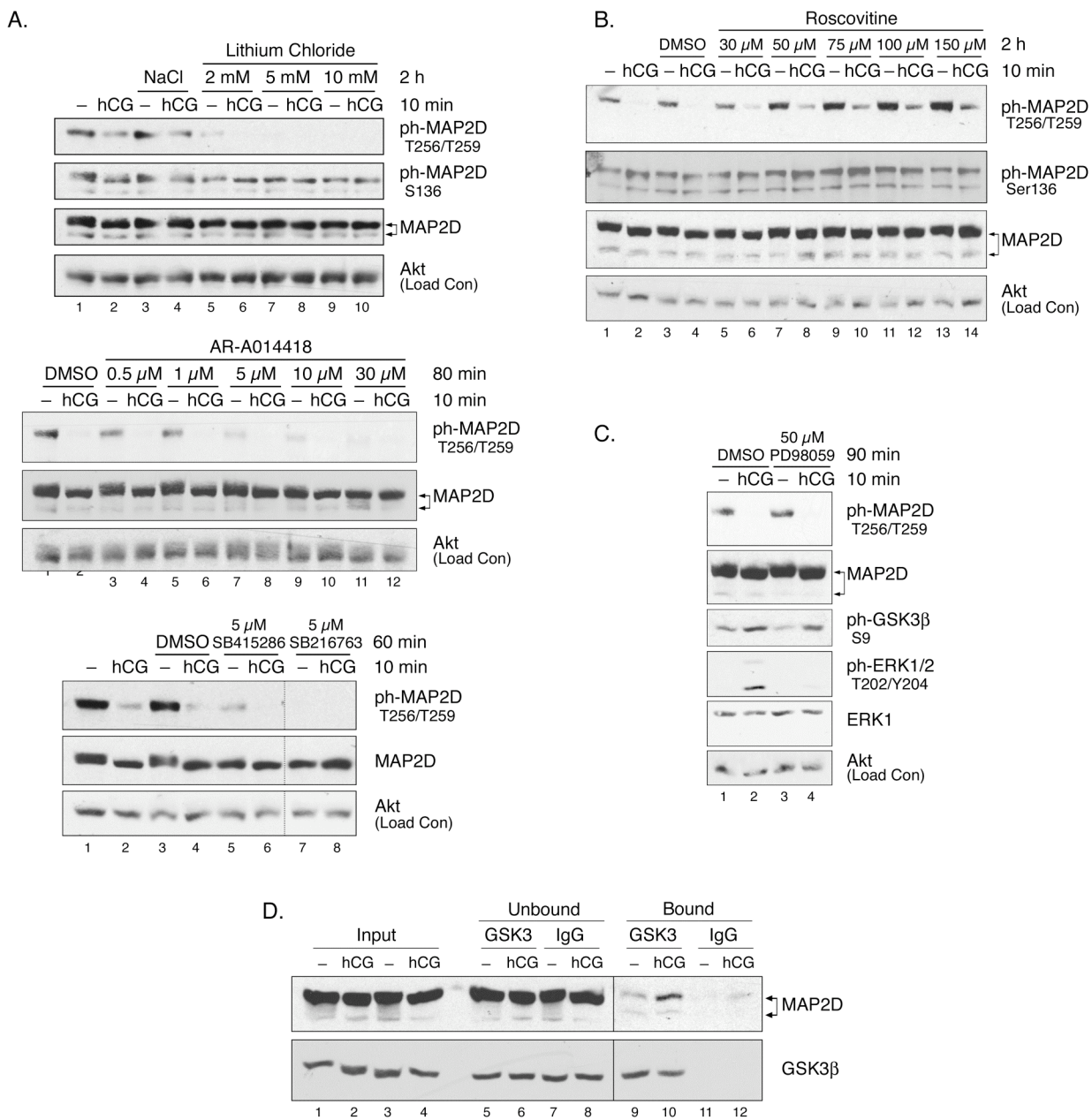
LH receptor signaling modulates phosphorylation of MAP2D at Thr256/Thr259 through regulation of both GSK3 β and PP2A.

LH receptor-regulated dephosphorylation of MAP2D at Thr256/Thr259 could be mediated not only by enhanced PP2A activity towards MAP2D but also by reduced activity of the kinase that phosphorylates MAP2D Thr256/Thr259. We initially investigated the kinase(s) responsible for basal phosphorylation of MAP2D Thr256/Thr259 in granulosa cells. *In vitro* phosphorylation of high-molecular weight MAP2 by proline-directed kinases, such as GSK3, cyclin-dependent kinases (CDKs), and mitogen-activated protein kinase (MAPK) superfamily members, has been demonstrated (119). PO granulosa cells were pretreated with a panel of GSK3 inhibitors, the CDK inhibitor roscovitine, or the MAPK extracellular signal-regulated kinase (ERK) pathway inhibitor PD98059 at a variety of doses prior to 10 min treatment with or without hCG. Western blot analysis of cell lysates indicated that inhibition of GSK3 activity by pretreatment with lithium chloride reduced basal state phosphorylation of MAP2D Thr256/Thr259 in the absence of hCG to undetectable levels (Fig. 9A, top panel, compare odd-numbered lanes). Basal state phosphorylation of Ser136, a recognized phosphorylation site on MAP2A/2B/2C for proline-

Figure 9 GSK3 inhibitors block basal state phosphorylation of MAP2D at**Thr256/Thr259**

In *Panel A*, PO granulosa cells were pretreated with the indicated concentrations of the GSK3 inhibitors lithium chloride, AR-A014418, SB415286, SB216763, or control (50 mM NaCl or dimethylsulfoxide) for the indicated times and then left untreated (–) or treated with 1 IU/ml hCG for 10 min. Results of lithium chloride and AR-A014418 pretreatments are representative of at least three separate experiments. In *Panel B*, PO granulosa cells were pretreated with the indicated concentrations of the CDK inhibitor roscovitine or vehicle control (dimethylsulfoxide) for 2 h and then left untreated (–) or treated with 1 IU/ml hCG for 10 min. Results are representative of two separate experiments. In *Panel C*, PO granulosa cells were pretreated with 50 μ M of the MEK inhibitor PD98059 or vehicle control (dimethylsulfoxide) for 90 min and then left untreated (–) or treated with 1 IU/ml hCG for 10 min. Western blot results are representative of three separate experiments. In *Panel D*, detergent soluble PO granulosa cell extracts from cells left untreated or treated with 1 IU/ml hCG for 10 min were subjected to co-immunoprecipitation, as described under *Materials and Methods*, with agarose-conjugated GSK3 α/β monoclonal antibody (Santa Cruz) or control agarose-conjugated mouse IgG (Santa Cruz). Input, unbound, and bound/immunoprecipitated proteins were probed by Western blot with the indicated antibodies. To avoid overexposure, input and unbound images shown for the MAP2 Western are from shorter exposures than bound/immunoprecipitated images. IP results are representative of three separate experiments. Input and unbound fractions reflect 6.25% of total lysate and bound reflects 100% of total lysate. DMSO, dimethylsulfoxide.

Figure 9



directed kinases (155), was not affected by the 2-h pretreatment with lithium chloride (Fig. 9A, *top panel, odd-numbered lanes*). Similar results were observed using the GSK3 inhibitors AR-A014418, SB415286, and SB216763 (Fig. 9A, *middle and bottom panels*). Inhibition of roscovitine-sensitive CDK activity by roscovitine pretreatment not only failed to reduce MAP2D phosphorylation but also appeared to enhance phosphorylation at this site (Fig. 9B, *compare odd numbered lanes*). Basal state phosphorylation of MAP2D at Ser136 was also not reduced by roscovitine pretreatment. Inhibition of ERK pathway activity by the MAPK kinase (MEK) inhibitor PD98059 reduced ERK activation (Fig. 9C, *compare lanes 2 and 4*) but failed to reduce MAP2D Thr256/Thr259 phosphorylation (*compare lanes 1 and 3*). Taken together, these results suggest that GSK3 is necessary for basal phosphorylation of MAP2D at Thr256/Thr259. Given that GSK3 inhibition reduced MAP2D phosphorylation at Thr256/Thr259 to undetectable levels, GSK3 appears to be responsible for most of the phosphorylation at these sites in granulosa cells. Consistent with these results, MAP2D co-immunoprecipitated with GSK3 from granulosa cells left untreated or treated with hCG (Fig. 9D, *lanes 9 and 10*) but was not pulled down with control IgG (*lanes 11 and 12*). The apparent increased association of GSK3 and MAP2D in hCG-treated cells was unexpected and is not understood.

GSK3 β is recognized to be basally active in most cells and to be inhibited by phosphorylation at Ser9 by a number of kinases, including Akt, p90^{RSK}, and PKA (reviewed in (156)). As the dephosphorylation of Thr256/Thr259 is both rapid and PKA-dependent, I determined whether LH receptor activation lead to phosphorylation of GSK3 β at Ser9 in granulosa cells. GSK3 β phosphorylation at Ser9 was detected at low levels in untreated cells (Fig. 5A, *lanes 1, 6, and 8*). Treatment with hCG (*lanes 2-5 and 7*) caused a rapid increase in

Ser9 phosphorylation, comparable in timing to the dephosphorylation of MAP2D Thr256/Thr259. The timing of this increased phosphorylation also corresponded with activation of PKA, as demonstrated by increased phosphorylation of CREB at Ser133. Indeed, it was found that cAMP/PKA signaling regulates GSK3 β phosphorylation, as treatment with forskolin or 8-CPT-cAMP was sufficient to induce Ser9 phosphorylation of GSK3 β (Fig. 10A) and pretreatment with the PKA inhibitor Myr-PKI blocked the hCG-induced increase in Ser9 phosphorylation (Fig. 10A, compare lanes 4 and 6). I next determined whether the effect of PKA on phosphorylation of GSK3 β Ser9 is direct or is mediated by signaling through Akt or p90^{RSK}. LH receptor activation by hCG induced Akt phosphorylation at Ser473 (Fig. 10B, compare lanes 1 and 2), and this activating phosphorylation was blocked by pretreatment with the PI 3-kinase inhibitor LY294002 (lanes 3 and 4). However, PI 3-kinase inhibition did not block phosphorylation of GSK3 β at Ser9. Ser9 phosphorylation of GSK3 β was also unaffected by the MEK inhibitor PD98059 (Fig. 9C). These results suggest that GSK3 β is rapidly inhibited upon activation of LH receptor signaling by PKA-catalyzed phosphorylation of Ser9 independent of PI 3-kinase/Akt signaling or MEK/ERK/p90^{RSK} signaling.

I next investigated the mechanism by which PP2A activity could be regulated. The PP2A holoenzyme consists of a catalytic C subunit, a scaffolding A subunit, and one of a large variety of possible regulatory B subunits (157). Although PP2A activity can be regulated by a variety of mechanisms targeting any one of these subunits (reviewed in (157)), the rapid timing and PKA-dependence of MAP2D dephosphorylation suggests that phospho-regulation is a likely mechanism for these events. Though regulation of PP2A activity by cAMP and/or PKA has been reported under a variety of conditions (158-161), the mechanism of this regulation was until

Figure 10 Modulation of MAP2D at Thr256/Thr259 through LH-mediated regulation of both GSK3 β and PP2A

In *Panel A*, PO granulosa cells were left untreated or pretreated with 50 μ M myristoylated-PKI (Myr-PKI) for 60 min and then left untreated (–) or treated with 10 μ M forskolin (Fsk), 500 μ M of 8-CPT-cAMP, or 1 IU/ml hCG for 10 min, as indicated. Western blot results are

representative of two separate experiments. Lines between lanes indicate cropped images. In

Panel B, PO granulosa cells were pretreated with 12.5 μ M of the PI 3-kinase inhibitor LY294002 in dimethylsulfoxide or an equivalent concentration of dimethylsulfoxide for 60 min and then left untreated (–) or treated with 1 IU/ml hCG for 10 min, as indicated. Western blot results are

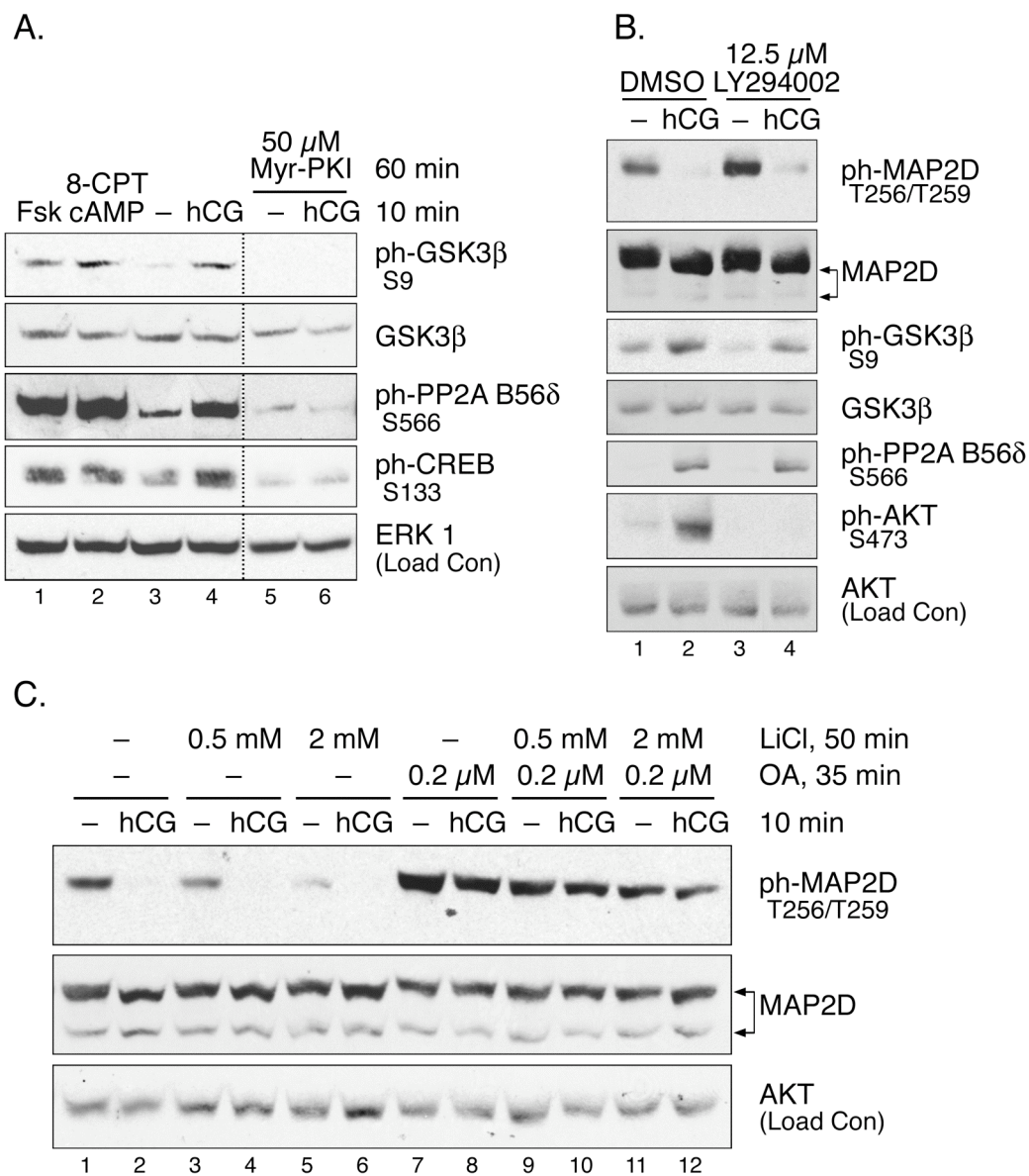
representative of three separate experiments. In *Panel C*, PO granulosa cells were first left untreated (–) or pretreated with the indicated concentrations of the GSK3 inhibitor lithium

chloride (LiCl) for 50 min; cells were then left untreated (–) or pretreated with the PP2A

inhibitor okadaic acid (OA) for an additional 35 min; cells were then left untreated (–) or treated with 1 IU/ml hCG for 10 min. Similar results were obtained using okadaic acid combined with

the GSK3 inhibitor AR-A014418 (not shown). DMSO, dimethylsulfoxide.

Figure 10



recently unknown. However, it has recently been shown that PKA phosphorylates the B56 δ regulatory subunit of PP2A *in vitro* and in HEK293 cells and, in particular, PKA phosphorylation of Ser566 of the B56 δ subunit was found to be necessary and sufficient for activation of PP2 (162). To observe possible LH receptor-dependent phospho-regulation of the B56 δ subunit, cultured granulosa cells were treated with or without hCG for various times and Western blots of total cell lysates were probed with a phospho-specific antibody against Ser566 of the B56 δ subunit of PP2A. Phosphorylation at Ser566 was detected at low levels in untreated cells (Fig. 5A, lanes 1, 6, and 8). hCG caused a rapid increase in phosphorylation of B56 δ Ser566 (lanes 2-5 and 7), comparable in timing to the dephosphorylation of MAP2D Thr256/Thr259 and with the activation of PKA. Indeed, treatment with forskolin or 8-CPT-cAMP was sufficient to induce Ser566 phosphorylation of the B56 δ subunit (Fig. 10A) and inhibition of PKA by Myr-PKI blocked Ser566 phosphorylation by LH receptor signaling (compare lanes 4 and 6). Pretreatment with the PI 3-kinase inhibitor LY294002 had no effect on B56 δ subunit phosphorylation at Ser566 (Fig. 10B, compare lanes 2 and 4). These results demonstrate that the B56 δ subunit of PP2A is rapidly phosphorylated in a PKA-dependent manner upon activation of LH receptor signaling, suggesting a mechanism for hormonal regulation of PP2A activity.

It could be argued that the role of PP2A in MAP2D phospho-regulation as demonstrated by inhibition with okadaic acid is a static one and that active regulation of Thr256/Thr259 occurs exclusively through inhibitory phosphorylation of GSK3 β . To determine whether PP2A activity against Thr256/Thr259 is actively regulated by LH receptor signaling, cultured granulosa cells were pretreated with a combination of inhibitors: first cells were pretreated without or with the

GSK3 β inhibitor lithium chloride for 50 min; next cells were further pretreated without or with the PP2A inhibitor okadaic acid for an additional 35 min; and finally, cells were treated for 10 min without or with hCG. In agreement with results shown in Figure 9A, lithium chloride pretreatment alone inhibited basal phosphorylation of MAP2D Thr256/Thr259 (Fig. 10C, lanes 1,3, and 5), but even with substantial inhibition of basal phosphorylation (approximately 18% of control; compare lanes 1 and 5), hCG treatment resulted in a decrease in the remaining phosphorylation at this site (compare lanes 5 and 6). However, even when combined with the same inhibitory concentrations of lithium chloride, PP2A inhibition by okadaic acid pretreatment was capable of potently inhibiting this hCG-induced decrease in phosphorylation (compare lanes 11 and 12). Similar results were observed using okadaic acid combined with the GSK3 inhibitor AR-A014418 (data not shown). Taken together, these results demonstrate that active regulation of both the kinase and the phosphatase is necessary for phospho-regulation of Thr256/Thr259.

Discussion

Activation of the LH receptor in PO granulosa cells triggers gene expression leading to ovulation, oocyte maturation, and differentiation of granulosa to luteal cells to radically remodel the structure and function of ovarian follicles. While many downstream transcriptional targets of LH have been identified (19), little is known about how LH signals to effect this dramatic transformation in granulosa cell structure and function. PO granulosa cells selectively express MAP2D, a lower molecular weight splice variant of the neuronal protein MAP2 that binds microtubules and microfilaments and regulates cytoskeletal dynamics in neurons (98-100, 102, 106). I have identified a novel LH-receptor signaling mechanism in granulosa cells by which LH orchestrates a coordinated increase of phosphatase activity and decrease of kinase activity

against MAP2D to promote selective dephosphorylation of Thr256/Thr259. Specifically, the LH analog hCG stimulates PKA-mediated phosphorylation of GSK3 β on Ser9 to inhibit GSK3 β activity and of the B56 δ regulatory subunit of PP2A on Ser566 to increase phosphatase activity towards Thr256/Thr259 on MAP2D.

MAP2 proteins are highly phosphorylated, particularly on Ser and Thr residues in the C-terminal proline-rich and microtubule-binding domains. MAP2 may be phosphorylated *in vitro* or in neuronal cells at numerous sites by a wide variety of kinases. Phosphorylation by one or more kinases is generally believed to alter the association between MAP2 and various cytoskeletal elements (reviewed in (86)).

MAP2D in granulosa cells also appears to be highly phosphorylated (see Fig. 4 and (14)). I focused on the phosphorylation state of two residues, Thr256/Thr259, located in the proline-rich domain adjacent to the first MTBD. These residues are 100% conserved in mouse, rat and human species and are also highly conserved in the corresponding domain of the related MAP, tau (133) and appear to be phosphorylated by GSK3 β resulting in inhibition of microtubule interactions (101).

Phosphorylation of MAP2D on Thr256/Thr259 in granulosa cells is coincident with FSH-induced increases in MAP2D expression (14). My results using a collection of cell-permeable inhibitors for GSK3, CDKs, and the ERK pathway indicate that GSK3 is required for most, if not all, of this basal phosphorylation of MAP2D at Thr256/Thr259 in granulosa cells. Moreover, GSK3 β is present in a protein complex with MAP2D, based on its co-immunoprecipitation with MAP2D in granulosa cells. GSK3 β exists in an active state in cells (163) consistent with the seemingly coincident expression and phosphorylation of MAP2D at these residues in granulosa

cells (14). Also, GSK3 has been shown to phosphorylate MAP2 at Thr256/Thr259 and tau at Ser199/Ser202 in neuronal systems (132, 164). While GSK3 phosphorylation of substrate proteins often occurs at residues that have been “primed” by prior phosphorylation, I found no indication that priming by CDK5 or ERK was necessary for phosphorylation of MAP2D at Thr256/Thr259, as inhibition of these kinases did not have an inhibitory effect on basal phosphorylation of this site. However, I cannot rule out the possibility that priming of nearby sites by another kinase may contribute to GSK3 β -dependent phosphorylation at MAP2D Thr256/Thr259 (128, 129, 165).

The LH receptor agonist hCG promotes a rapid yet transient dephosphorylation of MAP2D at Thr256/Thr259 in granulosa cells *in vitro* and *in vivo*. My results suggest that rather than promoting a global dephosphorylation of MAP2D, LH receptor signaling appears to be targeted specifically to Thr256/Thr259. While MAP2D in granulosa cells is also phosphorylated at Ser136, a site located near the N-terminal RII binding domain (155), phosphorylation at this site is not regulated by LH receptor signaling. MAP2D dephosphorylated at Thr256/Thr259 continues to migrate with the slower migrating 80 kDa band and not with the dephospho-MAP2D at 70 kDa (see Figs. 4 and 5). Finally, total levels of MAP2D phosphorylation, measured by $^{32}\text{P}_i$ incorporation, are not decreased by hCG treatment (14).

While the LH receptor couples to Gs, Gi, and Gq/11 in granulosa cells (21), the majority of LH receptor signaling appears to be mediated by cAMP/PKA (reviewed in (10, 13)). Indeed, LH is recognized to activate PKA (28) and to signal via PKA to activate ERK (34) and downstream ERK-regulated target genes such as the low density lipoprotein receptor, early growth response 1, and steroidogenic acute regulatory protein, thus contributing to enhanced

steroidogenesis and luteinization of granulosa cells (reviewed in (13)). LH also signals via cAMP to promote expression of EGF-like growth factors to activate the EGF receptor and ERK, among other possible targets, leading to expression of cyclooxygenase-2 and resulting cumulus expansion and oocyte maturation (55, 166) by a pathway dependent on PKA activation (33). However, not all of the LH receptor signaling is PKA dependent. LH signals via cAMP to activate p38 MAPK by an apparently PKA-independent pathway (34).

My results show that dephosphorylation of MAP2D Thr256/Thr259 in response to LH receptor signaling is also regulated by PKA, based on inhibition by Myr-PKI and ineffectiveness of the cAMP analog that serves as an agonist for the Rap1 guanine nucleotide exchange factor Epac but not for PKA (150). I reasoned that PKA-dependent dephosphorylation of MAP2D at Thr256/Thr259 could be mediated by either reduced activity of GSK3 β , by activation of a phosphatase, or by a combination of both. My data show that, indeed, both kinase and phosphatase activities are modulated by LH receptor signaling, resulting in rapid and potent dephosphorylation of MAP2D at Thr256/Thr259. First I showed that phosphorylation of GSK3 β at Ser9 increased rapidly upon activation of LH receptor signaling. LH receptor-stimulated phosphorylation of Ser9 on GSK3 β was not inhibited by the PI 3-kinase inhibitor LY294002 or by the MEK inhibitor PD98059 but was inhibited by Myr-PKI, suggesting that Ser9 on GSK3 β is a direct PKA target. This result is consistent with previous reports that PKA directly phosphorylates GSK3 β on Ser9 (reviewed in (167)). Second, my results support a role for PP2A in actively dephosphorylating MAP2D at Thr256/Thr259. This conclusion is based in part on the ability of preferential inhibition of PP2A by okadaic acid, at nM concentrations, to prevent dephosphorylation of MAP2D at Thr256/Thr259 compared to the ineffectiveness of preferential

PP1 inhibition by tautomycin (151-153, 168). Using a combination of PP2A and GSK3 β inhibitors, I demonstrate that, even in the absence of most GSK3 activity, PP2A is necessary for the hCG-induced decrease in phosphorylation. This result supports the hypothesis that both a decrease in kinase activity as well as an increase in phosphatase activity against MAP2D is responsible for regulation of phosphorylated Thr256/Thr259. Furthermore, immunoprecipitation and microcystin-agarose pulldown analyses demonstrated interactions between MAP2D and PP2A catalytic subunit in granulosa cells. My results thus suggest that PP2A binds to MAP2D and, upon stimulation by LH receptor signaling through PKA, actively dephosphorylates Thr256/Thr259.

The PP2A holoenzyme consists of a catalytic C subunit, a scaffolding A subunit, and one of a large variety of possible regulatory B subunits (reviewed in (157)). LH-dependent regulation of PP2A activity could occur by regulation of subunit expression, acute regulation of intrinsic C subunit activity by changes in Leu309 methylation (169, 170) and/or Tyr307 phosphorylation (171, 172), or regulation of the substrate specificity of C subunit activity through modification of regulatory B subunits (157). In granulosa cells, the rapid timing and PKA-dependence of PP2A activation suggests phospho-regulation is a likely mechanism. Activation of PP2A activity by cAMP and/or PKA has been reported previously under a variety of conditions (158-160). Earlier studies indicated that the B56 δ regulatory subunit (originally called B'' δ) can be phosphorylated *in vitro* by PKA leading to changes in substrate specificity of the PP2A holoenzyme (173). Expanding upon this report, it has recently been shown that PKA phosphorylates Ser566 on B56 δ *in vitro* and that phosphorylation of this residue by PKA is necessary and sufficient to activate PP2A in transfected HEK293 cells as well as in striatal neurons (162). My results here

show that the B56 δ regulatory subunit of PP2A in granulosa cells is rapidly phosphorylated at Ser566 by LH receptor signaling, and that this phosphorylation is inhibited by Myr-PKI. Taken together, these results suggest that the B56 δ regulatory subunit of PP2A is a direct PKA target in granulosa cells that accelerates the dephosphorylation of Thr256/Thr259 on MAP2D.

MAP2D was originally identified in granulosa cells based on its ability to bind to PKA RII subunits (140). I hypothesize, based on my co-immunoprecipitation results, that a multiprotein complex exists in granulosa cells, in which a pool of MAP2D phosphorylated on Thr256/Thr259 binds not only PKA but also the PP2A holoenzyme and GSK3 β (Fig. 19). In this signaling complex, both B56 δ PP2A regulatory subunit and GSK3 β appear to be direct PKA targets that selectively regulate the phosphorylation of MAP2D at Thr256/Thr259. I hypothesize that the convergence of PKA, GSK3 β , and PP2A with the pool of MAP2D phosphorylated at Thr256/Thr259 facilitates the ability of the LH receptor to signal to MAP2D to promote its dephosphorylation at these specific sites.

In summary, MAP2D in granulosa cells is basally phosphorylated (in the absence of LH-receptor signaling) on Thr256/Thr259 primarily by GSK3 β . LH receptor signaling in PO granulosa cells promotes rapid dephosphorylation of MAP2D Thr256/Thr259 via PKA-dependent phosphorylation of Ser566 on the B56 δ regulatory subunit of PP2A and PKA-dependent phosphorylation of Ser9 on GSK3 β . These phosphorylation events are recognized to promote activation of PP2A (162) and inactivation of GSK3 β (163), respectively. Moreover, these proteins appear to be present in a complex consisting of the AKAP MAP2D, PKA, GSK3 β , and PP2A. This is the first report of the regulation of the phosphorylation status of MAP2D Thr256/Thr259, sites that are conserved in MAP2C and the larger MAP2A/MAP2B isoforms, by

a PKA signaling pathway that both stimulates protein phosphatase activity and inhibits protein kinase activity. This mechanism might also contribute to regulation of these MAP2 phosphorylation sites, as well as corresponding sites in tau, in neuronal cells, where these MAPs are especially abundant and are believed to contribute to neurite outgrowth as well as cytoskeletal dynamics (87).

CHAPTER III: MAP2D PHOSPHORYLATION REGULATES BINDING TO VIMENTIN INTERMEDIATE FILAMENTS

Summary

A mid-cycle surge of LH activates receptors on granulosa cells of PO ovarian follicles to rapidly induce progesterone steroidogenesis, ovulation, and follicle luteinization. These acute changes in follicle function are likely dependent on dynamic changes in the granulosa cell cytoskeleton. We previously showed that MAP2D is expressed in primary rat PO granulosa cells and that LH receptor-mediated dephosphorylation of MAP2D at Thr256/Thr259 occurs through interaction with a signaling complex involving GSK3 β , PP2A B56 δ , and PKA. MAP2 family proteins have been extensively characterized in neuronal systems with a particular focus on their binding to microtubules, actin microfilaments, and intermediate filaments. Here I describe direct binding and colocalization of granulosa cell MAP2D and vimentin intermediate filaments. This binding is reduced by phosphorylation of MAP2D by GSK3 β . I present data supporting the hypothesis that LH receptor-mediated MAP2D dephosphorylation coordinates redistribution of MAP2D and associated PKA-signaling complex to vimentin filaments, allowing for PKA-dependent vimentin phosphorylation and reorganization of the vimentin cytoskeleton. I propose that such vimentin remodeling may facilitate the biosynthesis of progesterone that is obligatory for ovulation.

Introduction

The mid-cycle surge of pituitary LH stimulates granulosa cells of PO ovarian follicles to induce events essential for progesterone steroidogenesis, luteinization and ovulation. This response is initiated through binding of LH to surface LH receptors resulting in activation of adenylyl cyclase (135) and signaling primarily through the cAMP/PKA signaling pathway (28). We previously showed that the AKAP MAP2D is expressed in PO granulosa cells and binds the regulatory R subunits of PKA, suggesting that MAP2D may be important for particular PKA-dependent granulosa cell functions (14, 140).

MAP2 family members were first isolated from brain tissues and have typically been studied in neuronal systems (reviewed in (86, 95)). While, as an AKAP, they contain an N-terminal R-subunit binding domain that allows for binding to PKA (115, 123), MAP2 isoforms also bind to a number of cytoskeletal elements in neurons. Most renowned is their ability to bind microtubules, via three or four C-terminal MTBDs on MAP2 (96), resulting in increased microtubule assembly (97), stability and rigidity (98-100), and microtubule bundling in heterologous systems (101, 102), which appears to be required for neurite outgrowth (174, 175). MAP2 similarly may bind to and bundle actin microfilaments (105, 106), also via the MTBDs, leading to the hypothesis that MAP2 may coordinate the reorganization of microfilaments and microtubules during neurite outgrowth (87). Lastly, MAP2 has been reported to bind to at least two classes of intermediate filaments, vimentin and neurofilaments (83, 108-112), apparently using a binding site different than that used for microtubules (113), and it has been shown that MAP2 may form cross-bridges between microtubules and intermediate filaments (114). Phosphorylation of MAP2 appears to regulate binding to each of these cellular components

(101, 105, 106, 108), indicating the importance of MAP2 phospho-regulation in cytoskeletal dynamics.

The most abundant intermediate filament protein in PO granulosa cells is vimentin, a class III intermediate filament protein (67, 69, 70). While some types of keratin may also be prevalent in less mature human granulosa cells, these are decreased during granulosa cells maturation to the PO phenotype and are not detected at all in rat, porcine, and bovine granulosa cells (69, 70), emphasizing the importance of vimentin as these cells mature. Vimentin appears to be a good *in vitro* and *in vivo* substrate for PKA (71), and phosphorylation by this kinase has been reported to lead to reorganization of vimentin filaments (72-74). In particular, phosphorylation of vimentin at Ser38 and Ser72 in the N-terminal head domain has been linked to changes in the vimentin assembly/disassembly equilibrium (71). Though PKA signaling is the predominant pathway in PO granulosa cells, the potential for PKA-dependent phosphorylation of vimentin by LH receptor signaling has not been evaluated.

While a well recognized role of intermediate filaments is to provide cells with strength and flexibility against mechanical stress (reviewed in (176)), vimentin filaments are also involved in a large number of cellular functions, including cell adhesion, migration and motility, and signal transduction (reviewed in (177, 178)). Additionally, vimentin filaments may play a unique role in steroidogenic cells (reviewed in (75)). Evidence of such a role in adrenal cells includes the finding that vimentin filaments bind both cholesterol ester droplets (179, 180), the primary substrate of steroidogenesis, as well as mitochondria (181), the site of steroid hormone production. Similarly, binding of vimentin to these structures has been described in LH-responsive rat Leydig cells (182), which share some similarities with granulosa cells. Thus, it has

been proposed that, in steroidogenic cells, the tethering of these components to vimentin limits the access of cholesterol to the mitochondria until, with the appropriate stimulus, vimentin networks are rearranged, allowing these structures to come together and for cholesterol to enter the steroidogenic pathway (75). In agreement with this, chemical disruption of vimentin filaments has been reported to increase steroidogenesis in adrenal cells (77). The direct effect of vimentin disruption on progesterone synthesis in granulosa cells has not been evaluated.

Based on the physiological dephosphorylation of granulosa cell MAP2D at Thr256/Thr259 in response to the mid-cycle surge of LH, I sought to assess the importance of this phospho-regulation to granulosa cell functions. My results show that MAP2D phosphorylated at Thr256/Thr259 is predominantly soluble and, upon dephosphorylation at these sites, redistributes into a vimentin-enriched cell fraction. Confocal immunofluorescence imaging and solid phase overlay assays confirm that MAP2D binds both microtubules and vimentin filaments and that this interaction is inhibited by phosphorylation by GSK3 β . I also show that redistribution of MAP2D to the vimentin-enriched fraction occurs coincident with hCG-stimulated phosphorylation of vimentin and reorganization of vimentin intermediate filaments in granulosa cells. Finally, I present results consistent with the hypothesis that LH-stimulated dephosphorylation of MAP2D leads to vimentin remodeling and facilitates the biosynthesis of progesterone that is obligatory for ovulation.

Results

MAP2D dephosphorylated at Thr256/Thr259 by LH receptor signaling redistributes into a vimentin-enriched cell fraction.

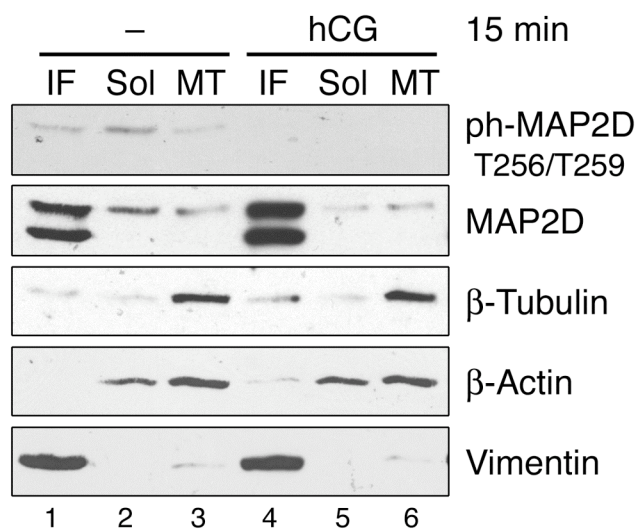
MAP2 family proteins are recognized to interact with a variety of cytoskeletal components, including microtubules (reviewed in (86)), microfilaments (105, 106, 183), and intermediate filaments (83, 108-114), and these cytoskeletal interactions are often blunted by MAP2 phosphorylation (86, 105, 108). To investigate the potential interaction between MAP2D and these components of the granulosa cell cytoskeleton, and to evaluate the possibility that phospho-regulation of MAP2D at Thr256/Thr259 modulates such an interaction, PO granulosa cells were treated with or without hCG for 15 min followed by cytoskeletal fractionation to distinguish proteins which were contained in intermediate filament, microtubule, and soluble fractions. The intermediate filament-enriched fraction contained nearly all detectable vimentin (Fig. 11A, lane 1), the predominant intermediate filament protein in PO granulosa cells (67); the majority of β -tubulin was detected in the microtubule-enriched fraction (lane 3); β -actin was detected in both the soluble and microtubule-enriched fractions (lanes 2 and 3). Unexpectedly, while some MAP2D protein was detected in both microtubule-enriched and soluble fractions, the majority (~75%) of MAP2D was detected in the vimentin-enriched fraction of vehicle-treated granulosa cells (lane 1). As reported in Chapter II, granulosa cell MAP2D migrates on SDS-PAGE as a faster band ~70 kDa and a slower band ~ 80 kDa, reflecting various states of phosphorylation. MAP2D phosphorylated on Thr256/Thr259 migrates at 80 kDa with the slower migrating band. However, as shown in Chapter II, migration position does not appear to be largely affected by this site as LH-receptor stimulated dephosphorylation of Thr256/Thr259 does not result in increased migration at 70 kDa. The majority (~60%) of the MAP2D phosphorylated at Thr256/Thr259 was localized to the soluble fraction in vehicle-treated cells (lane 2). Treatment of granulosa cells with hCG resulted in no detectable MAP2D phosphorylated at

Figure 11 Ovarian granulosa cell MAP2D co-isolates with vimentin intermediate filaments

In *Panel A*, PO granulosa cells were left untreated (–) or treated with 1 IU/ml hCG for 15 min before lysis at 37°C by sonication in Cytoskeletal Extraction Buffer. Intermediate-filament enriched fraction (IF) was pelleted by low speed centrifugation (13,000 x g; 35°C). Low speed supernatants were centrifuged at high speed (100K x g; 35°C) to separate intact microtubule networks and associated proteins (MT) from soluble protein (Sol). For further details, see *Materials and Methods*. Soluble fraction contains $58 \pm 10\%$ of MAP2D phosphorylated at Thr256/Thr259. Results are representative of five separate experiments. In *Panels B-D*, total MAP2D levels in the IF, Sol, and MT fractions of untreated (–) and 1 IU/ml hCG treated granulosa cells were quantified by densitometric analysis of Western blot results, as stated under *Materials and Methods*. Values are for MAP2D levels as a percentage of total MAP2D for each treatment condition, as indicated. Values are the mean \pm SE from five separate experiments, with $p = 0.07$, 0.03 (**), and 0.30 for IF, Sol, and MT fractions, respectively. In *Panel E*, the change in % of MAP2D in the IF and Sol fractions after hCG treatment (from *Panels B* and *C*) is shown, demonstrating similar changes to these fractions.

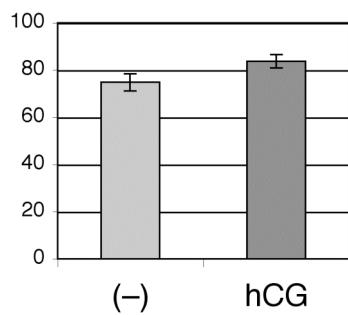
Figure 11

A.



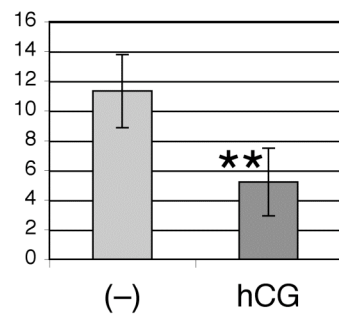
B.

% MAP2D in IF Fraction



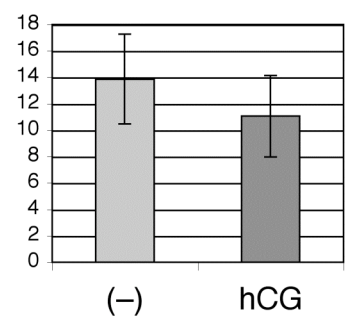
C.

% MAP2D in Sol Fraction



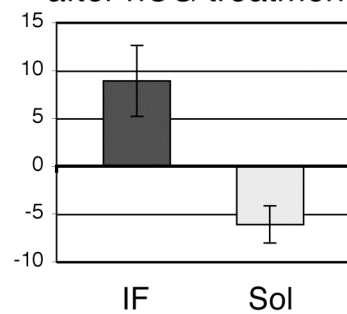
D.

% MAP2D in MT Fraction



E.

Change in % MAP2D after hCG treatment



Thr256/Thr259 (lanes 4-6), consistent with my previous observations of LH receptor-mediated dephosphorylation of these sites. Moreover, the total amount of MAP2D protein detected in the soluble fraction was significantly reduced by hCG treatment (Fig. 11A, compare lanes 2 and 5; Fig. 11C, from $11.3 \pm 2.5\%$ in untreated to $5.2 \pm 2.3\%$ in hCG-treated, as a percentage of total MAP2D protein detected in all three fractions; $n=5$, $p<0.05$). I consistently detected a corresponding increase in MAP2D in the vimentin-enriched fraction in hCG-treated cells (Fig. 11A, compare lanes 1 and 4), although the increase of the relatively small amount of MAP2D into the vimentin-enriched fraction was not statistically significant (Fig. 11B, from $74.8 \pm 3.6\%$ to $83.7 \pm 2.8\%$; $n=5$, $p=0.07$). The relative increase in % MAP2D in the vimentin-enriched fraction ($8.9\% \pm 3.7\%$) after hCG treatment corresponded closely with the consistent decrease in % MAP2D in the soluble fraction ($6.1 \pm 1.9\%$; Fig. 11E). The distribution of MAP2D to the microtubule-enriched fraction was not altered by hCG treatment (Fig. 11D, $n=5$, $p=0.30$). These results demonstrate that, while a portion of MAP2D is soluble or co-isolates with the microtubule cytoskeleton, a substantial portion of MAP2D co-isolates with vimentin and this interaction appears to be modulated by LH receptor-mediated phospho-regulation of MAP2D.

MAP2D colocalizes with the vimentin intermediate filament and microtubule cytoskeletons in granulosa cells.

In order to verify my fractionation results and to better characterize the location of MAP2D relative to components of the granulosa cell cytoskeleton, confocal immunofluorescence microscopy was utilized. Dual staining of fixed granulosa cells with antibodies against β -tubulin and MAP2D revealed that, as has been reported for other MAP2

family proteins, a substantial portion of MAP2D localizes to the microtubule cytoskeleton in PO granulosa cells (Fig. 12A). However, in agreement with cell fractionation results, dual staining for vimentin and MAP2D demonstrated that a large amount of MAP2D also localizes to vimentin intermediate filaments (Fig. 12B). This was particularly true for vimentin in the peri-nuclear region (Fig. 12B, arrowheads). Comparisons between MAP2D and microfilaments, as determined by staining for β -actin, revealed no colocalization (Fig. 12C), as we have shown previously (14). These results demonstrate that MAP2D localizes to both the microtubule and vimentin intermediate filament cytoskeletons in granulosa cells.

MAP2D and vimentin intermediate filament localization is dependent on microtubule stability in granulosa cells.

As vimentin particles largely rely on microtubule-dependent transport by molecular motors for the formation of filaments (reviewed in (85)), vimentin networks are often assembled in close proximity to the microtubule cytoskeleton (78, 84). This dependence on microtubules is such that microtubule destabilization often results in reorganization or even collapse of intermediate filaments into thickened “peri-nuclear cables” (67, 78-84). To evaluate the importance of microtubule stability for vimentin and MAP2D localization in granulosa cells, tubulin and vimentin were observed by dual staining confocal immunofluorescence microscopy. In untreated cells, vimentin and microtubule cytoskeletal networks were often found colocalized, particularly in the peri-nuclear region of granulosa cells (Fig. 13A). Furthermore, upon disruption of the microtubule cytoskeleton by treatment with 1 μ g/ml nocodazole for 60 min (Fig. 13B), vimentin networks became unorganized, disappearing from the periphery of cells and

Figure 12 MAP2D colocalizes with the vimentin intermediate filament and microtubule cytoskeletons in granulosa cells

Confocal microscopy was performed on PO granulosa cells plated on fibronectin-coated glass coverslips, fixed in methanol (-20°C), and visualized by indirect immunofluorescence as stated under *Materials and Methods*. In *Panel A*, cells were stained with MAP2 rabbit polyclonal antibody (red) and β -tubulin mouse monoclonal antibody (green). In *Panel B*, cells were stained with MAP2 rabbit polyclonal antibody (red) and vimentin mouse monoclonal antibody (green). Arrowheads indicate peri-nuclear colocalization of vimentin and MAP2D. In *Panel C*, cells were stained with MAP2 rabbit polyclonal antibody (red) and β -actin mouse monoclonal antibody (green). Results are representative of at least three separate experiments. Similar results were obtained using MAP2 mouse monoclonal antibody (not shown). Scale bars indicate 10 μ M.

Figure 12

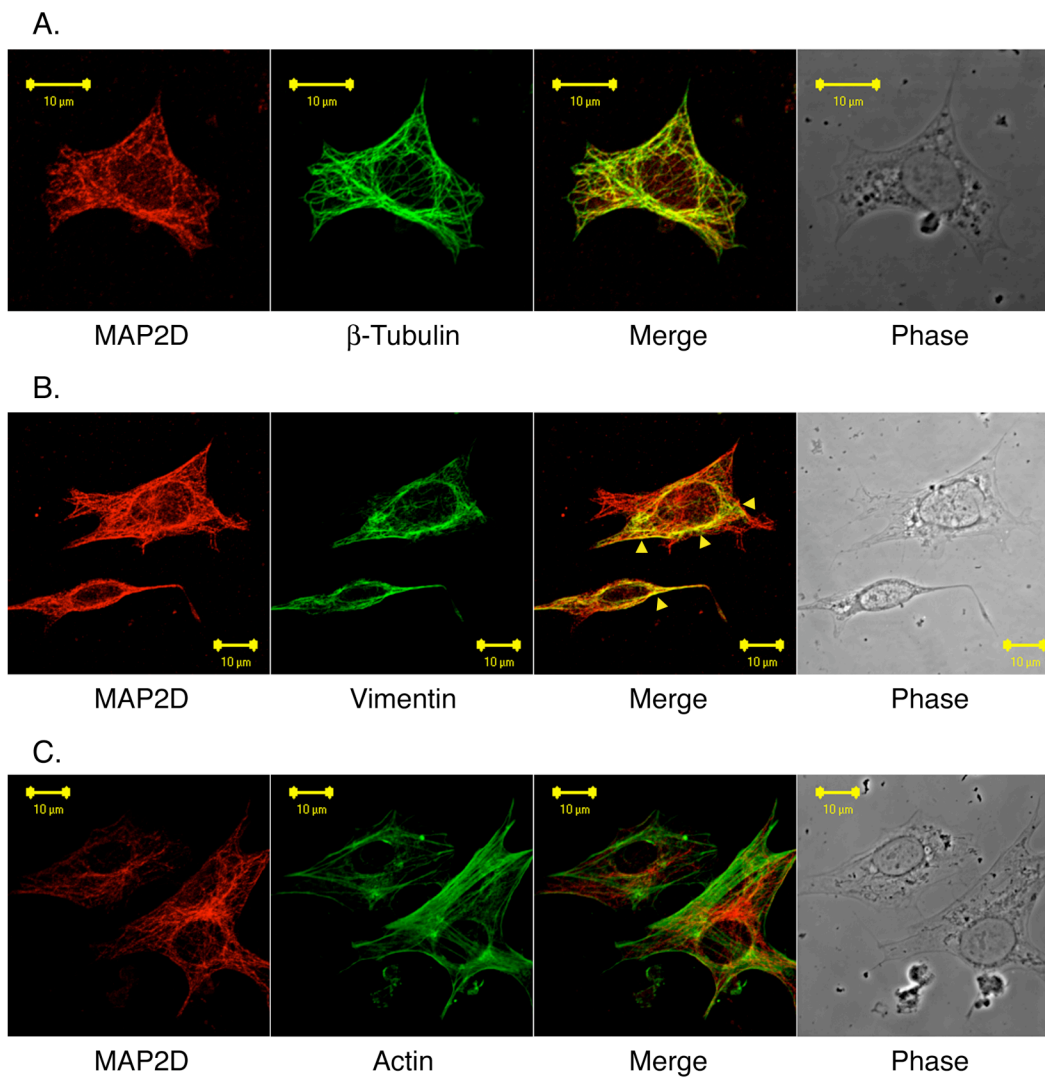
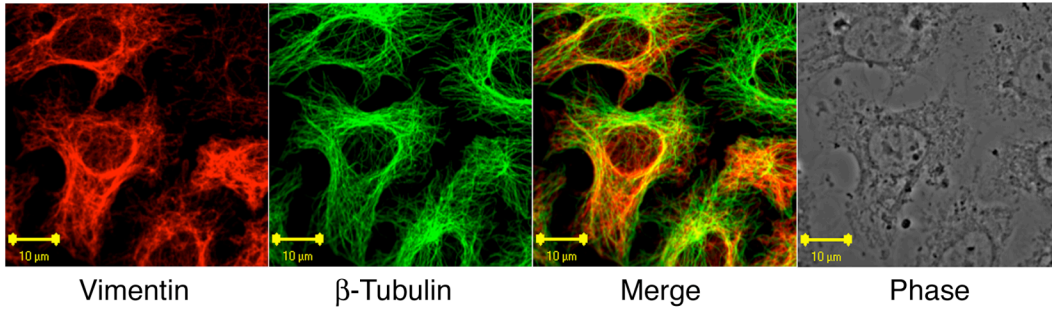


Figure 13 MAP2D and vimentin intermediate filament localization is dependent on microtubule stability in granulosa cells

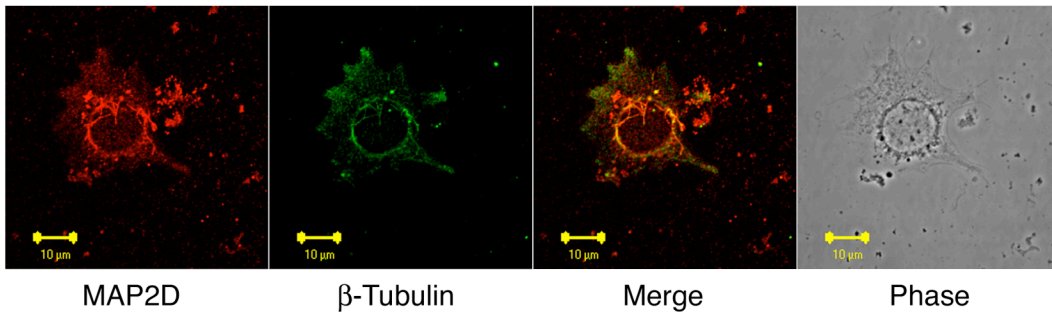
Confocal microscopy was performed on PO granulosa cells plated on fibronectin-coated glass coverslips, fixed in methanol (-20°C), and visualized by indirect immunofluorescence as stated under *Materials and Methods*. In *Panel A*, untreated cells were fixed and stained with antibodies against vimentin (red) and β -tubulin (green). In *Panels B and C*, PO granulosa cells were treated with 1 μ g/ml nocodazole for 60 min (+ Nocodazole) to destabilize microtubules. In *Panel B*, cells were stained with antibodies against MAP2 (red) and β -tubulin (green). In *Panel C*, cells were stained with antibodies against MAP2 (red) and vimentin (green). All results are representative of at least two separate experiments. Scale bars indicate 10 μ M.

Figure 13

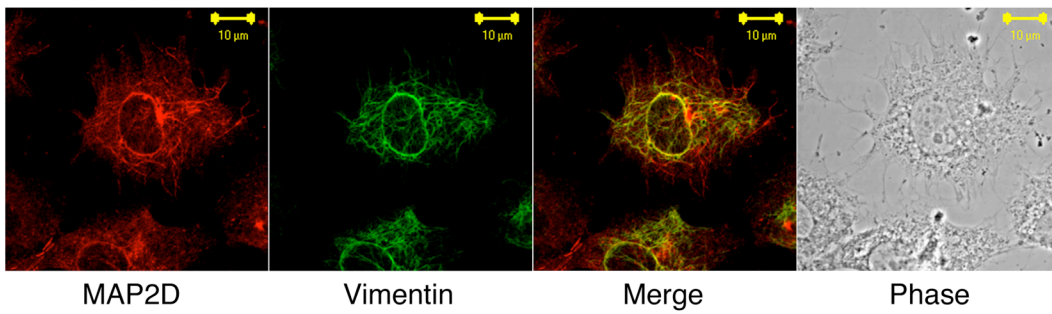
A.



B.

(+)
Nocodazole

C.

(+)
Nocodazole

collapsing into a thickened layer surrounding the nucleus (Fig 13C), as has been described previously (67). MAP2D was also localized to this region and remained colocalized with vimentin (Fig. 13C). These results confirm that MAP2D and vimentin are co-localized and their localization is dependent on microtubule stability in granulosa cells.

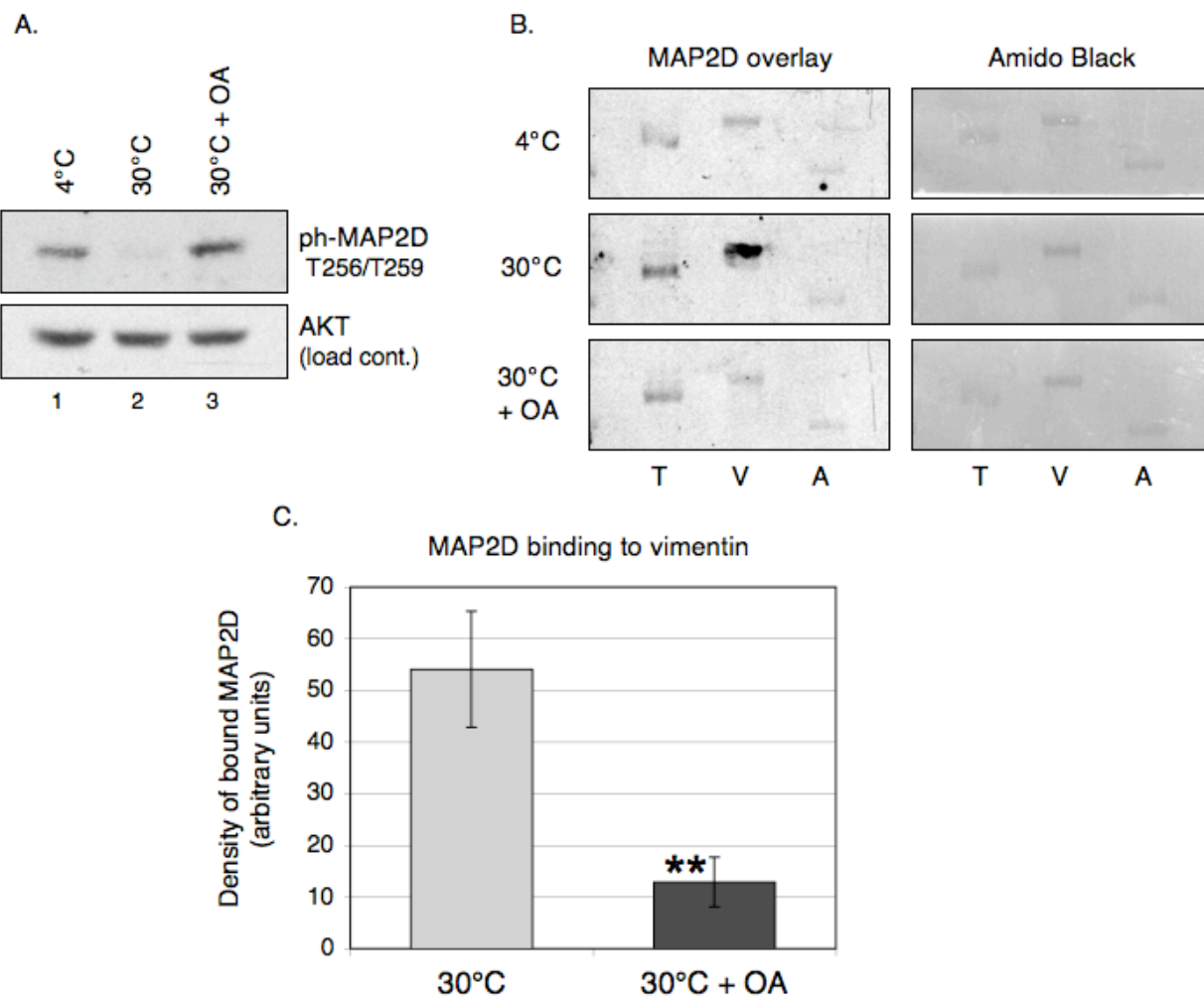
Granulosa cell MAP2D binds to vimentin in a phosphorylation-dependent manner.

To verify the interaction between granulosa cell MAP2D and vimentin and to further investigate the effect of MAP2D phosphorylation on this interaction, solid-phase overlay assays were performed using granulosa cell lysates containing MAP2D in various states of Thr256/Thr259 phosphorylation. Clarified granulosa cell lysates were incubated for 30 min at 4°C or 30°C with or without 0.2 μM okadaic acid, an inhibitor of PP2A and PP1, as indicated (Fig. 14A). Incubation of lysates at 4°C maintained phosphorylation of MAP2D at Thr256/Thr259 (lane 1). Incubation at 30°C resulted in dephosphorylation of MAP2D at Thr256/Thr259 (lane 2) by endogenous phosphatase activity. Inhibition of endogenous PP2A and PP1 by the addition of 0.2 μM okadaic acid was sufficient to block this dephosphorylation of Thr256/Thr259 at 30°C (lane 3). Solid-phase overlay assays were then performed, as described by others (113). Granulosa cell lysates from Fig. 14A were incubated with purified tubulin, vimentin, and actin immobilized on nitrocellulose membranes, and MAP2D bound to the immobilized protein was detected by MAP2 polyclonal antibody (Fig. 14B). MAP2D that was phosphorylated at Thr256/Thr259 (incubated at 4°C or 30°C with OA) bound in detectable amounts to vimentin and tubulin but only very weakly to actin (Fig. 14B, top and bottom). No change in actin binding was observed for MAP2D dephosphorylated at Thr256/Thr259

Figure 14 Granulosa cell MAP2D binds to vimentin in a phosphorylation-dependent manner

Plated PO granulosa cells were lysed by sonication in Overlay Buffer and centrifuged to remove insoluble material. Soluble extracts were incubated at 4°C or 30°C with or without 0.2 μM okadaic acid (OA), as indicated. For further details, see *Materials and Methods*. In *Panel A*, Western blots were performed post-incubation with the indicated antibodies to confirm the phosphorylation state of MAP2D in the extracts. In *Panel B*, 5 μg of the cytoskeletal proteins tubulin (T), vimentin (V), and actin (A) were electrophoretically separated and transferred to membrane for use in solid-phase overlay assays, as described under *Materials and Methods*. Membranes were incubated with rotation for 1.5 h in soluble granulosa cell extracts from (A). Membranes were washed and incubated with MAP2 polyclonal antibody followed by secondary antibody and ECL to detect MAP2D bound to immobilized cytoskeletal proteins. Total amounts of membrane-bound cytoskeletal proteins were verified by staining with Amido Black. Results are representative of 3 separate experiments. In *Panel C*, vimentin-bound MAP2D levels were quantified by densitometric analysis, as stated under *Materials and Methods*, and normalized to total vimentin protein levels as determined by Amido Black staining. Values are the mean ± SE from three separate experiments. **, $p < 0.05$.

Figure 14



(incubated at 30°C) and only a small increase in tubulin binding was observed (Fig. 14B, middle). In comparison, binding between vimentin and dephosphorylated MAP2D (incubated at 30°C) was ~4-fold greater ($p < 0.05$) than for phosphorylated MAP2D (incubated at 30°C with OA) (Fig. 14B, middle and Fig. 14C). No binding was detected when the assay was performed using cell-free buffer only, no primary antibody, or with an irrelevant primary antibody (data not shown.) These findings confirm that granulosa cell MAP2D binds directly or indirectly to vimentin and that this binding is dependent on MAP2D phosphorylation.

In vitro GSK3 β phosphorylation regulates direct binding between MAP2D and vimentin.

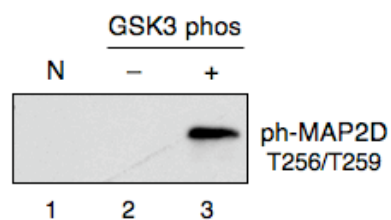
As shown in Chapter II, the kinase GSK3 β maintains basal phosphorylation of MAP2D at Thr256/Thr259 in unstimulated PO granulosa cells. To determine whether MAP2D can bind directly to vimentin and to investigate regulation of this interaction by GSK3 β -mediated phosphorylation of MAP2D, solid-phase overlays were performed using *in vitro* phosphorylated recombinant MAP2D. These experiments were performed by Sarah Fiedler and Dr. Daniel Carr at Oregon Health and Sciences University, in collaboration with my own research. Bacterially expressed and purified MAP2D was labeled with Alexa Fluor 680 and incubated in phosphorylation reactions with no kinase added, PKA catalytic subunit only, or in sequential reactions with PKA catalytic subunit and GSK3 β . Phosphorylation at MAP2D Thr256/Thr259 was not detected by Western blot on unphosphorylated or PKA-only phosphorylated MAP2D (Fig. 15A, lanes 1 and 2). However, the Thr256/Thr259 residues of MAP2D were strongly phosphorylated after sequential phosphorylation by PKA and GSK3 (lane 3). Solid-phase overlay assays were then performed by incubating Alexa Fluor 680-labeled MAP2D

Figure 15 *In vitro* GSK3 β phosphorylation regulates direct binding between MAP2D and vimentin

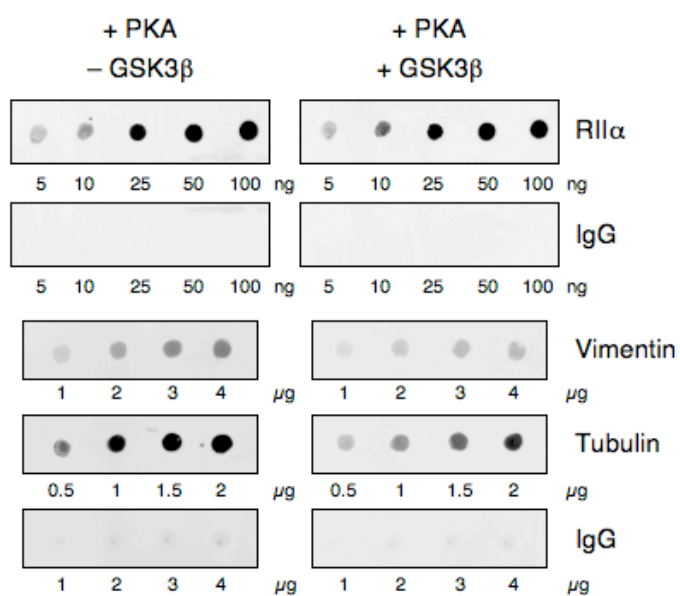
Bacterially expressed and purified MAP2D was labeled with AlexaFluor 680 and then subjected to sequential phosphorylation by PKA and GSK3 β , as stated under *Materials and Methods*. In *Panel A*, unphosphorylated MAP2D (N), MAP2D phosphorylated by PKA only (–), or MAP2D phosphorylated by PKA and GSK3 β sequentially (+) was analyzed by Western blot with a phospho-specific antibody against MAP2D Thr256/Thr259. In *Panel B*, the indicated amounts of RII α , tubulin, vimentin, and IgG were immobilized by spotting onto Immobilon-FL membrane and incubated overnight with PKA and GSK3 β phosphorylated (+ GSK3 β phos) or PKA-only phosphorylated (– GSK3 β phos) AlexaFluor 680-labeled MAP2D from (*A*). After washing, binding of AlexaFluor 680-labeled MAP2D was detected using the Odyssey Infrared Imaging System (LiCor). For further details, see *Materials and Methods*. In *Panel C*, densities of MAP2D bound to each amount of immobilized RII, vimentin, or tubulin protein were quantified as before. Values are the mean from three separate experiments. Significance was determined from raw values using a paired, two-tailed Student's t-test to compare all PKA values with all PKA/GSK3 β values. P values are 0.62, 0.004, and 0.014 for PKA/GSK3 β phospho-regulation of MAP2D binding to RII, vimentin, and tubulin, respectively. $p < 0.05$ was considered statistically significant. Slopes of line fit to plotted data were calculated. The ratio of slopes for PKA vs. PKA/GSK3 β phosphorylated MAP2D, which correlate with the fold increase in binding affinity due to GSK3 β phosphorylation, are 1.01, 2.03, 2.44 for RII, vimentin, and tubulin, respectively.

Figure 15

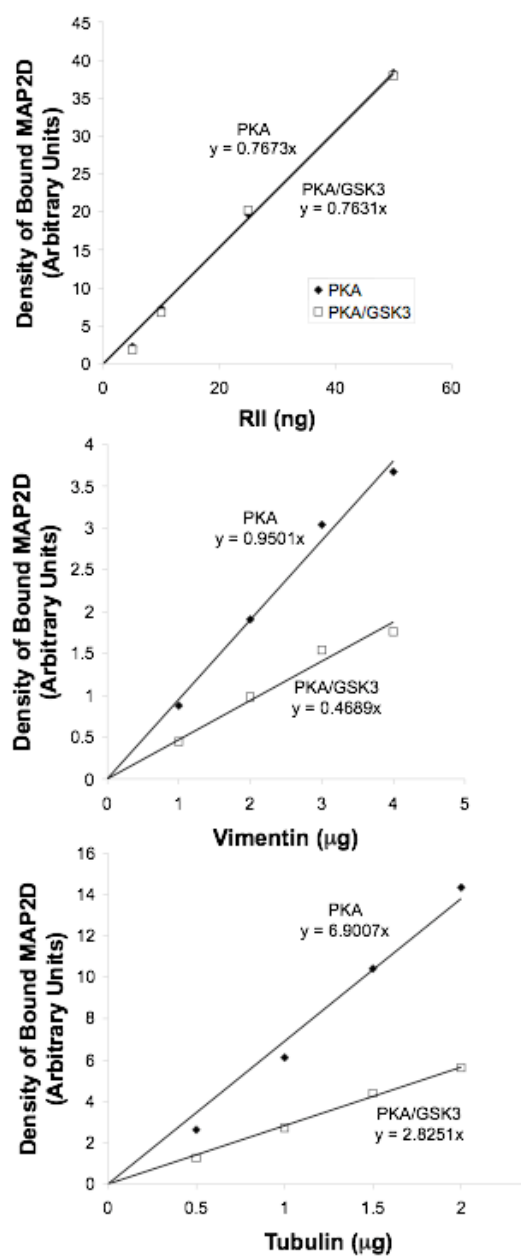
A.



B.



C.



phosphorylated by PKA-only or PKA and GSK3 β with various amounts of purified RII α , vimentin, or tubulin immobilized on Immobilon-FL membranes. MAP2D phosphorylated by PKA-only (labeled “– GSK3 β ”) bound strongly to RII α , tubulin, and vimentin (Fig. 15B, left side). In comparison, MAP2D sequentially phosphorylated by both PKA and GSK3 β (labeled “+ GSK3 β ”) displayed significantly reduced binding to tubulin and vimentin (Fig. 15B, right side). MAP2D binding to RII α , a well-characterized AKAP binding protein, was not regulated by GSK3 β phosphorylation of MAP2D. For all conditions, the density of bound MAP2D increased in a linear fashion with rising amounts of immobilized protein (Fig. 15C). Slopes of lines fit to the data were determined and the ratio of the PKA-alone slope to PKA and GSK3 β slope was calculated. These ratios, which correlate with the fold decrease in binding affinity due to GSK3 β phosphorylation, were 1.01, 2.03, and 2.44 for RII, vimentin, and tubulin, respectively. These results demonstrate that, similar to the well described interaction between MAP2 and tubulin, MAP2D binds directly to vimentin and the affinity of this interaction is reduced by GSK3 β phosphorylation at sites including Thr256/Thr259.

MAP2D recruitment to vimentin intermediate filaments is coincident with LH receptor-dependent phosphorylation of vimentin and redistribution of the vimentin cytoskeleton.

The function of AKAPs is to recruit PKA into close proximity with substrate proteins to allow for their efficient phosphorylation. It may be predicted, therefore, that relocation of a dynamic pool of the AKAP MAP2D under hormone treatment would allow more efficient PKA phosphorylation of a localized substrate. As vimentin is phosphorylated *in vivo* at Ser38 and Ser72 by PKA (71), the apparent LH-dependent redistribution of the AKAP MAP2D,

dephosphorylated at Thr256/Thr259, into the vimentin-enriched fraction (Fig. 11) prompted me to investigate the phosphorylation of vimentin at these sites. Treatment of granulosa cells with hCG for 10 or 30 min resulted in increased vimentin phosphorylation at Ser38 and Ser72 (Fig. 16A, lane 2) and pretreatment with the PKA inhibitor Myr-PKI blocked the hCG-induced increase in vimentin phosphorylation at Ser38 (Fig. 16B, compare lanes 2 and 4). These results indicate that coincident with PKA-dependent dephosphorylation of MAP2D at Thr256/Thr259 and its apparent redistribution to the vimentin-enriched cell fraction, vimentin is phosphorylated in a PKA-dependent manner at recognized PKA sites.

It has been well established that intermediate filaments are dynamic structures (reviewed in (85)) and are important for changes in cell shape and morphology (184). Furthermore, it has been shown that turnover of vimentin filaments is regulated by phosphorylation (71). In particular, phosphorylation of vimentin at Ser38 and Ser72 by PKA has been linked to disassembly of vimentin filaments *in vivo* (71). Based on my observation of LH receptor mediated phosphorylation of vimentin at these PKA sites, I sought to evaluate the effect of LH receptor signaling on the various components of the granulosa cell cytoskeleton. Cells were treated with or without 1 IU/ml hCG prior to visualization of vimentin and MAP2D protein by confocal immunofluorescence. In the untreated condition, granulosa cells were widely spread with vimentin filaments reaching into the periphery (Fig. 17, top panel). In comparison, after 30 min hCG treatment, granulosa cells were contracted and vimentin filaments were redistributed, appearing mostly in a thickened layer surrounding the nucleus (Fig. 17, bottom panel). MAP2D was clearly localized to the vimentin filaments surrounding the nucleus. These results demonstrate that, coincident with LH receptor signaling, vimentin is phosphorylated at two PKA

Figure 16 LH receptor activation results in vimentin phosphorylation at PKA sites

In *Panel A*, PO granulosa cells were treated with 1 IU/ml hCG for the indicated times. Results are representative of 3 separate experiments. In *Panel B*, cells were left untreated or pretreated with 50 μ M myristoylated-PKI (Myr-PKI) for 60 min and then left untreated (–) or treated with 1 IU/ml hCG for 10 min.

Figure 16

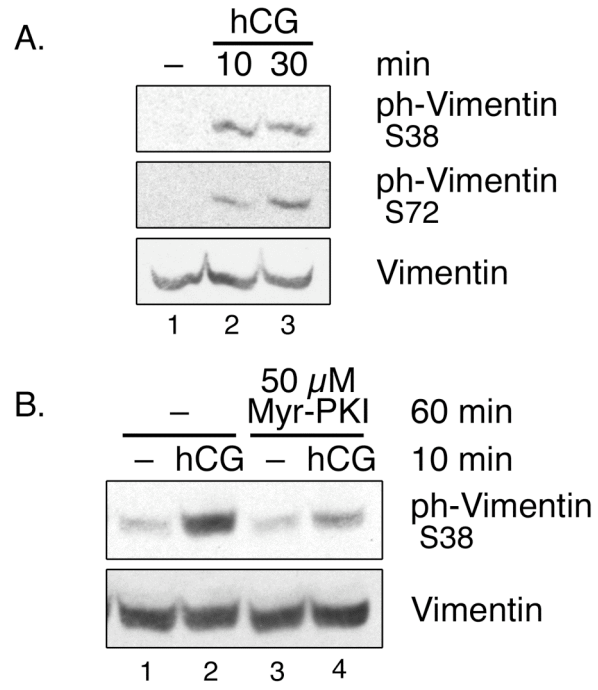
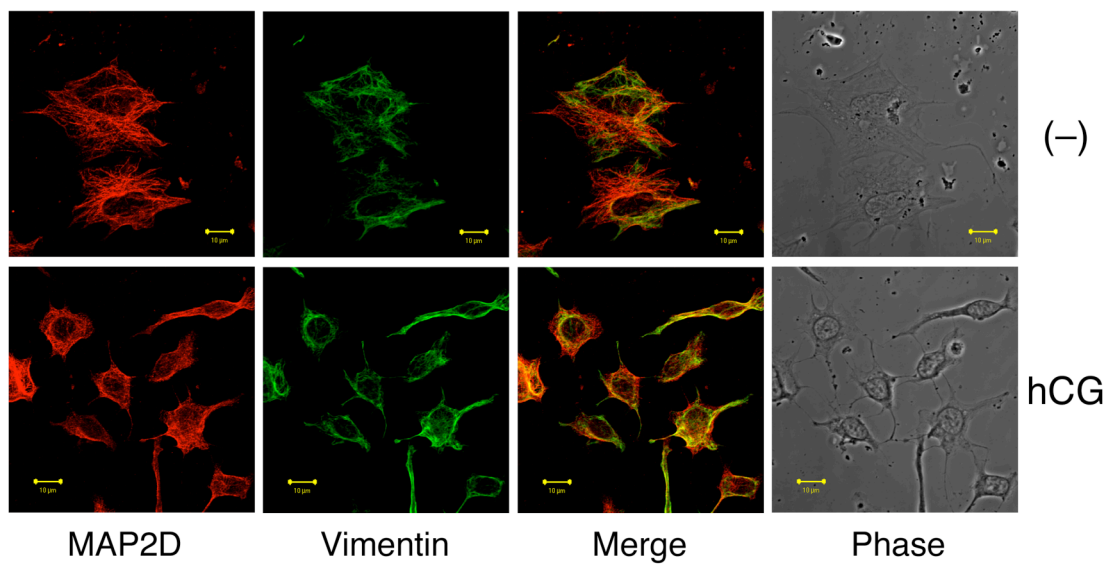


Figure 17 LH receptor signaling stimulates reorganization of the vimentin cytoskeleton

Granulosa cells plated on fibronectin-coated glass coverslips were left untreated (–) or treated with 1 IU/ml hCG for 30 min before being fixed in methanol (-20°C) and stained with antibodies against MAP2 (red) and vimentin (green). Confocal microscopy was performed by indirect immunofluorescence as stated under *Materials and Methods*. Clusters of granulosa cells were chosen for imaging as these cells appeared most responsive to hormonal treatment. Results are representative of at least three separate experiments. Scale bars indicate 10 μ M.

Figure 17



sites and granulosa cells contract as vimentin filaments are reorganized from the periphery into a thickened layer surrounding the nucleus.

Disruption of vimentin results in increased progesterone production in PO granulosa cells.

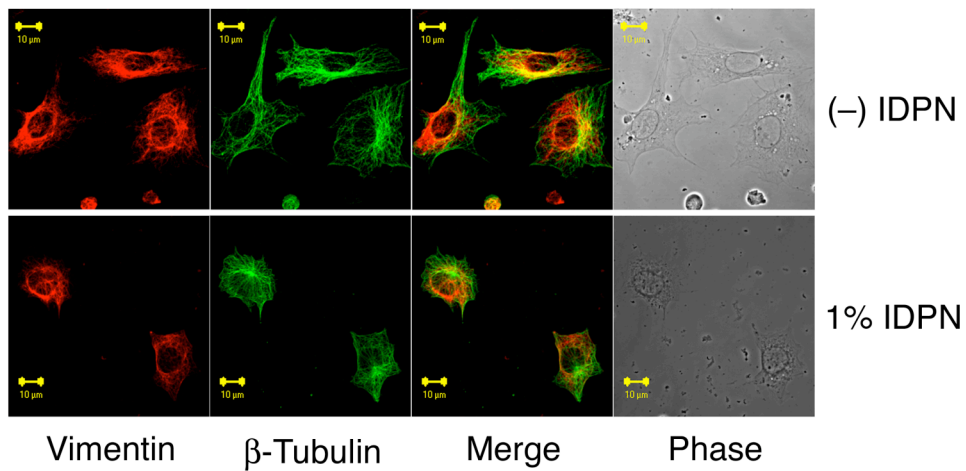
In view of the observed changes in granulosa cell morphology and vimentin reorganization following treatment with hCG, I sought to illuminate the possible functional consequences of these cytoskeletal changes by LH receptor signaling. A dynamic vimentin cytoskeleton is thought to play a unique role in steroidogenic cells by modulating the accessibility of cholesterol ester-containing lipid droplets to mitochondria (reviewed in (75)). Trophic hormones via PKA (185) promote the rapid mobilization of cholesterol from intracellular lipid droplets to the outer mitochondrial membrane (186) by a series of events that appear to include the disassembly of vimentin filaments (75-77). I therefore determined whether the disruption of the vimentin intermediate filament network affected LH-dependent granulosa cell progesterone production. Granulosa cells grown on glass coverslips were treated with 1% β,β' -iminodipropionitrile (IDPN) (v/v), a reversible intermediate filament disrupting agent (76, 82, 109, 187), for 60 min. This treatment successfully destabilized vimentin filaments, as they were observed in a thickened band surrounding the nucleus (Fig. 18A). Intermediate filament destabilization resulted in characteristic cell rounding but had no apparent effect on microtubule stability (Fig. 18A), in agreement with the observations of others (77, 82). Cell culture medium was collected from granulosa cells after IDPN treatment and secreted progesterone levels were measured by RIA. Disruption of vimentin assembly by IDPN treatment correlated with significantly increased progesterone levels (Fig. 18B). However, pretreatment with okadaic acid

Figure 18 Vimentin disruption stimulates increased progesterone secretion by granulosa cells

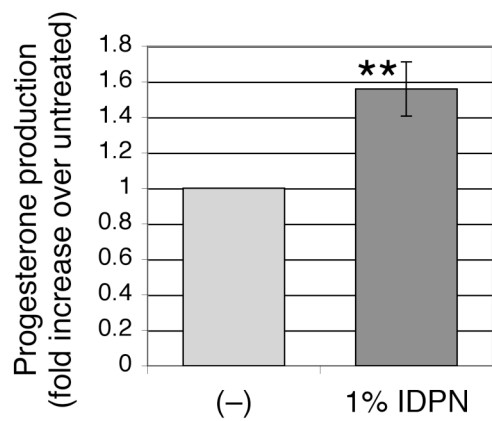
In *Panels A* and *B*, PO granulosa cells plated on glass coverslips were left untreated (–) or treated for 60 min with a 1% (v/v) β,β' -iminodipropionitrile (IDPN), an intermediate filament-disrupting agent. In *Panel A*, cells were stained with antibodies against vimentin (red) and β -tubulin (green) to confirm disruption of the vimentin cytoskeleton by IDPN treatment. Scale bars indicate 10 μ M. In *Panel B*, progesterone secretion levels from IDPN-treated granulosa cells were measured in the surrounding media by sensitive progesterone radioimmunoassay (RIA). Progesterone levels were normalized to untreated control levels (–) and values are presented as mean \pm SE of five separate experiments. $p < 0.05$ was considered statistically significant (**). Mean basal progesterone levels were 5.0 ng/ml. In *Panel C*, PO granulosa cells plated on glass coverslips were left untreated or pretreated for 60 min with 0.2 μ M okadaic acid (OA) prior to treatment with or without 1 IU/ml hCG for 4h. Progesterone secretion levels from OA-pretreated granulosa cells were measured from the surrounding media by sensitive RIA. Progesterone levels are normalized to untreated control levels at 0h, and values are presented as mean \pm SE of four determinations from one experiment. Mean basal progesterone levels were 2.9 ng/ml.

Figure 18

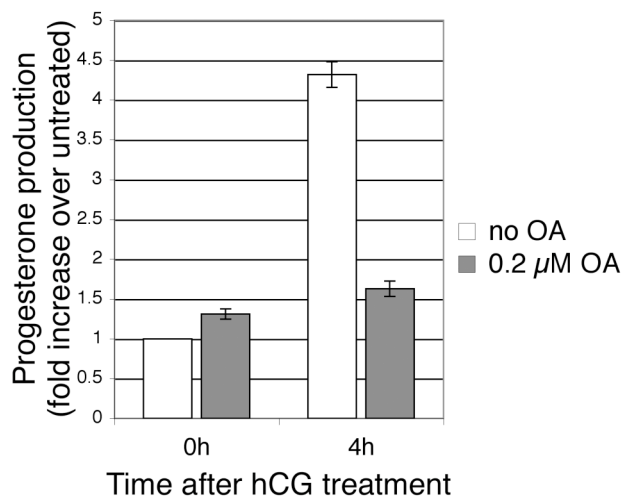
A.



B.



C.



abrogated LH receptor-dependent progesterone secretion by granulosa cells (Fig. 18C), similar to findings in luteal cells (188). Taken together, these results are consistent with the hypothesis that LH-dependent Thr256/Thr259 dephosphorylation of MAP2D by PP2A and the apparent movement of this dephosphorylated MAP2D into the vimentin-enriched fraction coupled with phosphorylation of vimentin on Ser38 and Ser72 facilitates vimentin disassembly that is necessary for progesterone production (Fig. 19).

Discussion

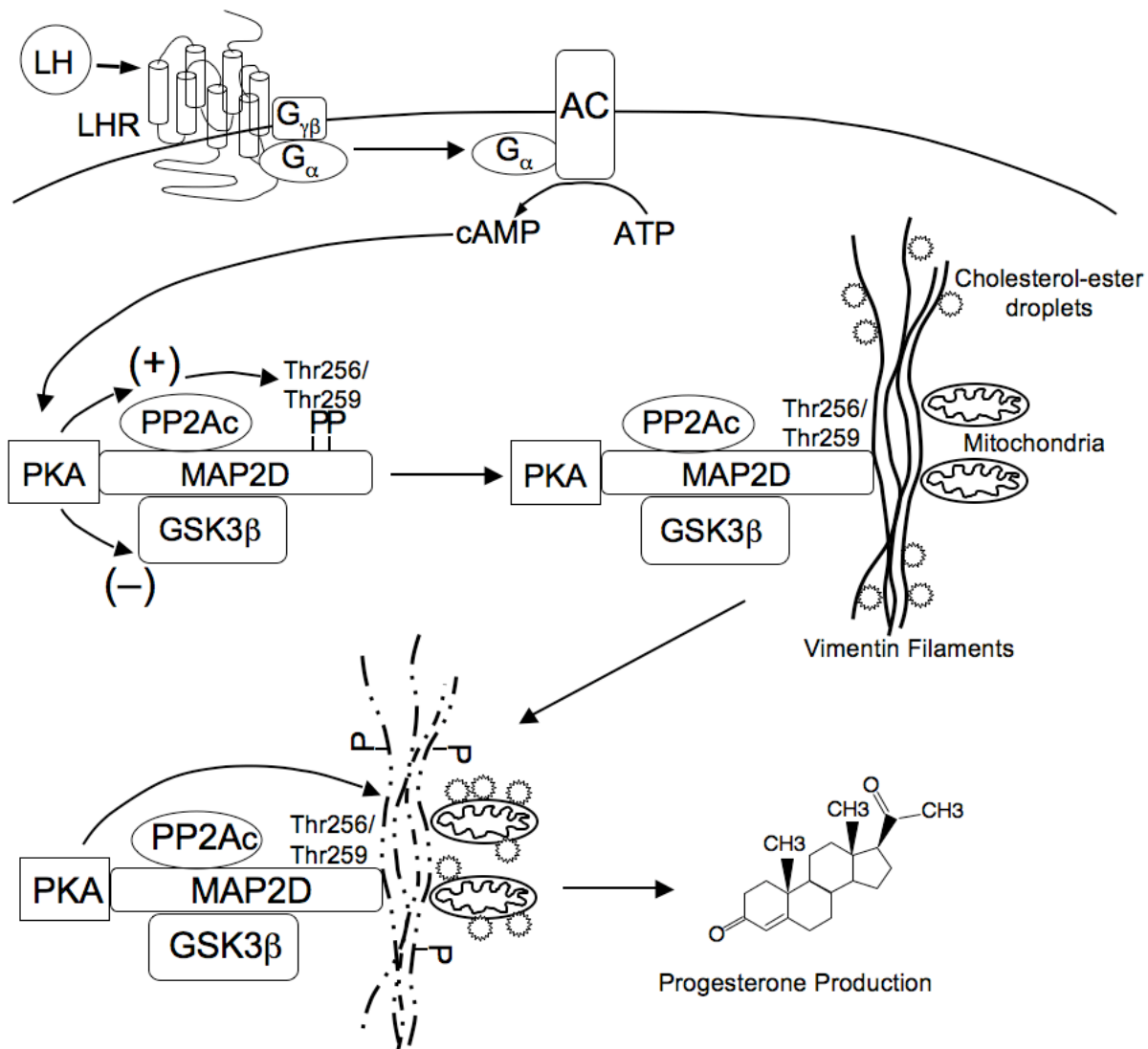
LH receptor activation in PO granulosa cells initiates extensive changes in the structure and function of ovarian follicles resulting in steroidogenesis, ovulation, and differentiation of granulosa to luteal cells. PO granulosa cells selectively express MAP2D, a lower molecular weight splice variant of the neuronal protein MAP2 that binds a variety of cytoskeletal elements in neurons (83, 99, 100, 102, 105, 106, 108, 109, 111, 114). Phosphorylation of MAP2 appears to regulate binding to each of these cellular components (101, 105, 106, 108). In granulosa cells, MAP2D is found in a complex containing PKA, GSK3 β , and PP2A B56 δ and regulation of these signaling molecules by LH receptor signaling results in phospho-regulation of MAP2D at Thr256/Thr259.

Here I have begun to elucidate the importance of LH-dependent MAP2D phospho-regulation to granulosa cell functions. Cytoskeletal fractionation was pursued in order to determine where the signaling complex containing MAP2D, PKA, GSK3 β , and PP2A B56 δ might be localized in granulosa cells. While one might predict that MAP2D would be primarily associated with microtubules, my results indicate that only a small portion of MAP2D was localized to the microtubules and another small portion remained soluble. The majority of

Figure 19 MAP2D functions as a scaffold for LH receptor signaling in preovulatory granulosa cells which may regulate vimentin cytoskeletal dynamics

Shown is a model for LH receptor signaling whereby MAP2D functions as a signaling scaffold for a protein complex composed of PKA, PP2A, and GSK3 β , allowing for rapid and selective dephosphorylation of MAP2D at Thr256/Thr259. This dephosphorylation recruits MAP2D and associated PKA to the vimentin cytoskeleton, allowing LH receptor-stimulated phosphorylation and reorganization of vimentin filaments. Vimentin reorganization promotes the rapid mobilization of cholesterol from intracellular lipid droplets to the outer mitochondrial membrane, facilitating progesterone steroidogenesis.

Figure 19



MAP2D was associated with the vimentin-enriched intermediate-filament fraction. There is evidence that other MAP2 family proteins bind to intermediate filaments including vimentin (83, 108-112), perhaps simultaneously with microtubules (113, 114). Moreover, the portion of MAP2D phosphorylated at Thr256/Thr259 localized primarily to the soluble fraction, suggesting that the signaling complex composed of PKA, MAP2D, PP2A B56 δ , and GSK3 β is contained within this soluble fraction.

In order to further elucidate the location of MAP2D, granulosa cells were examined by confocal immunofluorescence microscopy. Previously we reported that MAP2D was not bound to the granulosa cell cytoskeleton but instead appeared in a peri-nuclear region that localized with markers for the Golgi apparatus and was dispersed by the Golgi-disrupting chemical Brefeldin A (14). However, these experiments were not performed under conditions that maintained microtubule integrity. Based on the recognized dependence of vimentin filament localization on microtubule stability (67, 78-84), the reported interactions between vimentin and the Golgi apparatus (189-191), and the recent finding that Brefeldin A causes disruption of vimentin filaments (192), it appears likely that, in the absence of microtubules, MAP2D was localized to this region by an interaction with vimentin. Here I confirm that MAP2D is localized to both the microtubule and vimentin intermediate filament cytoskeletons when these networks are intact. Furthermore, I find that, upon disruption of microtubules by treatment with nocodazole, vimentin filaments and associated MAP2D collapse into a ring surrounding the nucleus. Therefore, my current findings are consistent with our previous observations of subcellular MAP2D localization and provide further evidence of an interaction with vimentin.

My results suggest that phospho-regulation of Thr256/Thr259 on MAP2D may modulate the association of MAP2D to the cytoskeleton. Indeed, in cytoskeletal fractionation experiments, most of the soluble MAP2D in untreated cells was shifted out of this fraction and apparently into the vimentin-enriched intermediate-filament fraction upon LH receptor activation. To better evaluate this regulation of MAP2D-vimentin binding, solid-phase overlay assays were performed with immobilized cytoskeletal proteins and either MAP2D from granulosa cell extracts or recombinant MAP2D. Dephosphorylated MAP2D from granulosa cell extracts incubated at 30°C bound vimentin significantly more than MAP2D from extracts incubated with OA, suggesting that regulation of Ser/Thr phosphorylation may effect this interaction. Moreover, *in vitro* phosphorylation of MAP2D sites by GSK3 β may also change vimentin binding. Recombinant MAP2D was phosphorylated at Thr256/Thr259 by sequential incubation with PKA and GSK3 β but was not phosphorylated at these sites by PKA alone. (Incubation with GSK3 β alone also did not phosphorylate Thr256/Thr259, suggesting that a prior priming phosphorylation (167) of MAP2D at a nearby site may be necessary for efficient phosphorylation of Thr256/Thr259 by GSK3 β). MAP2D phosphorylated by PKA and GSK3 β bound vimentin less avidly than MAP2D phosphorylated by PKA alone. While I cannot rule out a role for phosphorylation of other MAP2D sites by GSK3 β , the putative change in vimentin association after LH receptor signaling in cytoskeletal fractionation experiments and my extensive data demonstrating phospho-regulation of Thr256/Thr259 by GSK3 β and PP2A suggests that phospho-regulation of these sites may be important for modulation of the vimentin-MAP2D interaction.

Vimentin is the predominant intermediate filament protein and one of the most abundant phospho-proteins in granulosa cells (67). Phosphorylation by PKA is recognized to modify intermediate filament protein organization, often collapsing the filaments into tight bundles (72-74). In particular, the *in vivo* phosphorylation of vimentin at Ser38 and Ser72 enhances vimentin dynamics by increasing the extent of vimentin disassembly (71). In light of the well established role of MAP2D as an AKAP and my data suggesting the recruitment of a dynamic pool of this AKAP into the vimentin-enriched fraction upon LH receptor activation, I hypothesized that MAP2D phospho-regulation might function to enhance efficient PKA activity against vimentin at Ser38 and Ser72, resulting in remodeling of the intermediate filament cytoskeleton. Results presented herein demonstrate that LH receptor signaling through cAMP/PKA leads to phosphorylation of vimentin at these critical residues. Furthermore, following LH receptor activation and coincident with these events, vimentin filaments are collapsed away from the periphery into the region surrounding the nucleus. Though this effect is very similar to the reorganization of vimentin observed after microtubule destabilization, the microtubule cytoskeleton remains intact in hCG-treated cells. I have not yet directly linked the movement of MAP2D dephosphorylated at Thr256/Thr259 into the vimentin-enriched fraction to the vimentin phosphorylation and filament reorganization observed after LH receptor activation. However, based on these observations, I hypothesize that localization of MAP2D to vimentin filaments allows for more efficient vimentin phosphorylation by PKA at Ser38 and Ser72, resulting in an imbalance between filament assembly and disassembly and subsequent changes in the granulosa cell cytoskeleton.

One of the most prominent actions of the mid-cycle surge of LH is the induction of progesterone biosynthesis. Indeed, progesterone receptor null mice do not ovulate (193) and blockade of LH-stimulated progesterone biosynthesis with the P-450 SCC inhibitor aminoglutethimide blocks ovulation (194). Cholesterol, the substrate for all steroid hormone biosynthesis, is stored in steroidogenic cells in cholesterol-ester lipid droplets (reviewed in (186)). Upon stimulation of steroidogenic cells by trophic hormones such as LH, cholesterol is de-esterified and transported to the outer membrane of the mitochondria via a PKA-dependent pathway (185). Thereafter, cholesterol moves from the outer to the inner mitochondrial membrane, mediated by the activity of StAR and is then cleaved to pregnenolone by P-450 SCC (186, 195). The cellular mechanisms that mediate the transfer of cholesterol from lipid droplets to the outer mitochondrial membrane are poorly understood. My findings here demonstrate that inhibition of PP2A by pretreatment with okadaic acid inhibits LH receptor-stimulated progesterone production in PO granulosa cells without effecting basal progesterone levels. Similarly, reports have shown that both LH-stimulated and cAMP analog-stimulated progesterone secretion in luteal cells is inhibited by low doses of okadaic acid, without effecting basal progesterone levels (188). Interestingly, in these cells PP2A inhibition did not appear to interfere with the activity of the steroidogenic enzymes as 22R-hydroxycholesterol, a freely diffusible substrate for P-450-SCC, stimulated progesterone production in the presence of okadaic acid (188). This has led to the hypothesis that inhibition of progesterone steroidogenesis by okadaic acid occurs at a step occurring after PKA activation but prior to P-450 SCC activity, perhaps in the transport of cholesterol to the mitochondrial surface (188).

There is evidence that cholesterol ester lipid droplets are caged in vimentin-enriched structures (196, 197), and that vimentin disassembly in various steroidogenic cell models is necessary for cholesterol trafficking to mitochondria (75-77). Similarly, it has been reported that, after destabilization of PO granulosa cell microtubules with nocodazole or colchicine which also results in vimentin destabilization, progesterone production was increased (61). My results showing enhanced progesterone production in granulosa cells in response to the vimentin filament disrupting agent IDPN (76, 82) are consistent with the notion that cholesterol mobilization is facilitated by disruption of the vimentin intermediate filament network (76, 77).

One of the PKA-dependent steps in cholesterol mobilization is activation of cholesterol ester hydrolase to de-esterify cholesterol (198). However, there may be additional PKA-dependent steps in this pathway leading to cholesterol mobilization, such as MAP2D dephosphorylation and vimentin phosphorylation. The ability of okadaic acid to abrogate LH receptor-dependent progesterone biosynthesis by granulosa cells is consistent with the notion that MAP2D dephosphorylation may be necessary for proper cholesterol trafficking. However, direct proof for the involvement of vimentin phosphorylation and MAP2D dephosphorylation in progesterone production requires additional studies.

In summary, my results support the hypothesis that phospho-regulation of MAP2D at Thr256/Thr259 serves to regulate the association of MAP2D and possibly PKA with the intermediate filament protein vimentin. This association may facilitate efficient phosphorylation of vimentin at Ser38 and Ser72 by PKA, resulting in the observed restructuring of vimentin intermediate filaments after hCG treatment. Finally, binding between MAP2D and vimentin and

subsequent vimentin remodeling may play a role in the LH-dependent progesterone production by granulosa cells, which is essential for fertility.

CHAPTER IV: MATERIALS AND METHODS

Materials – The following were purchased: rabbit skeletal muscle actin, recombinant Syrian hamster vimentin, and bovine brain tubulin from Cytoskeleton, Inc. (Denver, CO); human chorionic gonadotropin (hCG) from Abraxis Pharmaceutical Products (Schaumburg, IL); pregnant mare serum gonadotropin (PMSG), forskolin, pepstatin A, leupeptin, benzamidine, phenylmethylsulfonyl fluoride (PMSF), soybean trypsin inhibitor (STI), SB415286, SB216763, and Amido Black total protein stain from Sigma-Aldrich (St. Louis, MO); antipain dihydrochloride, calpain inhibitor II, E-64, and aprotinin from Roche; protein A/G PLUS-agarose from Santa Cruz Biotechnology (Santa Cruz, CA); λ Protein Phosphatase and Reaction Buffer from New England Biolabs (Ipswich, MA); adenosine 3',5'-cyclic monophosphate, 8-(4-chlorophenylthio) cAMP (8-CPT-cAMP), myristoylated PKA inhibitor amide 14-22 (Myr-PKI), lithium chloride, AR-A014418 (GSK-3 β Inhibitor VIII), roscovitine, and PD98059 from EMD Biosciences/Calbiochem (La Jolla, CA); 8-(4-chlorophenylthio)-2'-O-methyl cAMP (8-pCPT-2'-O-Me-cAMP) from Biolog Life Science Institute (Bremen, Germany); okadaic acid and tautomycin from Alexis Biochemicals (Lausen, Switzerland); human fibronectin from BD Biosciences (San Jose, CA); β,β' -iminodipropionitrile (IDPN) from Fisher Scientific/Acros Organics (Waltham, MA); Immobilon-FL membrane was from Millipore (Billerica, MA), and ECL reagents, Rainbow molecular weight markers, and Hybond-C Extra nitrocellulose membranes from Amersham Biosciences/GE Healthcare (Buckinghamshire, UK).

Antibodies – Anti-phospho PP2A-B56 δ (Ser566) and total PP2A-B56 δ polyclonal antibodies, generated against the phospho-peptide LRRKpSELPQC or purified rat B56 δ , respectively (162), were a gift from Dr. Juhn Ahn, Dr. Thomas McAvoy, and Dr. Angus Nairn. Vimentin (serum

314) rabbit polyclonal antibody, generated against bacterially produced hamster vimentin, was a gift from Dr. Robert Goldman. Phospho-MAP2 (Thr1620/Thr1623) antibody was purchased from Cell Signaling Technology (Danvers, MA) and was purified and tested for phospho-specific reactivity by this company. This antibody was used for Western blot detection of MAP2D phosphorylation at residues Thr256/Thr259 (equivalent to Thr1620/Thr1623 in MAP2A/B). The following were purchased: MAP2 (HM-2), β -Actin (AC-15), β -Tubulin (TUB 2.1), and Vimentin (V9) mouse monoclonal antibodies from Sigma-Aldrich (St. Louis, MO); MAP2, Akt, phospho-MAP2 (Ser136), phospho-myosin light chain (MLC) 2 (Ser19), phospho-p44/42 MAP kinase (Thr202/Tyr204) (ph-ERK1/2), phospho-Akt (Ser473), and phospho-GSK3 α/β (Ser21/9) rabbit polyclonal antibodies, GSK3 β (27C10) rabbit monoclonal antibody, and anti-HA tag (6E2) mouse monoclonal antibody from Cell Signaling Technology (Danvers, MA); phospho-CREB (Ser133) (10E9) and PP2Ac (1D6) mouse monoclonal antibodies, PP1 and PP2Ac rabbit polyclonal antibodies, and microcystin-agarose from Upstate Biotechnology/Millipore (Lake Placid, NY); MAP kinase (Zymed ERK-798) mouse monoclonal, Alexa Fluor 488 goat anti-mouse IgG, and Alexa Fluor 568 goat anti-rabbit IgG antibodies from Invitrogen (Carlsbad, CA); phospho-Vimentin (Ser72) (EP1070Y) rabbit monoclonal antibody from Epitomics (Burlingame, CA); and phospho-Vimentin (Ser38) rabbit polyclonal antibody, GSK3 α/β mouse monoclonal-agarose conjugate and normal mouse IgG-agarose conjugate from Santa Cruz Biotechnology (Santa Cruz, CA).

Animals – Sprague-Dawley rats (Charles River Laboratories, Inc., Portage, MI) were obtained at 17 days of age, housed at Northwestern University animal care facilities, and maintained in

accordance with the *Guidelines for the Care and Use of Laboratory Animals* by protocols approved by the Northwestern University ACUC committee.

PO Granulosa Cell Culture – Granulosa cells were mechanically isolated from ovaries of 24-day-old rats primed by subcutaneous injections of 10 IU PMSG in 0.1 ml PBS on day 22 to promote maturation of follicles to the PO phenotype. Collected cells were utilized immediately or plated overnight on fibronectin (BD; San Jose, CA)-coated plastic dishes in DMEM/F12 serum-free medium supplemented with 10 nM estradiol-17 β , 100 U/ml penicillin, and 100 μ g/ml streptomycin, and treated with indicated additions ~20 h after plating (199).

Protease Inhibition – Protease Inhibitor Cocktail was prepared and added to various buffers such that final concentrations included 10 μ g/ml pepstatin A, 10 μ g/ml aprotinin, 10 μ g/ml leupeptin, 50 μ g/ml STI, 25 mM benzamidine, 10 μ g/ml E-64, 1 mM PMSF, 7 μ g/ml calpain inhibitor II, and 50 μ g/ml antipain dihydrochloride.

Whole Ovarian Extracts – Twenty-four-day-old rats, primed by subcutaneous injections with 10 IU PMSG 48 h prior, were given intraperitoneal injections of 50 IU hCG or saline. Ovaries were harvested at various time points after injections; dissected free of bursa, fat, and oviducts; weighed; and homogenized at 4°C in homogenization buffer (10 mM Tris, pH 7.0, 5 mM EDTA, 1 mM EGTA, 0.32 M sucrose, 1 mM sodium orthovanadate, 20 mM sodium fluoride, 2.5 mM sodium pyrophosphate and Protease Inhibitor Cocktail) using 12 strokes with a ground glass homogenizer. Homogenates were clarified by centrifugation at 10,000 x g at 4°C for 20 min. Supernatants were added to 0.5 x volume SDS-sample buffer and denatured by boiling. Protein concentrations were controlled by homogenization at a 10:1 ratio of homogenization buffer (ml)/wet tissue weight (g) followed by loading equal volumes for each SDS-PAGE gel lane.

Electrophoresis and Western Blot Analysis – For plated cells, treatments were terminated by aspirating medium and rinsing cells once with PBS. Total cell extracts were collected by scraping cells in SDS-sample buffer (28) and denatured by boiling. Protein concentrations were controlled by plating identical cell numbers per plate in each experiment followed by loading equal volumes for each SDS-PAGE gel lane. Separation of ovarian lysate protein was by SDS-PAGE using 10% or 13% separating gels (200). Separated protein was electrophoretically transferred to Hybond-C Extra nitrocellulose membrane (Amersham Pharmacia Biotech). Membranes were incubated with primary antibody overnight at 4°C, and protein-antibody complexes were detected using HRP-linked anti-IgG (Cell Signaling Technology, Danvers, MA) and enhanced chemiluminescence (Amersham Biosciences/GE Healthcare, Buckinghamshire, UK). Films were scanned with an Epson 1640SU scanner and Adobe Photoshop version 7.0 software with minimal processing. Relative protein quantities were calculated from densitometric measurements of Western band intensities using Molecular Analyst software (Bio-Rad Laboratories, Inc., Hercules, CA). Statistical analyses are presented as mean ± SE and were performed by paired Student's t-test; $p < 0.05$ was accepted as significant (201).

In Vitro Phosphatase Assay for Electrophoretic Migration Analysis – PO rat granulosa cells in suspension were collected and lysed by sonication in Minimal Buffer A (50 mM PIPES, pH 6.6, 100 mM NaCl, 0.5% Nonidet P-40, 2 mM EGTA, and Protease Inhibitor Cocktail), Complete Buffer A (Minimal Buffer A plus 1 mM EDTA, 1 mM sodium orthovanadate, 20 mM sodium fluoride, and 2.5 mM sodium pyrophosphate), or MnCl₂ Phosphatase Reaction Buffer (50 mM Tris HCl, pH 7.5, 100 mM dithiothreitol, 0.1 mM EGTA, 0.01% Brij 35, 2 mM MnCl₂, 0.5% Nonidet P-40, 2 mM EGTA, and Protease Inhibitor Cocktail). Lysates were clarified by

centrifugation at 10,000 x g for 5 min, then incubated at 30°C for 30 min, with or without the addition of exogenous Lambda protein phosphatase (New England Biolabs).

Co-immunoprecipitation and Microcystin Pulldown Analysis – Primary rat PO granulosa cells in suspension were collected and lysed by sonication in Complete Buffer A. Lysates were clarified by centrifugation at 10,000 x g for 5 min, after which a fraction was removed as input. For immunoprecipitation, detergent soluble cell extracts were precleared by incubation with protein A/G PLUS-agarose for 30 min at 4°C on a rotator. Extracts were then incubated overnight at 4°C on a rotator in the presence of 60 µl microcystin-agarose, protein A/G PLUS-agarose and 10 µl mouse monoclonal antibodies against MAP2, PP2A catalytic subunit, or an irrelevant epitope (HA-Tag mAb), or 40 µl GSK3β mAb-agarose or IgG-agarose conjugates. Unbound protein in the flow-through was collected and denatured in SDS-PAGE sample buffer. Agarose beads were washed in Complete Buffer A with 10% glycerol added. Bound proteins were eluted and denatured in SDS-PAGE sample buffer.

Confocal Immunofluorescence Microscopy – Treatments of granulosa cells cultured on fibronectin-coated glass coverslips were terminated by aspirating medium and rinsing cells once with PBS. Cells were fixed in -20°C methanol for 5 min, rinsed in PBS for 20 min at room temp, blocked in 1 mg/ml normal goat serum (Jackson ImmunoResearch) for 15 min at 37°C, and incubated in primary antibody for 30 min at 37°C. Coverslips were washed once in 0.05% Tween-20 in PBS and twice in PBS before incubation for 30 min at 37°C with goat anti-mouse IgG or goat anti-rabbit IgG antibody conjugated to Alexa Fluor 488 or Alexa Fluor 568, respectively (Invitrogen, Carlsbad, CA). Coverslips were washed as before, dried, and mounted with Gelvatol onto glass slides. Slides were analyzed at the Cell Imaging Facility, Northwestern

University Feinberg School of Medicine, using a Zeiss LSM510 laser-scanning confocal microscope.

Cytoskeletal Fractionation – Primary PO rat granulosa cells were treated with hormone in suspension, collected, and lysed at 37°C by sonication in Cytoskeletal Extraction Buffer (50 mM PIPES, pH 6.6, 0.5% Nonidet P-40, 2 mM EGTA, 1 mM MgCl₂, 2 mM dithiothreitol, 1 mM sodium orthovanadate, 20 mM sodium fluoride, 2.5 mM sodium pyrophosphate, and Protease Inhibitor Cocktail). To ensure observation of the endogenous cytoskeletal environment with minimal disruptions, paclitaxel was not added. Intermediate filament-enriched fractions were pelleted by low speed centrifugation (9,000 x g) for 10 min at 35°C. Low speed supernatant was centrifuged at high speed (100K x g) at 35°C for 30 min to pellet microtubule-enriched 1 fraction. Remaining supernatant contained soluble fraction. Samples were heat denatured in SDS-PAGE sample buffer.

Solid-phase Overlay Assays with Granulosa Cell MAP2D – Overlays were performed according to methods described by Heimann et al. (113), with some modifications. 5 µg of tubulin, vimentin, or actin protein were separated by SDS-PAGE in 10% separating gels. Separated protein was electrophoretically transferred to nitrocellulose membrane to immobilize protein. Membranes were blocked with Overlay Blocking Buffer (5% bovine serum albumin in 0.05 M Tris, pH 7.4, containing 5 mM EDTA, 0.19 M NaCl, and 2.5% Triton X-100) for 3 h to remove bound SDS and saturate nonspecific binding sites on the nitrocellulose. Primary PO rat granulosa cells were plated on fibronectin overnight and then lysed by sonication in Overlay Lysis Buffer (12.5 mM Tris, pH 7.2, 100 mM NaCl, 0.5% Nonidet P-40, 1 mM EGTA, and Protease Inhibitor Cocktail). Lysates were centrifuged at 16,000 x g for 20 min at 4°C to remove detergent

insoluble material and supernatants were incubated for 30 min at 4°C or 30°C, with or without the addition of 0.2 μ M OA. Phosphatase inhibitors were then added (1 mM sodium orthovanadate, 20 mM sodium fluoride, 2.5 mM sodium pyrophosphate, and 0.2 μ M OA, if not already added) to stop endogenous phosphatase activity. Nitrocellulose-immobilized cytoskeletal proteins were incubated with the resulting granulosa cell extracts at room temp for 1.5 h with rotation, washed three times in Overlay Wash Buffer (12.5 mM Tris, pH 7.2, 100 mM NaCl with 1 mM sodium orthovanadate, 20 mM sodium fluoride, 2.5 mM sodium pyrophosphate, and 0.2 μ M okadaic acid added for the first wash only), and incubated for 2 h at room temp with MAP2 primary antibody (Cell Signaling Technology, 1:500 dilution in 5% milk-TBS). Membranes were washed as before, incubated with secondary antibody for 1 h at room temp, washed again, and bound MAP2 protein/primary antibody/secondary antibody complexes were detected by enhanced chemiluminescence. Membranes were stained with Amido Black to visualize total protein.

Solid-phase Overlay Assays with Recombinant MAP2D – These procedures were performed by Sarah Fiedler and Dr. Daniel Carr at Oregon Health and Sciences University, in collaboration with our own research. Full-length rat MAP2D-pET30a was expressed in *E. coli* BL21 (DE3) pLysS (Novagen) by 1mM IPTG (Sigma-Aldrich) induction and purified in a HiTrap Chelating HP column (GE Healthcare). Purification was confirmed by western blot (not shown). After purification, MAP2D-pET30 was dialyzed into PBS, and then labeled with the AlexaFluor680 Protein Labeling Kit, according to kit instructions (Molecular Probes, Eugene, OR). Purified, AlexaFluor680-labeled MAP2D-pET30 was incubated in kinase buffer (50mM MOPS, 10mM MgCl₂, 0.25mg/ml BSA, pH7.0) with 2mM MgATP, and 0.22 μ g PKA C subunit (or water for

non-phos control) for 20 min at room temp. GSK3 β (2 μ l, or water for non-phos and PKA-only controls) was then added and incubated for 1 h at 30°C. Purified recombinant murine RII α -pET11 (described previously (140)), rabbit IgG, microtubules, and unpolymerized vimentin were spotted onto Immobilon-FL membrane (Millipore). Membranes were allowed to dry completely and then blocked 2 h in 5% milk-PBS, before overnight incubation with the AlexaFluor680-labeled, phosphorylated MAP2D-pET30. Membranes were then washed 4X in PBS and bound MAP2D detected using the Odyssey Infrared Imaging System (LiCor).

Progesterone Radioimmunoassay – Sensitive progesterone radioimmunoassay (RIA) was performed by the University of Virginia Center for Research in Reproduction Ligand Assay and Analysis Core; NICHD (SCCPRR) U54-HD28934.

CHAPTER V : CONCLUSIONS AND FUTURE DIRECTIONS

Conclusions

Signaling downstream of the LH receptor in PO granulosa cells, predominantly through the cAMP/PKA pathway, triggers a radical remodeling of the structure and function of ovarian follicles to support ovulation, oocyte maturation, and luteinization. While many downstream transcriptional targets of LH have been identified (19), little is known about how LH signals via PKA to effect this dramatic transformation in granulosa cells, nor have changes in the granulosa cell cytoskeleton been thoroughly evaluated as a necessary step in these events. PO granulosa cells selectively express MAP2D, a cytoskeletal-associated signaling protein with the unique ability and temporal expression appropriate to coordinate PKA signaling and dynamic cytoskeletal reorganization in granulosa cells.

I have identified a novel LH-receptor signaling mechanism in granulosa cells by which LH signaling by PKA coordinates increased PP2A activity and decreased GSK3 β activity against MAP2D to promote rapid and selective dephosphorylation of Thr256/Thr259. This coordinated phospho-regulation is made possible, I propose, by the ability of MAP2D to function as a signaling scaffold for a protein complex composed of PKA, PP2A, and GSK3 β (Fig. 19). The ability to act as a signaling scaffold is shared by other AKAP proteins and likely allows for strict spatial and temporal control over PKA signaling (117, 139). In the PO granulosa cell, MAP2D serves as both scaffold and substrate. This likely allows for very rapid and precise regulation of MAP2D phosphorylation by the bound kinase and phosphatase. Indeed, the phosphorylation of MAP2D at Thr256/Thr259 concurrent with induction of MAP2D expression suggests that

GSK3 β becomes immediately bound to newly generated MAP2D and, by maintaining this interaction, preserves Thr256/Thr259 phosphorylation until LH receptor activation of PKA turns it off. Similarly, LH receptor-mediated dephosphorylation MAP2D at Thr256/Thr259 is detected within 2 min, likely reflecting the close association of PKA with GSK3 β and PP2A.

Based on GSK3 β phosphorylation-dependent *in vitro* binding of MAP2D to immobilized vimentin, LH receptor-mediate phosphorylation of vimentin at PKA sites reported to regulate filament disassembly, and observations of vimentin rearrangement in PO granulosa cells after LH receptor activation, I have proposed a model by which LH receptor signaling may induce remodeling of the vimentin cytoskeleton to allow transport of cholesterol esters to the mitochondrial membrane. Regulation of vimentin networks by trophic hormones to promote steroidogenesis has been described in other steroidogenic systems, such as ACTH stimulation of adrenal cells and LH stimulation of Leydig cells (75). Furthermore, a report using nocodazole to disrupt microtubules in PO granulosa cells found vimentin was also disrupted and progesterone levels were increased (61). Thus, my evidence of increased progesterone production after vimentin disruption is supportive of the hypothesis that a vimentin-dependent steroidogenic regulatory mechanism exists in PO granulosa cells.

Future Directions

Disruption of PKA/AKAP interactions by AKAP inhibitory peptides

The data presented above supports the hypothesis that PO granulosa cell MAP2D functions as an AKAP to target PKA signaling to the vimentin cytoskeleton. The design and use of synthetic peptides that bind with the RII subunit of PKA to disrupt PKA/AKAP interactions have been described (202, 203). Therefore, application of these AKAP inhibitory peptides to

granulosa cell signaling would be useful in testing the hypothesis that the AKAP function of MAP2D is required for vimentin phosphorylation at PKA sites, for vimentin remodeling after LH receptor activation, and for LH receptor-dependent progesterone production.

Knockdown of PP2A B56 δ subunit or vimentin expression by adenoviral delivered siRNA

Knockdown of gene expression levels can be achieved through the expression of siRNA (short interfering RNA) to trigger RNA interference pathways. As our cultured primary granulosa cells are non-dividing and have very low (<5%) transfection efficiency, use of an adenoviral delivery system will ensure highly efficient expression (204).

One potential target for gene silencing is the B56 δ regulatory subunit of PP2A. As demonstrated above, B56 δ is acutely phosphorylated at Ser566 by PKA-dependent LH receptor signaling, an event which is necessary and sufficient for activation of PP2 in other systems (162). Knockdown of B56 δ mRNA and protein levels will further test the hypothesis that a PP2A holoenzyme containing this regulatory subunit is necessary for MAP2D dephosphorylation under LH receptor signaling. Moreover, disruption of signaling through this specific PP2A holoenzyme may clarify the importance of phospho-regulation of MAP2D at Thr256/Thr259 under LH receptor signaling for vimentin binding and remodeling and progesterone production.

Another potential target for gene silencing is vimentin. Knockdown of vimentin mRNA and protein leads to disruption of the vimentin filamentous cytoskeleton and has been used as a confirmation of observations made after treatments with the vimentin disruptor IDPN (82). By disrupting granulosa cell vimentin filaments in this way, I might confirm my hypothesis that vimentin disruption stimulates progesterone production.

MAP2D mutations to determine specificity of Thr256/Thr259 phosphorylation on vimentin binding.

Above I have presented evidence that GSK3 β phosphorylation of MAP2D reduces its ability to bind to immobilized vimentin protein. Furthermore, I show that GSK3 β activity in granulosa cells is required for basal levels of MAP2D phosphorylation at Thr256/Thr259 and that bacterially-expressed recombinant MAP2D is phosphorylated at these sites by sequential *in vitro* phosphorylation by PKA and GSK3 β but not by PKA alone. This data supports that hypothesis that phosphorylation of MAP2D at Thr256/Thr259 contributes to the regulation of MAP2D-vimentin binding, however I cannot rule out the possibility that phosphorylation by GSK3 β at another site is responsible for this effect. Two MAP2D expressing constructs with either Thr to Ala or Thr to Glu point mutations at both Thr residues (256 and 259) have been designed by our collaborator, Dr. Daniel Carr at Oregon Health and Sciences University. Mutations from Thr to Ala will provide a MAP2D mutant protein that can not be phosphorylated at the amino acid residues 256 and 259. Inversely, mutations from Thr to the negatively charged amino acid Glu may mimic post-translational phosphorylation at these sites in regard to interactions with binding partners (205). Therefore, use of mutant MAP2D protein expressed from these constructs in solid-phase overlay assays would test the hypothesis that phosphorylation of MAP2D specifically at Thr256/Thr259 is necessary for regulation of the MAP2D-vimentin interaction.

REFERENCES

1. **Larsen PR, Kronenberg HM, Melmed S, Polonsky KS** 2003 Williams Textbook of Endocrinology. 10th ed. Philadelphia: Saunders
2. **Beckmann CRB, Ling FW, Herbert WNP, Laube DW, Smith RP, Barzansky BM** 1998 Obstetrics and Gynecology. 3rd ed. Baltimore: Lippincott Williams & Wilkins
3. **Dorrington JH, Moon YS, Armstrong DT** 1975 Estradiol-17beta biosynthesis in cultured granulosa cells from hypophysectomized immature rats; stimulation by follicle-stimulating hormone. *Endocrinology* 97:1328-1331
4. **Armstrong DT, Papkoff H** 1976 Stimulation of aromatization of exogenous and endogenous androgens in ovaries of hypophysectomized rats in vivo by follicle-stimulating hormone. *Endocrinology* 99:1144-1151
5. **Rani CS, Salhanick AR, Armstrong DT** 1981 Follicle-stimulating hormone induction of luteinizing hormone receptor in cultured rat granulosa cells: an examination of the need for steroids in the induction process. *Endocrinology* 108:1379-1385
6. **Peng XR, Hsueh AJ, LaPolt PS, Bjersing L, Ny T** 1991 Localization of luteinizing hormone receptor messenger ribonucleic acid expression in ovarian cell types during follicle development and ovulation. *Endocrinology* 129:3200-3207
7. **Lawrence TS, Dekel N, Beers WH** 1980 Binding of human chorionic gonadotropin by rat cumuli oophori and granulosa cells: a comparative study. *Endocrinology* 106:1114-1118
8. **Magnusson C, Billig H, Eneroth P, Roos P, Hillensjo T** 1982 Comparison between the progesterin secretion responsiveness to gonadotrophins of rat cumulus and mural granulosa cells in vitro. *Acta Endocrinol (Copenh)* 101:611-616
9. **Channing CP, Bae IH, Stone SL, Anderson LD, Edelson S, Fowler SC** 1981 Porcine granulosa and cumulus cell properties. LH/hCG receptors, ability to secrete progesterone and ability to respond to LH. *Mol Cell Endocrinol* 22:359-370
10. **Conti M, Hsieh M, Park JY, Su YQ** 2006 Role of the epidermal growth factor network in ovarian follicles. *Mol Endocrinol* 20:715-723
11. **Matzuk MM, Lamb DJ** 2002 Genetic dissection of mammalian fertility pathways. *Nature cell biology* 4 Suppl:s41-49
12. **Stocco C, Telleria C, Gibori G** 2007 The molecular control of corpus luteum formation, function, and regression. *Endocr Rev* 28:117-149
13. **Hunzicker-Dunn M, Mayo KE** 2006 Gonadotropin Signaling in the Ovary. In: Neill JD ed. *Knobil and Neill's Physiology of Reproduction*. 3 ed: Elsevier; 547-592
14. **Salvador LM, Flynn MP, Avila J, Reierstad S, Maizels ET, Alam H, Park Y, Scott JD, Carr DW, Hunzicker-Dunn M** 2004 Neuronal Microtubule-associated Protein 2D Is a Dual A-kinase Anchoring Protein Expressed in Rat Ovarian Granulosa Cells. *J Biol Chem* 279:27621-27632

15. **Huhtaniemi I, Zhang FP, Kero J, Hamalainen T, Poutanen M** 2002 Transgenic and knockout mouse models for the study of luteinizing hormone and luteinizing hormone receptor function. *Mol Cell Endocrinol* 187:49-56
16. **Themmen APN, Huhtaniemi IT** 2000 Mutations of gonadotropins and gonadotropin receptors: elucidating the physiology and pathophysiology of pituitary-gonadal function. *Endocr Rev* 21:551-583
17. **Hillier SG** 2001 Gonadotropic control of ovarian follicular growth and development. *Mol Cell Endocrinol* 179:39-46
18. **Goldring NB, Durica JM, Lifka J, Hedin L, Ratoosh SL, Miller WL, Orly J, Richards JS** 1987 Cholesterol side-chain cleavage P450 messenger RNA: evidence for hormonal regulation in rat ovarian follicles and constitutive expression in corpora lutea. *Endocrinology* 120:1942-1950
19. **Espey LL, Richards JS** 2002 Temporal and spatial patterns of ovarian gene transcription following an ovulatory dose of gonadotropin in the rat. *Biol Reprod* 67:1662-1670
20. **Rajagopalan-Gupta RM, Rasenick MM, Hunzicker-Dunn M** 1997 LH/choriogonadotropin-dependent, cholera toxin-catalyzed adenosine 5'-diphosphate (ADP)-ribosylation of the long and short forms of G α and pertussis toxin-catalyzed ADP-ribosylation of G β . *MolEndo* 11:538-549
21. **Rajagopalan-Gupta RM, Lamm ML, Mukherjee S, Rasenick MM, Hunzicker-Dunn M** 1998 Luteinizing hormone/choriogonadotropin receptor-mediated activation of heterotrimeric guanine nucleotide binding proteins in ovarian follicular membranes. *Endocrinology* 139:4547-4555
22. **Kosugi S, Mori T, Shenker A** 1996 The role of Asp⁵⁷⁸ in maintaining the inactive conformation of the human lutropin/choriogonadotropin receptor. *JBiolChem* 271:31813-31817
23. **Kosugi S, Van Dop C, Geffner ME, Rabl W, Carel J, Chaussain J, Mori T, Merendino JJ, Shenker A** 1995 Characterization of heterogeneous mutations causing constitutive activation of the luteinizing hormone receptor in familial male precocious puberty. *Human Molecular Genetics* 4:183-188
24. **Kosugi S, Mori T, Shenker A** 1998 An anionic residue at position 564 is important for maintaining the inactive conformation of the human lutropin/choriogonadotropin receptor. *MolPharm* 53:894-901
25. **Russell DL, Doyle KM, Gonzales-Robayna I, Pipaon C, Richards JS** 2003 Egr-1 induction in rat granulosa cells by follicle-stimulating hormone and luteinizing hormone: combinatorial regulation by transcription factors cyclic adenosine 3',5'-monophosphate regulatory element binding protein, serum response factor, sp1, and early growth response factor-1. *Mol Endocrinol* 17:520-533
26. **Sirois J, Richards JS** 1993 Transcriptional regulation of the the rat prostaglandin endoperoxide synthase 2 gene in granulosa cells. *JBiolChem* 268:21931-21938
27. **Park-Sarge O-K, Mayo KE** 1994 Regulation of the progesterone receptor gene by gonadotropins and cyclic adenosine 3',5'-monophosphate in rat granulosa cells. *Endocrinology* 134:709-718
28. **Hunzicker-Dunn M** 1981 Selective activation of rabbit ovarian protein kinase isozymes in rabbit ovarian follicles and corpora lutea. *JBiolChem* 256:12185-12193

29. **Broillet MC, Firestein S** 1999 Cyclic nucleotide-gated channels. Molecular mechanisms of activation. *Ann N Y Acad Sci* 868:730-740
30. **de Rooij J, Rehmann H, van Triest M, Cool RH, Wittinghofer A, Bos JL** 2000 Mechanism of Regulation of the Epac Family of cAMP-dependent RapGEFs. *J Biol Chem* 275:20829-20836
31. **de Rooij J, Zwartkruis FJ, Verheijen MH, Cool RH, Nijman SM, Wittinghofer A, Bos JL** 1998 Epac is a Rap1 guanine-nucleotide-exchange factor directly activated by cyclic AMP. *Nature* 396:474-477
32. **Conti M** 2002 Specificity of the cyclic adenosine 3',5'-monophosphate signal in granulosa cell function. *Biol Reprod* 67:1653-1661
33. **Morris JK, Richards JS** 1995 Luteinizing hormone induces prostaglandin endoperoxide synthase-2 and luteinization in vitro by A-kinase and C-kinase pathways. *Endocrinology* 136:1549-1558
34. **Salvador LM, Maizels E, Hales DB, Miyamoto E, Yamamoto H, Hunzicker-Dunn M** 2002 Acute signaling by the LH receptor is independent of protein kinase C activation. *Endocrinology* 143:2986-2994
35. **Mukherjee A, Park-Sarge OK, Mayo KE** 1996 Gonadotropins induce rapid phosphorylation of the 3',5'-cyclic adenosine monophosphate response element binding protein in ovarian granulosa cells. *Endocrinology* 137:3234-3245
36. **Manna PR, Dyson MT, Eubank DW, Clark BJ, Lalli E, Sassone-Corsi P, Zeleznik AJ, Stocco DM** 2002 Regulation of steroidogenesis and the steroidogenic acute regulatory protein by a member of the cAMP response-element binding protein family. *MolEndocrinol* 16:184-199
37. **Hirakawa T, Ascoli M** 2003 The lutropin/choriogonadotropin receptor-induced phosphorylation of the extracellular signal-regulated kinases in leydig cells is mediated by a protein kinase a-dependent activation of ras. *Mol Endocrinol* 17:2189-2200
38. **Cottom J, Salvador LM, Maizels ET, Reierstad S, Park Y, Carr DW, Davare MA, Hell JW, Palmer SS, Dent P, Kawakatsu H, Ogata M, Hunzicker-Dunn M** 2003 Follicle-stimulating hormone activates extracellular signal-regulated kinase but not extracellular signal-regulated kinase kinase through a 100-kDa phosphotyrosine phosphatase. *J Biol Chem* 278:7167-7179
39. **Sugawara T, Saito M, Fujimoto S** 2000 Sp1 and SF-1 interact and cooperate in the regulation of human steroidogenic acute regulatory protein gene expression. *Endocrinology* 141:2895-2903
40. **Sugawara T, Holt JA, Kiriakidou M, Strauss Jr JF** 1996 Steroidogenic factor 1-dependent promoter activity of the human steroidogenic acute regulatory protein (StAR) gene. *Biochemistry* 35:9052-9059
41. **Clemens JW, Lala DS, Parker KL, Richards JS** 1994 Steroidogenic factor-1 binding and transcriptional activity of the cholesterol side-chain cleavage promoter in rat granulosa cells. *Endocrinology* 134:1499-1508
42. **Monte D, DeWitte F, Hum DW** 1998 Regulation of the human P450scc gene by steroidogenic factor 1 is mediated by CBP/p300. *JBiolChem* 273:4585-4591

43. **Desclozeaux M, Krylova IN, Horn F, Fletterick RJ, Ingraham HA** 2002 Phosphorylation and intramolecular stabilization of the ligand binding domain in the nuclear receptor steroidogenic factor 1. *Mol Cell Biol* 22:7193-7203
44. **Herrlich A, Kuhn B, Grosse R, Schmid A, Schultz G, Gudermann T** 1996 Involvement of G_s and G_i proteins in dual coupling of the luteinizing hormone receptor to adenylyl cyclase and phospholipase C. *JBiolChem* 271:16764-16772
45. **Gudermann T, Nichols C, Levy FO, Birnbaumer M, Birnbaumer L** 1992 Calcium mobilization by the LH receptor expressed in *Xenopus* oocytes independent of 3',5'-cyclic adenosine monophosphate formation: evidence for parallel activation of two signaling pathways. *MolEndo* 6:272-278
46. **Gudermann T, Birnbaumer M, Birnbaumer L** 1992 Evidence for dual coupling of the murine luteinizing hormone receptor to adenylyl cyclase and phosphoinositide breakdown and Ca²⁺ mobilization. *JBiolChem* 267:4479-4488
47. **Davis JS, Weakland LL, West LA, Farese RV** 1986 Luteinizing hormone stimulates the formation of inositol triphosphate and cyclic AMP in rat granulosa cells. *BiochemJ* 238:597-604
48. **Kuhn B, Gudermann T** 1999 The luteinizing hormone receptor activates phospholipase C via preferential coupling to Gi2. *Biochemistry* 38:12490-12498
49. **Ascoli M, Fanelli F, Segaloff DL** 2002 The lutropin/choriogonadotropin receptor, a 2002 perspective. *Endocr Rev* 23:141-174
50. **Morris JK, Richards JS** 1993 Hormone induction of luteinization and prostaglandin endoperoxide synthase-2 involves multiple cellular signalling pathways. *Endocrinology* 133:770-779
51. **Park JI, Park HJ, Lee YI, Seo YM, Chun SY** 2003 Regulation of NGFI-B expression during the ovulatory process. *Mol Cell Endocrinol* 202:25-29
52. **Wu Y, Ghosh S, Nishi Y, Yanase T, Nawata H, Hu Y** 2005 The orphan nuclear receptors NURR1 and NGFI-B modulate aromatase gene expression in ovarian granulosa cells: a possible mechanism for repression of aromatase expression upon luteinizing hormone surge. *Endocrinology* 146:237-246
53. **Maizels ET, Mukherjee A, Sithanandam G, Peters CA, Cottom J, Mayo KE, Hunzicker-Dunn M** 2001 Developmental regulation of mitogen-activated protein kinase-activated kinases-2 and -3 (MAPKAPK-2/-3) in vivo during corpus luteum formation in the rat. *Mol Endocrinol* 15:716-733
54. **Peng X, Hsueh AJW, Lapolt PS, Bjersing L, Ny T** 1991 Localization of luteinizing hormone receptor messenger ribonucleic acid expression in ovarian cell types during follicle development and ovulation. *Endocrinology* 129:3200-3207
55. **Park JY, Su YQ, Ariga M, Law E, Jin SL, Conti M** 2004 EGF-like growth factors as mediators of LH action in the ovulatory follicle. *Science* 303:682-684
56. **Ashkenazi H, Cao X, Motola S, Popliker M, Conti M, Tsafirri A** 2005 Epidermal growth factor family members: endogenous mediators of the ovulatory response. *Endocrinology* 146:77-84
57. **Albertini DF, Herman B** 1984 Cell shape and membrane receptor dynamics. Modulation by the cytoskeleton. *Cell and muscle motility* 5:235-253

58. **Herman B, Albertini DF** 1984 A time-lapse video image intensification analysis of cytoplasmic organelle movements during endosome translocation. *J Cell Biol* 98:565-576
59. **Herman B, Albertini DF** 1982 The intracellular movement of endocytic vesicles in cultured granulosa cells. *Cell Motil* 2:583-597
60. **Carnegie JA, Byard R, Dardick I, Tsang BK** 1988 Culture of granulosa cells in collagen gels: the influence of cell shape on steroidogenesis. *Biol Reprod* 38:881-890
61. **Carnegie JA, Dardick I, Tsang BK** 1987 Microtubules and the gonadotropic regulation of granulosa cell steroidogenesis. *Endocrinology* 120:819-828
62. **Carnegie JA, Tsang BK** 1987 Microtubules and the calcium-dependent regulation of rat granulosa cell steroidogenesis. *BiolRepro* 36:1007-1015
63. **Herman B, Albertini DF** 1983 Microtubule regulation of cell surface receptor topography during granulosa cell differentiation. *Differentiation; research in biological diversity* 25:56-63
64. **Saltarelli D** 1999 Heterotrimeric Gi/o proteins control cyclic AMP oscillations and cytoskeletal structure assembly in primary human granulosa-lutein cells. *Cellular signalling* 11:415-433
65. **Ben-Ze'ev A, Amsterdam A** 1989 Regulation of cytoskeletal protein organization and expression in human granulosa cells in response to gonadotropin treatment. *Endocrinology* 124:1033-1041
66. **Herman B, Langevin MA, Albertini DF** 1983 The effects of taxol on the organization of the cytoskeleton in cultured ovarian granulosa cells. *European journal of cell biology* 31:34-45
67. **Albertini DF, Kravit NG** 1981 Isolation and biochemical characterization of ten-nanometer filaments from cultured ovarian granulosa cells. *J Biol Chem* 256:2484-2492
68. **Sasson R, Rimon E, Dantes A, Cohen T, Shinder V, Land-Bracha A, Amsterdam A** 2004 Gonadotrophin-induced gene regulation in human granulosa cells obtained from IVF patients. Modulation of steroidogenic genes, cytoskeletal genes and genes coding for apoptotic signalling and protein kinases. *Molecular human reproduction* 10:299-311
69. **van den Hurk R, Dijkstra G, van Mil FN, Hulshof SC, van den Ingh TS** 1995 Distribution of the intermediate filament proteins vimentin, keratin, and desmin in the bovine ovary. *Molecular reproduction and development* 41:459-467
70. **Czernobilsky B, Moll R, Levy R, Franke WW** 1985 Co-expression of cytokeratin and vimentin filaments in mesothelial, granulosa and rete ovarii cells of the human ovary. *European journal of cell biology* 37:175-190
71. **Eriksson JE, He T, Trejo-Skalli AV, Harmala-Brasken AS, Hellman J, Chou YH, Goldman RD** 2004 Specific in vivo phosphorylation sites determine the assembly dynamics of vimentin intermediate filaments. *J Cell Sci* 117:919-932
72. **Evans RM** 1988 Cyclic AMP-dependent protein kinase-induced vimentin filament disassembly involves modification of the N-terminal domain of intermediate filament subunits. *FEBS Lett* 234:73-78
73. **Inagaki M, Nishi Y, Nishizawa K, Matsuyama M, Sato C** 1987 Site-specific phosphorylation induces disassembly of vimentin filaments in vitro. *Nature* 328:649-652

74. **Lamb NJ, Fernandez A, Feramisco JR, Welch WJ** 1989 Modulation of vimentin containing intermediate filament distribution and phosphorylation in living fibroblasts by the cAMP-dependent protein kinase. *J Cell Biol* 108:2409-2422
75. **Hall PF, Almahbobi G** 1997 Roles of microfilaments and intermediate filaments in adrenal steroidogenesis. *Microscopy research and technique* 36:463-479
76. **Lee HS, Mrotek JJ** 1984 The effect of intermediate filament inhibitors on steroidogenesis and cytoskeleton in Y-1 mouse adrenal tumor cells. *Cell Biol Int Rep* 8:463-482
77. **Shiver TM, Sackett DL, Knipling L, Wolff J** 1992 Intermediate filaments and steroidogenesis in adrenal Y-1 cells: acrylamide stimulation of steroid production. *Endocrinology* 131:201-207
78. **Albertini DF, Clark JI** 1981 Visualization of assembled and disassembled microtubule protein by double label fluorescence microscopy. *Cell Biol Int Rep* 5:387-397
79. **Hynes RO, Destree AT** 1978 10 nm filaments in normal and transformed cells. *Cell* 13:151-163
80. **Starger JM, Goldman RD** 1977 Isolation and preliminary characterization of 10-nm filaments from baby hamster kidney (BHK-21) cells. *Proc Natl Acad Sci U S A* 74:2422-2426
81. **Monck JR, Fernandez JM** 1996 The fusion pore and mechanisms of biological membrane fusion. *Curr Opin Cell Biol* 8:524-533
82. **Kumar N, Robidoux J, Daniel KW, Guzman G, Floering LM, Collins S** 2007 Requirement of vimentin filament assembly for beta3-adrenergic receptor activation of ERK MAP kinase and lipolysis. *J Biol Chem* 282:9244-9250
83. **Bloom GS, Vallee RB** 1983 Association of microtubule-associated protein 2 (MAP 2) with microtubules and intermediate filaments in cultured brain cells. *J Cell Biol* 96:1523-1531
84. **Gurland G, Gundersen GG** 1995 Stable, detyrosinated microtubules function to localize vimentin intermediate filaments in fibroblasts. *J Cell Biol* 131:1275-1290
85. **Helfand BT, Chang L, Goldman RD** 2004 Intermediate filaments are dynamic and motile elements of cellular architecture. *J Cell Sci* 117:133-141
86. **Sanchez C, Diaz-Nido J, Avila J** 2000 Phosphorylation of microtubule-associated protein 2 (MAP2) and its relevance for the regulation of the neuronal cytoskeleton function. [Review] [483 refs]. *Progress in Neurobiology* 61:133-168
87. **Dehmelt L, Smart FM, Ozer RS, Halpain S** 2003 The role of microtubule-associated protein 2c in the reorganization of microtubules and lamellipodia during neurite initiation. *J Neurosci* 23:9479-9490
88. **Kindler S, Schulz B, Goedert M, Garner CC** 1990 Molecular structure of microtubule-associated protein 2b and 2c from rat brain. *J Biol Chem* 265:19679-19684
89. **Kindler S, Schwanke B, Schulz B, Garner CC** 1990 Complete cDNA sequence encoding rat high and low molecular weight MAP2. *Nucleic acids research* 18:2822
90. **Doll T, Meichsner M, Riederer BM, Honegger P, Matus A** 1993 An isoform of microtubule-associated protein 2 (MAP2) containing four repeats of the tubulin-binding motif. *J Cell Sci* 106:633-639

91. **Ferhat L, Ben-Ari Y, Khrestchatisky M** 1994 Complete sequence of rat MAP2d, a novel MAP2 isoform. *Comptes rendus de l'Academie des sciences* 317:304-309
92. **Ferhat L, Bernard A, Ribas dP, Ben-Ari Y, Khrestchatisky M** 1994 Structure, regional and developmental expression of rat MAP2d, a MAP2 splice variant encoding four microtubule-binding domains. *Neurochemistry International* 25:327-338
93. **Obar RA, Dingus J, Bayley H, Vallee RB** 1989 The RII subunit of cAMP-dependent protein kinase binds to a common amino-terminal domain in microtubule-associated proteins 2A, 2B, and 2C. *Neuron* 3:639-645
94. **Rubino HM, Dammerman M, Shafit-Zagardo B, Erlichman J** 1989 Localization and characterization of the binding site for the regulatory subunit of type II cAMP-dependent protein kinase on MAP2. *Neuron* 3:631-638
95. **Dehmelt L, Halpain S** 2005 The MAP2/Tau family of microtubule-associated proteins. *Genome biology* 6:204
96. **Lewis SA, Wang DH, Cowan NJ** 1988 Microtubule-associated protein MAP2 shares a microtubule binding motif with tau protein. *Science* 242:936-939
97. **Kim H, Binder LI, Rosenbaum JL** 1979 The periodic association of MAP2 with brain microtubules in vitro. *J Cell Biol* 80:266-276
98. **Gamblin TC, Nachmanoff K, Halpain S, Williams RC, Jr.** 1996 Recombinant microtubule-associated protein 2c reduces the dynamic instability of individual microtubules. *Biochemistry* 35:12576-12586
99. **Weisshaar B, Doll T, Matus A** 1992 Reorganisation of the microtubular cytoskeleton by embryonic microtubule-associated protein 2 (MAP2c). *Development (Cambridge, England)* 116:1151-1161
100. **Felgner H, Frank R, Biernat J, Mandelkow EM, Mandelkow E, Ludin B, Matus A, Schliwa M** 1997 Domains of neuronal microtubule-associated proteins and flexural rigidity of microtubules. *J Cell Biol* 138:1067-1075
101. **Sanchez C, Perez M, Avila J** 2000 GSK3beta-mediated phosphorylation of the microtubule-associated protein 2C (MAP2C) prevents microtubule bundling. *European journal of cell biology* 79:252-260
102. **Weisshaar B, Matus A** 1993 Microtubule-associated protein 2 and the organization of cellular microtubules. *Journal of neurocytology* 22:727-734
103. **Ferralli J, Doll T, Matus A** 1994 Sequence analysis of MAP2 function in living cells. *J Cell Sci* 107 (Pt 11):3115-3125
104. **Ludin B, Ashbridge K, Funfschilling U, Matus A** 1996 Functional analysis of the MAP2 repeat domain. *J Cell Sci* 109:91-99
105. **Ozer RS, Halpain S** 2000 Phosphorylation-dependent localization of microtubule-associated protein MAP2c to the actin cytoskeleton. *Molecular biology of the cell* 11:3573-3587
106. **Roger B, Al-Bassam J, Dehmelt L, Milligan RA, Halpain S** 2004 MAP2c, but not tau, binds and bundles F-actin via its microtubule binding domain. *Curr Biol* 14:363-371
107. **Kwei SL, Clement A, Faissner A, Brandt R** 1998 Differential interactions of MAP2, tau and MAP5 during axogenesis in culture. *Neuroreport* 9:1035-1040

108. **Miyata Y, Hoshi M, Nishida E, Minami Y, Sakai H** 1986 Binding of microtubule-associated protein 2 and tau to the intermediate filament reassembled from neurofilament 70-kDa subunit protein. Its regulation by calmodulin. *J Biol Chem* 261:13026-13030
109. **Papasozomenos SC, Binder LI, Bender PK, Payne MR** 1985 Microtubule-associated protein 2 within axons of spinal motor neurons: associations with microtubules and neurofilaments in normal and beta,beta'-iminodipropionitrile-treated axons. *J Cell Biol* 100:74-85
110. **Falconer MM, Vielkind U, Brown DL** 1989 Association of acetylated microtubules, vimentin intermediate filaments, and MAP 2 during early neural differentiation in EC cell culture. *Biochemistry and cell biology = Biochimie et biologie cellulaire* 67:537-544
111. **Bigot D, Hunt SP** 1991 The effects of quisqualate and nocodazole on the organization of MAP2 and neurofilaments in spinal cord neurons in vitro. *Neurosci Lett* 131:21-26
112. **Bloom GS, Luca FC, Vallee RB** 1985 Cross-linking of intermediate filaments to microtubules by microtubule-associated protein 2. *Ann N Y Acad Sci* 455:18-31
113. **Heimann R, Shelanski ML, Liem RK** 1985 Microtubule-associated proteins bind specifically to the 70-kDa neurofilament protein. *J Biol Chem* 260:12160-12166
114. **Hirokawa N, Hisanaga S, Shiomura Y** 1988 MAP2 is a component of crossbridges between microtubules and neurofilaments in the neuronal cytoskeleton: quick-freeze, deep-etch immunoelectron microscopy and reconstitution studies. *J Neurosci* 8:2769-2779
115. **Theurkauf WE, Vallee RB** 1982 Molecular characterization of the cAMP-dependent protein kinase bound to microtubule-associated protein 2. *JBiolChem* 257:3284-3290
116. **Beene DL, Scott JD** 2007 A-kinase anchoring proteins take shape. *Curr Opin Cell Biol* 19:192-198
117. **Wong W, Scott JD** 2004 AKAP signalling complexes: focal points in space and time. *Nature reviews* 5:959-970
118. **Diviani D, Scott JD** 2001 AKAP signaling complexes at the cytoskeleton. *JCell Sci* 114:1431-1437
119. **Sanchez C, Tompa P, Szucs K, Friedrich P, Avila J** 1996 Phosphorylation and dephosphorylation in the proline-rich C-terminal domain of microtubule-associated protein 2. *European journal of biochemistry / FEBS* 241:765-771
120. **Zamora-Leon SP, Bresnick A, Backer JM, Shafit-Zagardo B** 2005 Fyn phosphorylates human MAP-2c on tyrosine 67. *J Biol Chem* 280:1962-1970
121. **Zamora-Leon SP, Lee G, Davies P, Shafit-Zagardo B** 2001 Binding of Fyn to MAP-2c through an SH3 binding domain. Regulation of the interaction by ERK2. *J Biol Chem* 276:39950-39958
122. **Lim RW, Halpain S** 2000 Regulated association of microtubule-associated protein 2 (MAP2) with Src and Grb2: evidence for MAP2 as a scaffolding protein. *JBiolChem* 275:20578-20587
123. **Sloboda RD, Rudolph SA, Rosenbaum JL, Greengard P** 1975 Cyclic AMP-dependent endogenous phosphorylation of a microtubule-associated protein. *Proc Natl Acad Sci U S A* 72:177-181
124. **Schulman H** 1984 Phosphorylation of microtubule-associated proteins by a Ca²⁺/calmodulin-dependent protein kinase. *J Cell Biol* 99:11-19

125. **Akiyama T, Nishida E, Ishida J, Saji N, Ogawara H, Hoshi M, Miyata Y, Sakai H** 1986 Purified protein kinase C phosphorylates microtubule-associated protein 2. *J Biol Chem* 261:15648-15651
126. **Tsuyama S, Bramblett GT, Huang KP, Flavin M** 1986 Calcium/phospholipid-dependent kinase recognizes sites in microtubule-associated protein 2 which are phosphorylated in living brain and are not accessible to other kinases. *J Biol Chem* 261:4110-4116
127. **Illenberger S, Drewes G, Trinczek B, Biernat J, Meyer HE, Olmsted JB, Mandelkow EM, Mandelkow E** 1996 Phosphorylation of microtubule-associated proteins MAP2 and MAP4 by the protein kinase p110mark. Phosphorylation sites and regulation of microtubule dynamics. *J Biol Chem* 271:10834-10843
128. **Chang L, Jones Y, Ellisman MH, Goldstein LS, Karin M** 2003 JNK1 is required for maintenance of neuronal microtubules and controls phosphorylation of microtubule-associated proteins. *Dev Cell* 4:521-533
129. **Bjorkblom B, Ostman N, Hongisto V, Komarovski V, Filen JJ, Nyman TA, Kallunki T, Courtney MJ, Coffey ET** 2005 Constitutively active cytoplasmic c-Jun N-terminal kinase 1 is a dominant regulator of dendritic architecture: role of microtubule-associated protein 2 as an effector. *J Neurosci* 25:6350-6361
130. **Alexa A, Schmidt G, Tompa P, Ogueta S, Vazquez J, Kulcsar P, Kovacs J, Dombradi V, Friedrich P** 2002 The phosphorylation state of threonine-220, a uniquely phosphatase-sensitive protein kinase A site in microtubule-associated protein MAP2c, regulates microtubule binding and stability. *Biochemistry* 41:12427-12435
131. **Gong CX, Wegiel J, Lidsky T, Zuck L, Avila J, Wisniewski HM, Grundke-Iqbal I, Iqbal K** 2000 Regulation of phosphorylation of neuronal microtubule-associated proteins MAP1b and MAP2 by protein phosphatase-2A and -2B in rat brain. *Brain research* 853:299-309
132. **Sanchez Martin C, Diaz-Nido J, Avila J** 1998 Regulation of a site-specific phosphorylation of the microtubule-associated protein 2 during the development of cultured neurons. *Neuroscience* 87:861-870
133. **Chapin SJ, Bulinski JC** 1992 Microtubule stabilization by assembly-promoting microtubule-associated proteins: a repeat performance. *Cell motility and the cytoskeleton* 23:236-243
134. **Anderton BH, Betts J, Blackstock WP, Brion JP, Chapman S, Connell J, Dayanandan R, Gallo JM, Gibb G, Hanger DP, Hutton M, Kardalinou E, Leroy K, Lovestone S, Mack T, Reynolds CH, Van Slegtenhorst M** 2001 Sites of phosphorylation in tau and factors affecting their regulation. *Biochemical Society symposium*:73-80
135. **Marsh JM** 1970 The stimulatory effect of luteinizing hormone on adenylylcyclase in the bovine corpus luteum. *J Biol Chem* 245:1596-1603
136. **Richards JS** 1994 Hormonal control of gene expression in the ovary. *Endocr Rev* 15:725-751
137. **Richards JS, Fitzpatrick SL, Clemens JW, Morris JK, Alliston T, Sirois J** 1995 Ovarian cell differentiation: a cascade of multiple hormones, cellular signals, and regulated genes. *RecProgHormRes* 50:223-254

138. **Feliciello A, Gottesman ME, Avvedimento EV** 2001 The biological functions of A-kinase anchor proteins. *J Mol Biol* 308:99-114
139. **Smith FD, Langeberg LK, Scott JD** 2006 The where's and when's of kinase anchoring. *Trends in biochemical sciences* 31:316-323
140. **Carr DW, DeManno DA, Atwood A, Hunzicker-Dunn M, Scott JD** 1993 Follicle-stimulating hormone regulation of A-kinase anchoring proteins in granulosa cells. *JBiolChem* 268:20729-20732
141. **Garner CC, Matus A** 1988 Different forms of microtubule-associated protein 2 are encoded by separate mRNA transcripts. *Journal of Cell Biology* 106:779-783
142. **Ferhat L, Ben-Ari Y, Khrestchatisky M** 1994 Complete sequence of rat MAP2d, a novel MAP2 isoform. *Comptes Rendus de l Academie des Sciences - Serie Iii, Sciences de la Vie* 317:304-309
143. **Kalcheva N, Albala J, O'Guin K, Rubino H, Garner C, Shafit-Zagardo B** 1995 Genomic structure of human microtubule-associated protein 2 (MAP-2) and characterization of additional MAP-2 isoforms. *Proceedings of the National Academy of Sciences of the United States of America* 92:10894-10898
144. **Olesen OF** 1994 Expression of low molecular weight isoforms of microtubule-associated protein 2. Phosphorylation and induction of microtubule assembly in vitro. *Journal of Biological Chemistry* 269:32904-32908
145. **Arias C, Sharma N, Davies P, Shafit-Zagardo B** 1993 Okadaic acid induces early changes in microtubule-associated protein 2 and tau phosphorylation prior to neurodegeneration in cultured cortical neurons. *J Neurochem* 61:673-682
146. **Sanchez C, Diaz-Nido J, Avila J** 1995 Variations in in vivo phosphorylation at the proline-rich domain of the microtubule-associated protein 2 (MAP2) during rat brain development. *Biochem J* 306 (Pt 2):481-487
147. **Cai L, Chu Y, Wilson SE, Schlender KK** 1995 A metal-dependent form of protein phosphatase 2A. *Biochem Biophys Res Commun* 208:274-279
148. **Longin S, Jordens J, Martens E, Stevens I, Janssens V, Rondelez E, De Baere I, Derua R, Waelkens E, Goris J, Van Hoof C** 2004 An inactive protein phosphatase 2A population is associated with methylesterase and can be re-activated by the phosphotyrosyl phosphatase activator. *Biochem J* 380:111-119
149. **Kawasaki H, Springett GM, Mochizuki N, Toki S, Nakaya M, Matsuda M, Housman DE, Grabel AM** 1998 A family of cAMP-binding proteins that directly activate Rap1. *Science* 282:2275-2279
150. **Enserink JM, Christensen AE, de Rooij J, van Triest M, Schwede F, Genieser HG, Doskeland SO, Blank JL, Bos JL** 2002 A novel Epac-specific cAMP analogue demonstrates independent regulation of Rap1 and ERK. *Nature cell biology* 4:901-906
151. **Favre B, Turowski P, Hemmings BA** 1997 Differential inhibition and posttranslational modification of protein phosphatase 1 and 2A in MCF7 cells treated with calyculin-A, okadaic acid, and tautomycin. *J Biol Chem* 272:13856-13863
152. **Resjo S, Oknianska A, Zolnierowicz S, Manganiello V, Degerman E** 1999 Phosphorylation and activation of phosphodiesterase type 3B (PDE3B) in adipocytes in response to serine/threonine phosphatase inhibitors: deactivation of PDE3B in vitro by protein phosphatase type 2A. *Biochem J* 341 (Pt 3):839-845

153. **Yan Y, Mumby MC** 1999 Distinct roles for PP1 and PP2A in phosphorylation of the retinoblastoma protein. PP2a regulates the activities of G(1) cyclin-dependent kinases. *J Biol Chem* 274:31917-31924
154. **Cohen P, Holmes CFB, Tsukitani Y** 1990 Okadaic acid: a new probe for the study of cellular regulation. *TIBS* 15:98-102
155. **Berling B, Wille H, Roll B, Mandelkow EM, Garner C, Mandelkow E** 1994 Phosphorylation of microtubule-associated proteins MAP2a,b and MAP2c at Ser136 by proline-directed kinases in vivo and in vitro. *European journal of cell biology* 64:120-130
156. **Joep RS, Johnson GV** 2004 The glamour and gloom of glycogen synthase kinase-3. *Trends in biochemical sciences* 29:95-102
157. **Sontag E** 2001 Protein phosphatase 2A: the Trojan Horse of cellular signaling. *Cellular signalling* 13:7-16
158. **Feschenko MS, Stevenson E, Nairn AC, Sweadner KJ** 2002 A novel cAMP-stimulated pathway in protein phosphatase 2A activation. *The Journal of pharmacology and experimental therapeutics* 302:111-118
159. **Floer M, Stock J** 1994 Carboxyl methylation of protein phosphatase 2A from *Xenopus* eggs is stimulated by cAMP and inhibited by okadaic acid. *Biochem Biophys Res Commun* 198:372-379
160. **Nishi A, Bibb JA, Snyder GL, Higashi H, Nairn AC, Greengard P** 2000 Amplification of dopaminergic signaling by a positive feedback loop. *Proc Natl Acad Sci U S A* 97:12840-12845
161. **Kim Y, Sung JY, Ceglia I, Lee KW, Ahn JH, Halford JM, Kim AM, Kwak SP, Park JB, Ho Ryu S, Schenck A, Bardoni B, Scott JD, Nairn AC, Greengard P** 2006 Phosphorylation of WAVE1 regulates actin polymerization and dendritic spine morphology. *Nature* 442:814-817
162. **Ahn JH, McAvoy T, Rakhilin SV, Nishi A, Greengard P, Nairn AC** 2007 Protein kinase A activates protein phosphatase 2A by phosphorylation of the B56delta subunit. *Proc Natl Acad Sci U S A* 104:2979-2984
163. **Dajani R, Fraser E, Roe SM, Young N, Good V, Dale TC, Pearl LH** 2001 Crystal structure of glycogen synthase kinase 3 beta: structural basis for phosphate-primed substrate specificity and autoinhibition. *Cell* 105:721-732
164. **Li T, Paudel HK** 2006 Glycogen synthase kinase 3beta phosphorylates Alzheimer's disease-specific Ser396 of microtubule-associated protein tau by a sequential mechanism. *Biochemistry* 45:3125-3133
165. **Bach S, Knockaert M, Reinhardt J, Lozach O, Schmitt S, Baratte B, Koken M, Coburn SP, Tang L, Jiang T, Liang DC, Galons H, Dierick JF, Pinna LA, Meggio F, Totzke F, Schachtele C, Lerman AS, Carnero A, Wan Y, Gray N, Meijer L** 2005 Roscovitine targets, protein kinases and pyridoxal kinase. *J Biol Chem* 280:31208-31219
166. **Hsieh M, Lee D, Panigone S, Horner K, Chen R, Theologis A, Lee DC, Threadgill DW, Conti M** 2007 Luteinizing hormone-dependent activation of the epidermal growth factor network is essential for ovulation. *Mol Cell Biol* 27:1914-1924
167. **Doble BW, Woodgett JR** 2003 GSK-3: tricks of the trade for a multi-tasking kinase. *J Cell Sci* 116:1175-1186

168. **Chatfield K, Eastman A** 2004 Inhibitors of protein phosphatases 1 and 2A differentially prevent intrinsic and extrinsic apoptosis pathways. *Biochem Biophys Res Commun* 323:1313-1320
169. **De Baere I, Derua R, Janssens V, Van Hoof C, Waelkens E, Merlevede W, Goris J** 1999 Purification of porcine brain protein phosphatase 2A leucine carboxyl methyltransferase and cloning of the human homologue. *Biochemistry* 38:16539-16547
170. **Ogris E, Du X, Nelson KC, Mak EK, Yu XX, Lane WS, Pallas DC** 1999 A protein phosphatase methyltransferase (PME-1) is one of several novel proteins stably associating with two inactive mutants of protein phosphatase 2A. *J Biol Chem* 274:14382-14391
171. **Brautigan DL** 1995 Flicking the switches: phosphorylation of serine/threonine protein phosphatases. *Seminars in cancer biology* 6:211-217
172. **Begum N, Ragolia L** 1996 cAMP counter-regulates insulin-mediated protein phosphatase-2A inactivation in rat skeletal muscle cells. *J Biol Chem* 271:31166-31171
173. **Usui H, Inoue R, Tanabe O, Nishito Y, Shimizu M, Hayashi H, Kagamiyama H, Takeda M** 1998 Activation of protein phosphatase 2A by cAMP-dependent protein kinase-catalyzed phosphorylation of the 74-kDa B" (delta) regulatory subunit in vitro and identification of the phosphorylation sites. *FEBS Lett* 430:312-316
174. **Dinsmore JH, Solomon F** 1991 Inhibition of MAP2 expression affects both morphological and cell division phenotypes of neuronal differentiation. *Cell* 64:817-826
175. **Caceres A, Mautino J, Kosik KS** 1992 Suppression of MAP2 in cultured cerebellar macroneurons inhibits minor neurite formation. *Neuron* 9:607-618
176. **Wagner OI, Rammensee S, Korde N, Wen Q, Leterrier JF, Janmey PA** 2007 Softness, strength and self-repair in intermediate filament networks. *Experimental cell research* 313:2228-2235
177. **Chou YH, Flitney FW, Chang L, Mendez M, Grin B, Goldman RD** 2007 The motility and dynamic properties of intermediate filaments and their constituent proteins. *Experimental cell research* 313:2236-2243
178. **Ivaska J, Pallari HM, Nevo J, Eriksson JE** 2007 Novel functions of vimentin in cell adhesion, migration, and signaling. *Experimental cell research* 313:2050-2062
179. **Almahbobi G, Williams LJ, Hall PF** 1992 Attachment of steroidogenic lipid droplets to intermediate filaments in adrenal cells. *J Cell Sci* 101 (Pt 2):383-393
180. **Almahbobi G, Hall PF** 1990 The role of intermediate filaments in adrenal steroidogenesis. *J Cell Sci* 97 (Pt 4):679-687
181. **Almahbobi G, Williams LJ, Hall PF** 1992 Attachment of mitochondria to intermediate filaments in adrenal cells: relevance to the regulation of steroid synthesis. *Experimental cell research* 200:361-369
182. **Almahbobi G, Williams LJ, Han XG, Hall PF** 1993 Binding of lipid droplets and mitochondria to intermediate filaments in rat Leydig cells. *Journal of reproduction and fertility* 98:209-217
183. **Griffith LM, Pollard TD** 1982 The interaction of actin filaments with microtubules and microtubule-associated proteins. *Journal of Biological Chemistry* 257:9143-9151
184. **Goldman RD, Khuon S, Chou YH, Opal P, Steinert PM** 1996 The function of intermediate filaments in cell shape and cytoskeletal integrity. *J Cell Biol* 134:971-983

185. **Rae PA, Gutmann NS, Tsao J, Schimmer BP** 1979 Mutations in cyclic AMP-dependent protein kinase and corticotropin (ACTH)-sensitive adenylate cyclase affect adrenal steroidogenesis. *Proc Natl Acad Sci U S A* 76:1896-1900
186. **Liscum L, Dahl NK** 1992 Intracellular cholesterol transport. *Journal of lipid research* 33:1239-1254
187. **Griffin JW, Hoffman PN, Clark AW, Carroll PT, Price DL** 1978 Slow axonal transport of neurofilament proteins: impairment of beta,beta'-iminodipropionitrile administration. *Science* 202:633-635
188. **Abayasekara DR, Ford SL, Persaud SJ, Jones PM** 1996 Role of phosphoprotein phosphatases in the corpus luteum: II control of progesterone secretion by isolated rat luteal cells. *J Endocrinol* 150:213-221
189. **Styers ML, Salazar G, Love R, Peden AA, Kowalczyk AP, Faundez V** 2004 The endo-lysosomal sorting machinery interacts with the intermediate filament cytoskeleton. *Molecular biology of the cell* 15:5369-5382
190. **Gao YS, Vrieland A, MacKenzie R, Sztul E** 2002 A novel type of regulation of the vimentin intermediate filament cytoskeleton by a Golgi protein. *European journal of cell biology* 81:391-401
191. **Gao Y, Sztul E** 2001 A novel interaction of the Golgi complex with the vimentin intermediate filament cytoskeleton. *J Cell Biol* 152:877-894
192. **Styers ML, Kowalczyk AP, Faundez V** 2006 Architecture of the vimentin cytoskeleton is modified by perturbation of the GTPase ARF1. *J Cell Sci* 119:3643-3654
193. **Lydon JP, DeMayo FJ, Funk CR, Mani SK, Hughes AR, Montgomery CA, Jr., Shyamala G, Conneely OM, O'Malley BW** 1995 Mice lacking progesterone receptor exhibit pleiotropic reproductive abnormalities. *Genes Dev* 9:2266-2278
194. **Szabo M, Knox KL, Ringstrom SJ, Perlyn CA, Sutandi S, Schwartz NB** 1996 Mechanism of the inhibitory action of RU486 on the secondary follicle-stimulating hormone surge. *Endocrinology* 137:85-89
195. **Stocco DM** 2000 Intramitochondrial cholesterol transfer. *Biochimica et biophysica acta* 1486:184-197
196. **Niswender GD** 2002 Molecular control of luteal secretion of progesterone. *Reproduction* 123:333-339
197. **Franke WW, Hergt M, Grund C** 1987 Rearrangement of the vimentin cytoskeleton during adipose conversion: formation of an intermediate filament cage around lipid globules. *Cell* 49:131-141
198. **Trzeciak WH, Boyd GS** 1973 The effect of stress induced by ether anaesthesia on cholesterol content and cholesteryl-esterase activity in rat-adrenal cortex. *European journal of biochemistry / FEBS* 37:327-333
199. **Salvador LM, Park Y, Cottom J, Maizels ET, Jones JCR, Schillace RV, Carr DW, Cheung P, Allis CD, Jameson JL, Hunzicker-Dunn M** 2001 Follicle stimulating hormone stimulates protein kinase A mediated histone H3 phosphorylation and acetylation leading to select gene activation in ovarian granulosa cells. *JBiolChem* 276:40146-40155

200. **Hunzicker-Dunn M, Cutler RE, Jr., Maizels ET, DeManno DA, Lamm MLG, Erlichman J, Sanwal BD, LaBarbera AR** 1991 Isozymes of cAMP-dependent protein kinase present in the rat corpus luteum. *JBiolChem* 266:7166-7175
201. **Bender FE, Douglass LW, Kramer A** 1982 Statistical methods for Food and Agriculture. Westport,CT.: AVI Publishing Co., Inc.
202. **Alto NM, Soderling SH, Hoshi N, Langeberg LK, Fayos R, Jennings PA, Scott JD** 2003 Bioinformatic design of A-kinase anchoring protein-in silico: a potent and selective peptide antagonist of type II protein kinase A anchoring. *Proc Natl Acad Sci U S A* 100:4445-4450
203. **Carr DW, Hausken ZE, Fraser IDC, Stofko-Hahn RE, Scott JD** 1992 Association of the type II cAMP-dependent protein kinase with a human thyroid RII-anchoring protein. *JBiolChem* 267:13376-13382
204. **Alam H, Maizels ET, Park Y, Ghaey S, Feiger ZJ, Chandel NS, Hunzicker-Dunn M** 2004 Follicle-stimulating hormone activation of hypoxia-inducible factor-1 by the phosphatidylinositol 3-kinase/AKT/Ras homolog enriched in brain (Rheb)/mammalian target of rapamycin (mTOR) pathway is necessary for induction of select protein markers of follicular differentiation. *J Biol Chem* 279:19431-19440
205. **Rankin CA, Sun Q, Gamblin TC** 2005 Pseudo-phosphorylation of tau at Ser202 and Thr205 affects tau filament formation. *Brain Res Mol Brain Res* 138:84-93

CURRICULUM VITAE

Maxfield P. Flynn

ADDRESS: 759 West Melrose Street
Chicago, Illinois 60657
773-665-8090 (tel)
mflynn005@northwestern.edu (e-mail)

EDUCATION: M.D. (expected) 2001-2003, 2007-2009
Northwestern University Feinberg School of Medicine, Chicago, IL
Ph.D. (Cell and Molecular Biology) 2003-2007
Northwestern University Feinberg School of Medicine, Chicago, IL
B.S. (Cell and Molecular Biology, Physics) 1997-2001
Tulane University, New Orleans, LA

AWARDS

AND HONORS: • Tulane University Dean's Honor Scholarship
• 2000 Endocrine Society Summer Research Fellowship
• 2001 Tulane College William Wallace Peery Society
• Magna Cum Laude, Honors in Cell and Molecular Biology, Tulane University
• Endocrinology Training Grant Fellowship, Northwestern University
• 2006 1st Place Poster Award, Annual Minisymposium on Reproductive Biology

SCIENTIFIC

EXPERIENCE: Undergraduate Student Research with Dr. David Hurley, 1997-2001
Department of Cell and Molecular Biology, Tulane University
• Mathematical modeling of an ultrasensitive receptor system
• Characterization of the genomic structure of transcription factor Zn-16

N.I.H. Medical Scientist Training Program 2001-2009
Northwestern University Feinberg School of Medicine

Graduate Student Research with Dr. Mary Hunzicker-Dunn 2003-2007
Department of Cell and Molecular Biology, Northwestern University
• Luteinizing hormone receptor signaling to regulate MAP2D in preovulatory ovarian granulosa cells

SCIENTIFIC

MEETINGS: • The Endocrine Society Annual Meeting, Toronto, 2000.
• The Endocrine Society Annual Meeting, Denver, 2001.
• The Society for the Study of Reproduction Annual Meeting, Vancouver, 2004.
• The Society for the Study of Reproduction Annual Meeting, Quebec, 2005.
• Minisymposium on Reproductive Biology, Evanston, 2005.
• The Endocrine Society Annual Meeting, Boston, 2006.
• Minisymposium on Reproductive Biology, Evanston, 2006.

SOCIETIES AND

MEMBERSHIPS: • The Endocrine Society Since 2000
• Society for the Study of Reproduction Since 2003

TEACHING

EXPERIENCE:	Teaching Assistant, Histology <i>Dr. Larry Cochard, Course Director.</i>	2004, 2005, 2006
	Teaching Assistant, Microbiology <i>Dr. Karla Satchell, Course Director.</i>	2004, 2005

BIBLIOGRAPHY: THESIS

1. Flynn, M.P. (2007) Luteinizing hormone receptor signaling regulates MAP2D phosphorylation in preovulatory granulosa cells. Ph.D. thesis, Cell and Molecular Biology, Northwestern University.

BIBLIOGRAPHY: ORIGINAL JOURNAL ARTICLES

1. Voss, T.C., Flynn, M.P., and Hurley, D.L. (2001) IGF-1 causes an ultrasensitive reduction in GH mRNA levels via an extracellular mechanism involving IGF binding proteins. *Mol. Endocrinol.* 15, 1549-58.
2. Salvador, L.M., Flynn, M.P., Avila, J., Reierstad, S., Maizels, E.T., Alam, H., Park, Y., Scott, J.D., Carr, D.W., and Hunzicker-Dunn, M. (2004) Neuronal microtubule-associated protein 2D is a dual A-kinase anchoring protein expressed in rat ovarian granulosa cells. *J. Biol. Chem.* 279, 27621-32.
3. Flynn, M.P., and Hurley, D.L. (2006) Growth hormone transcription factor ZN-16 genomic coding regions are composed of a single exon and are evolutionarily conserved in mammals. *Gene* 368, 78-83.
4. Flynn, M.P., Maizels, E.T., Karlsson, A.B., McAvoy, T., Ahn, J.-H., Nairn, A.C., Hunzicker-Dunn, M. (2008) Luteinizing hormone receptor activation in ovarian granulosa cells promotes protein kinase A-dependent dephosphorylation of MAP2D. *Mol. Endocrinol.* 22, 1695-710.

BIBLIOGRAPHY: ABSTRACTS AND PRESENTATIONS

1. Voss, T.C., Flynn, M.P. and Hurley, D.L. (2000) Growth hormone mRNA expression in rat MtT/S somatotroph cells is decreased by insulin-like growth factor-1 in a switch-like manner via an extracellular mechanism of ultrasensitive kinetics. Endocrine Society Annual Meeting, Toronto, ON.
2. Flynn, M.P. and Hurley, D.L. (2001) Genomic structure of pituitary transcription factor Zn-16 in mouse and human is compact and conserved. Endocrine Society Annual Meeting, Denver, CO.
3. Flynn, M.P., Carr, D.W., and Hunzicker-Dunn, M. (2004) Existence of a putative type I PKA trimer in rat preovulatory follicles. Society for the Study of Reproduction Annual Meeting, Vancouver, BC.
4. Flynn, M.P., Maizels, E.T., Hunzicker-Dunn, M. (2005) LH-dependent dephosphorylation of MAP2D by PP2A in ovarian granulosa cells. Annual Minisymposium on Reproductive Biology, Evanston, IL.
5. Flynn, M.P., Maizels, E.T., Hunzicker-Dunn, M. (2006) Luteinizing hormone receptor activation in ovarian granulosa cells promotes PKA-dependent dephosphorylation of the AKAP MAP2D on Thr256/Thr259. Endocrine Society Annual Meeting, Boston, MA.
6. Flynn, M.P., Maizels, E.T., Hunzicker-Dunn, M. (2006) Luteinizing hormone receptor activation in ovarian granulosa cells promotes PKA-dependent dephosphorylation of the AKAP MAP2D on Thr256/Thr259. Annual Minisymposium on Reproductive Biology, Evanston, IL.